TEXAS INSTRUMENTS

U1-780130-F

SPACECRAFT APPLICATIONS OF ADVANCED GLOBAL POSITIONING SYSTEM TECHNOLOGY

FINAL REPORT

Prepared by:

Texas Instruments Incorporated
Defense Systems & Electronics Group
P.O. Box 869305
Plano, Texas 75086

15 June 1988

Reference Contract No. NAS 9-17781

Prepared for:

National Aeronautics and Space Administration
Lyndon B. Johnson Space Center
Houston, Texas 77058

TABLE OF CONTENTS

LIST OF ILLUSTRATIONS

LIST OF TABLES

SPACECRAFT APPLICATIONS OF ADVANCED GLOBAL POSITIONING SYSTEM TECHNOLOGY

INTERIM REPORT

SECTION 1

INTRODUCTION

This is the final report on the Texas Instruments Incorporated (TI) simulations study of Spacecraft Applications of Advanced Global Positioning System (GPS) Technology. This work was conducted for the NASA Lyndon B. Johnson Space Center (JSC) under contract NAS 9–17781. GPS, in addition to its baselined capability as a highly accurate spacecraft navigation system, can provide traffic control, attitude control, structural control and a uniform time base. In Phase I of this program, another contractor investigated the potential of GPS in these four areas and compared GPS to other techniques. This contract was for the Phase II effort, to study the performance of GPS for these spacecraft applications through computer simulations. TI had previously developed simulation programs for GPS differential navigation and attitude measurement. These programs were adapted for these specific spacecraft applications. In addition, TI has extensive expertise in the design and production of advanced GPS receivers, including space-qualified GPS receivers. We have drawn on this background to augment the simulation results in the system level overview, which is Section 2 of this report.

1.1 FINAL REPORT STRUCTURE

This report has four sections:

Section 1. Introduction

Section 2. System Level Overview

Section 3. Analytical Basis for Study and Simulations

Section 4. Simulation Results.

Section 2 is intended to be easy, fluent and informative reading with sufficient quantitative information to provide a system-level understanding based on the simulation results and on TI's previous experience with advanced GPS receiver applications.

Section 3 addresses the analytical basis for the two major simulation study topics: GPS Attitude Measurement Analysis and GPS Relative Navigation Analysis.

Section 4 describes the simulation environment and presents the simulation results for the two major simulation study topics: GPS Attitude Measurement Simulation Results and GPS Relative Navigation Simulation Results.

1.2 TECHNICAL STAFF

The program manager and lead system engineer was Phil Ward. Principal system engineer and analyst for the GPS attitude simulations was Dr. Jagannath Rath. Principal system engineer and

analyst for GPS relative navigation simulations was Ann Collier. Dennis Henson provided system engineering consulting support.

1.3 TIME PERIOD OF STUDY

The authorization for TI to proceed for this study was given 15 July 1987 and the duration of the contract was 6 months, ending 15 January 1988. TI requested a no-cost extension of the contract to 15 June 1988 to consider the study of multipath and masking effects in GPS relative navigation between the space station and the shuttle orbiter during a typical docking maneuver.

The kickoff meeting was 21 May 1987 at NASA-JSC. TI and another contractor, Axiomatix, presented their approaches to the Phase II Computer Simulation Study. The following guidelines were agreed upon.

1.4 SUMMARY OF COMPUTER SIMULATIONS GUIDELINES

The differential studies were confined to less than 20 nautical miles (35 km) of separation between space vehicles and were not to include docking maneuvers. The simulations were to demonstrate clearly the benefits (if any) of the more complex relative navigation techniques involving pseudorange differencing versus the simple differencing of the navigation state vector of each space vehicle. With respect to the "bent pipe" techniques involving L-band translation, the relative navigation performance was to be inferred from conventional GPS relative navigation simulations. The bent pipe study was to address only the advantages of this technique (if any) and the bandwidth requirements. The study was confined to pure GPS applications, not integrated GPS and inertial navigation systems. Only the standard GPS earth-centered, earth-fixed (ECEF) coordinate system was required. The simulations do not require absolute navigation techniques to be developed. The scope of the attitude determination with GPS was limited to measurement performance, not attitude control of the space vehicle. The scope of the structural oscillations study was limited to an extension of the attitude measurement performance results. No value judgements were to be provided, only comparisons of advantages and disadvantages.

At subsequent technical interchange meetings with NASA-JSC, TI received the following additional guidelines. Assume that the GPS attitude measurement accuracy of the space station to be 0.01 degree (RMS 1 sigma) and that the GPS relative navigation accuracy for the space station and any other spacecraft to be 30 meters or 1 percent of the range between the two spacecraft (RMS 1 sigma), whichever is the greater.

1.5 MAJOR CONCLUSIONS OF THE STUDY

1.5.1 GPS Attitude Measurement

It can be concluded from the GPS attitude measurement simulations results that the space station attitude measurement accuracy of 0.01 degree can be obtained by using simultaneous GPS carrier doppler phase measurements. These measurements must be from each of three GPS antennas located at the apexes of an approximately equilateral triangle whose sides are 5 or more meters in length. The same three GPS satellites must be tracked at each antenna and the carrier phase noise of each measurement must be less than 2 degrees. To achieve this, necessary

precautions must be taken to maintain a high carrier signal-to-noise ratio by proper antenna/receiver design and by minimizing the effect of differential carrier multipath. Differential multipath effects are caused by the reflected path *differences* experienced at each antenna phase center, not the absolute effects. Differential multipath is minimized by using a low-profile GPS antenna and microwave-absorbing material about 20 centimeters (one carrier wavelength) around each antenna base. The antenna design should provide sharp attenuation to multipath signals which tend to occur at elevation angles below 10 degrees. The antenna phase centers must be matched by using identical antenna designs with stable phase centers so that phase center migrations with satellite elevation angle tend to cancel when the carrier doppler phases are differenced. The antennas should have identical orientation marks on the antenna mounting base, and these should all be aligned in the same direction when mounted on the space station.

1.5.2 GPS Relative Navigation

It can be concluded that the relative navigation accuracy performance of 30 meters or 1 percent, whichever is greater, can be met by differencing the navigation state vector. Certain precautions must be taken, however. The same four satellites should be tracked by both spacecraft to remove all space and control segment common bias errors. Both receivers should use the antispoofing/selective availability (AS/SA) key consistently; i.e., typically both will apply the SA correction function to the navigation state to achieve the best absolute navigation accuracy or, alternatively, both must not apply the SA correction function to the navigation state. If the SA correction function is not applied to the navigation state, to achieve the relative navigation accuracy performance, both navigation states must have their measurement incorporation cycles synchronized to the same GPS time. Both spacecraft may use P(Y)-code or C/A-code receivers or one may use a P(Y)-code and the other a C/A-code receiver (provided that both spacecraft correct their navigation position accuracy with the SA function or both synchronize to the same GPS measurement incorporation time without the SA function).

Relative navigation by differencing the navigation state vector of two spacecraft is the recommended baseline for all traffic control applications. However, pseudorange difference techniques are recommended when the highest relative positioning accuracy is required (for example, for docking maneuvers). Taking pseudorange differences ensures that all measurement bias errors and both receiver clock errors are eliminated in the GPS observables, independent of the navigation state filter mechanization or the accuracy of the satellite orbit predictions. Naturally, the technique also ensures that the same four satellites will be used. The SA correction is not required to achieve maximum relative navigation precision if the raw measurements of both receivers are synchronized to the same GPS time, because time skew between the measurements of the two spacecraft is removed automatically. For example, if both spacecraft use C/A-code receivers without the AS/SA key, synchronized GPS measurements would achieve the same relative navigation performance as if both C/A-code receivers had applied the SA correction. The SA correction is the same at the same GPS time and therefore the difference cancels.

The navigation state vector difference is recommended as the coarse relative navigation baseline because of the possibility that the two spacecraft might not be able to track the same satellites under certain masking or other outage conditions. Another consideration in favor of the navigation state vector difference as the baseline is that the navigation state vector might be augmented by other navigation aids, such as an inertial navigation system, which will carry it through masking or other outage conditions.

SECTION 2
SYSTEM-LEVEL OVERVIEW

2.1 TASK 1. ATTITUDE CONTROL AND POINTING

The functions of star trackers, inertial measurement units, and rate gyros to determine attitude and attitude rate can be replaced by a plurality of GPS antennas and the use of GPS interferometry techniques. GPS interferometry techniques have been used extensively in precision geodetic applications. GPS interferometry is a method of determining relative position by comparing the carrier doppler phase of signals from two or more GPS antennas receiving the same satellite signal at the same time. The method of determining attitude from the relative position information derived from differential GPS carrier doppler phase measurements is very similar to the techniques used in geodetic applications, except that the baseline between the GPS antennas is much shorter and the magnitude of the antenna phase center separation is known fairly accurately beforehand.

2.1.1 Method of Determining Attitude

Figure 2-1 illustrates the differential measurement of the carrier doppler phase from the same SV at two antennas. This single difference corresponds to a time difference of arrival of the carrier wavefront at the phase centers of the antennas. Note that there is an ambiguity in this time difference of arrival at every wavelength of the carrier frequency. Since the separation of

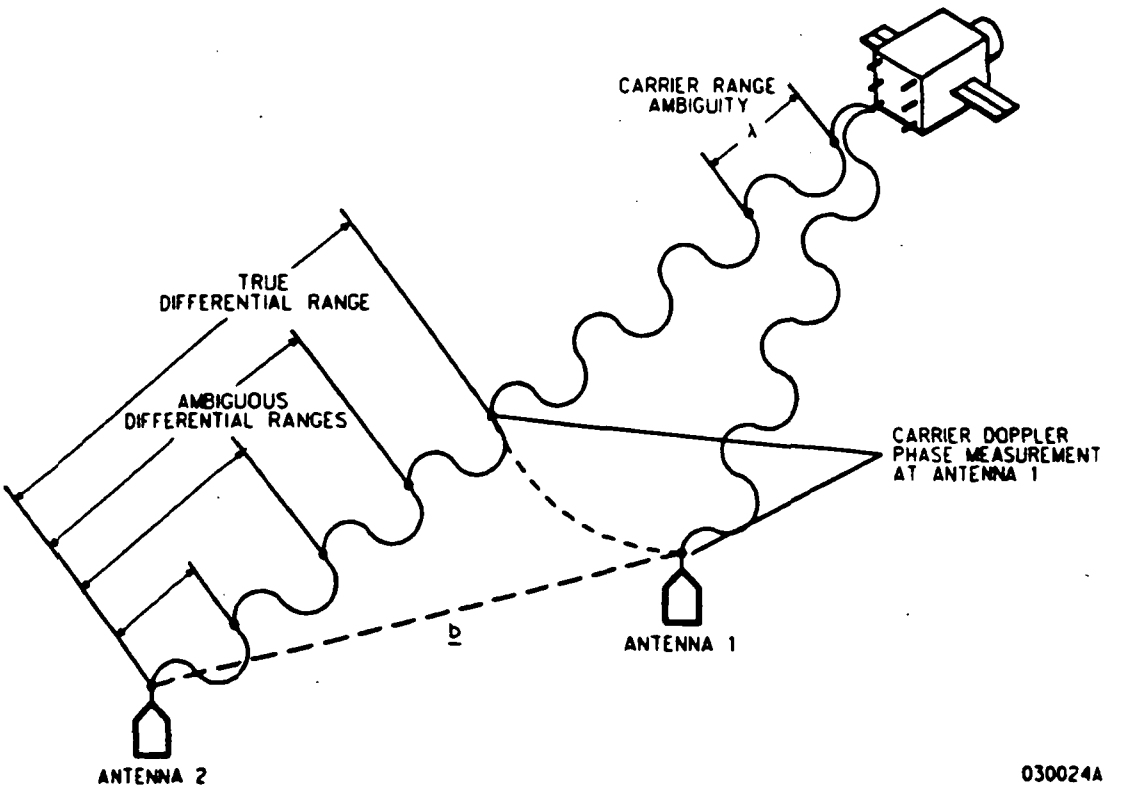

Figure 2-1. Carrier Doppler Phase Difference Measurement

the antenna phase centers for attitude control and pointing applications is precisely known, the angle of the line joining the two phase centers with respect to the line of sight to the satellite can be determined, after the ambiguity problem has been solved. The plane containing the antenna baseline can be rotated about the antenna baseline axis and orthogonally to this axis in a manner which does not change the time difference of arrival measurement. The remaining degree of rotational freedom of the plane is the only one whose attitude is measurable with one pair of antennas located in a plane. Thus, for each pair of antennas and for one set of interferometric observables from one SV, one degree of freedom of attitude can be measured. If three antennas are arranged to define a plane on the spacecraft, then by measuring a multiplicity of carrier phase differences to at least three satellites, the plane and, therefore, the spacecraft attitude, can be measured.

The geometry of the plane with respect to the geometry of the SVs determines the orthogonality of the interferometry measurements. This, in turn, determines the sensitivity of the measurements to noise in the observables. Attitude measurement with GPS satellite signals can be very accurate, since the operational GPS satellites will provide good geometry and the proper GPS receiver hardware design will keep the noise quite small. The spacecraft attitude rate can be measured by calculating the differential rate of phase change (differential frequency) between antenna phase centers. This is the same as differential doppler between antenna phase centers. If the local oscillator noise is properly managed, the major source of residual error by this multiple differencing technique is carrier thermal noise which decreases with signal strength and increases with receiver noise figure. Carrier doppler phase difference noise can be filtered to yield less than a degree of RMS phase error. For the GPS L1 frequency at 1575.42 MHz, the carrier wavelength is 19.03 centimeters. A phase error of one degree in a 360- degree wavelength corresponds to 0.52 millimeter of relative position error which, in turn, for a baseline separation between antennas of 1 meter corresponds to 0.52 milliradian. Thus, the fundamental measurement accuracy of the GPS interferometry technique is approximately 0.5 milliradian per meter of antenna separation per degree of carrier phase difference measurement noise.

Not every GPS receiver can provide the carrier phase measurements used in the interferometry technique. Receivers using analog voltage controlled oscillator techniques in their carrier tracking loops are unsuitable for precision carrier phase measurements because the phase measurement is not directly observable. They measure "delta pseudorange" by differencing two carrier phase values separated by a short time interval but they cannot provide continuous phase. Sequential single-channel receivers provide these data for one SV at a time, with the data from subsequent SVs at a different time. Measurements from the same SVs could be a few seconds apart, and this is too long an interval to extrapolate without excessive error.

2.1.2 GPS Receiver Design for Determining Attitude

There are several design approaches to GPS receivers used for determining attitude. In all design approaches, the receiver design must be able to produce the continuously counted carrier doppler phase measurements from three or more GPS satellites and from three or more GPS antennas simultaneously.

2.1.2.1 ***Multiple Receiver Approach.*** A straightforward approach, which does not require a specialized GPS receiver, it to use one conventional GPS receiver per antenna. Each performs the normal GPS tracking functions essentially independently (and redundantly), but constrained

to continuously track three or more of the same satellites in phase lock. The code and carrier tracking loops would be conventional (only one set each per satellite tracked) and would be designed to operate at full tracking dynamics required. In each GPS receiver, there would be a dedicated channel per satellite. It is important that the GPS receiver be a modern one with digitalization prior to correlation and designed in such a manner that the multiple continuous channels do not introduce interchannel bias errors.

Each GPS receiver would provide synchronized carrier doppler phase measurements to a central control processor which would perform the differencing process and determine the attitude measurement. This multiple conventional GPS receiver approach has appeal since the size and cost of modern conventional receivers are being reduced significantly through higher levels of component integration and by amortizing the software development cost over a large number of receivers.

*2.1.2.2 **Multiplexed Antenna Approach.*** Another approach is to multiplex the measurements from a single GPS receiver across multiple GPS antennas. The obvious advantage to this approach is the classical advantage of multiplexing GPS receivers: reduced GPS receiver hardware because the same hardware is time shared across multiple satellites and, in this case, across multiple antennas. The disadvantage is that the tracking threshold of the multiplexing receiver is significantly reduced. The multiplexing process involves a loss of effective signal-to-noise ratio because the dwell time on each satellite (and therefore the available carrier power) is reduced. The fact that the same GPS satellites are being tracked on all antennas permits clever but highly specialized tracking schemes such as sum and difference loops to be implemented which provide the desired differential measurements and yet minimize the effective tracking threshold loss of multiplexing.

For example, one multiplexed tracking scheme uses sum and difference loops. In the case of three antenna, multiplex tracking, four code and carrier tracking loops would be formed for each satellite tracked. There would be a sum loop:

$$S(n) = A1(n) + A2(n) + A3(n)$$

where A1(n) is the tracking state corresponding to the satellite(n) on antenna 1 and three difference loops:

$$D1(n) = A1(n) - A2(n)$$
$$D2(n) = A2(n) - A3(n)$$
$$D3(n) = A3(n) - A1(n)$$

When visiting a particular antenna on a multiplexed dwell cycle, the tracking state placed into the receiver tracking hardware is predicted from the algebraic combination of the sum loop and appropriate difference loops. For example:

$$A1(n) = [S(n) + D1(n) - D3(n)]/3$$

The sum loop is tracking the full dynamics, while the difference loops are tracking only the mild differential dynamics. The attitude observables would be derived from these difference loops. The code difference loops provide the coarse attitude measurements and are used to minimize

the ambiguity problem. The carrier difference loops provide the precision attitude observables. Since the difference loops track only the mild dynamics of the attitude changes, their tracking loop bandwidth can (usually) be significantly reduced in comparison with the sum loop bandwidth. This, in turn, reduces the differential measurements noise and improves tracking threshold which partially compensates for the loss in tracking threshold due to the time division multiplexing between antennas.

2.1.2.3 Single GPS Receiver Approach. A third approach is a single GPS receiver approach, wherein one specialized GPS receiver design can perform GPS attitude measurements from multiple GPS antennas with the minimum hardware that supports continuous tracking of each satellite and each antenna. This is a TI invention which has already been implemented in the TI 420 GPS receiver hardware design so that this 5 channel, 10 pound man-portable receiver can accomplish GPS pointing when a second GPS antenna assembly is provided. TI has the only GPS receiver design with built-in pointing capability. A patent disclosure has been filed on this minimal hardware technique.

The invention assumes that there is proximity of the GPS antennas used for GPS pointing or attitude measurements: i.e., the correlation interval of P(Y)-code at 60 meters or C/A-code at 600 meters is very large in comparison with a typical GPS antenna separation of 5 meters or less when used for pointing or attitude measurement of a platform.

The GPS pointing invention block diagram shown in Figure 2–1a depicts the key features of the invention using two GPS antennas as implemented in the TI 420 for pointing. The same concepts can be readily implemented for three or more GPS antennas for attitude measurement. Referring to Figure 2–1a, one antenna and its precorrelation electronics output is designated the primary signal and the other is designated the secondary signal. In a modern digital GPS receiver like the TI 420, the precorrelation electronics provide preamplification, downconversion to an intermediate frequency (IF) and analog-to-digital conversion at IF. Thereafter, the only duplication of hardware is one carrier mixer and three code correlators per antenna signal. One set of replica carrier and code generators, one oscillator (clock) and one processor are shared in common with the dual port mixer and correlators. Since these are digital mixers and correlators, they do not require much additional circuit real estate to duplicate, especially when implemented on an application specific integrated circuit (ASIC). In the TI 420 these dual functions as well as the remainder of the GPS receiver are implemented in an ASIC called the channel-on-a-chip (COAC). There are 5 dual-port COACs in the TI–420.

Walking through the COAC portion of the block diagram, the primary (digital) signal feeds the primary carrier mixer and the secondary signal feeds the secondary carrier mixer. The common replica carrier generator produces a complex in-phase (I) and quadrature (Q) signal which feeds both the primary and the secondary carrier mixers. The complex I and Q outputs from the primary carrier mixer feed all three primary code correlators. Similarly, the complex I and Q outputs from the secondary carrier mixer feed all three secondary code correlators. The common replica code generator feeds the three primary code correlators and the three secondary code correlators with an early (E), prompt (P) and late (L) code which are phased half a chip apart. The result is that three complex I and Q outputs (E_P, P_P and L_P) are produced from the primary GPS signal. E_P, P_P and L_P are processed and tracked in the conventional manner by the receiver baseband processor. As a by-product, three complex I and Q outputs (E_S, P_S and L_S) are

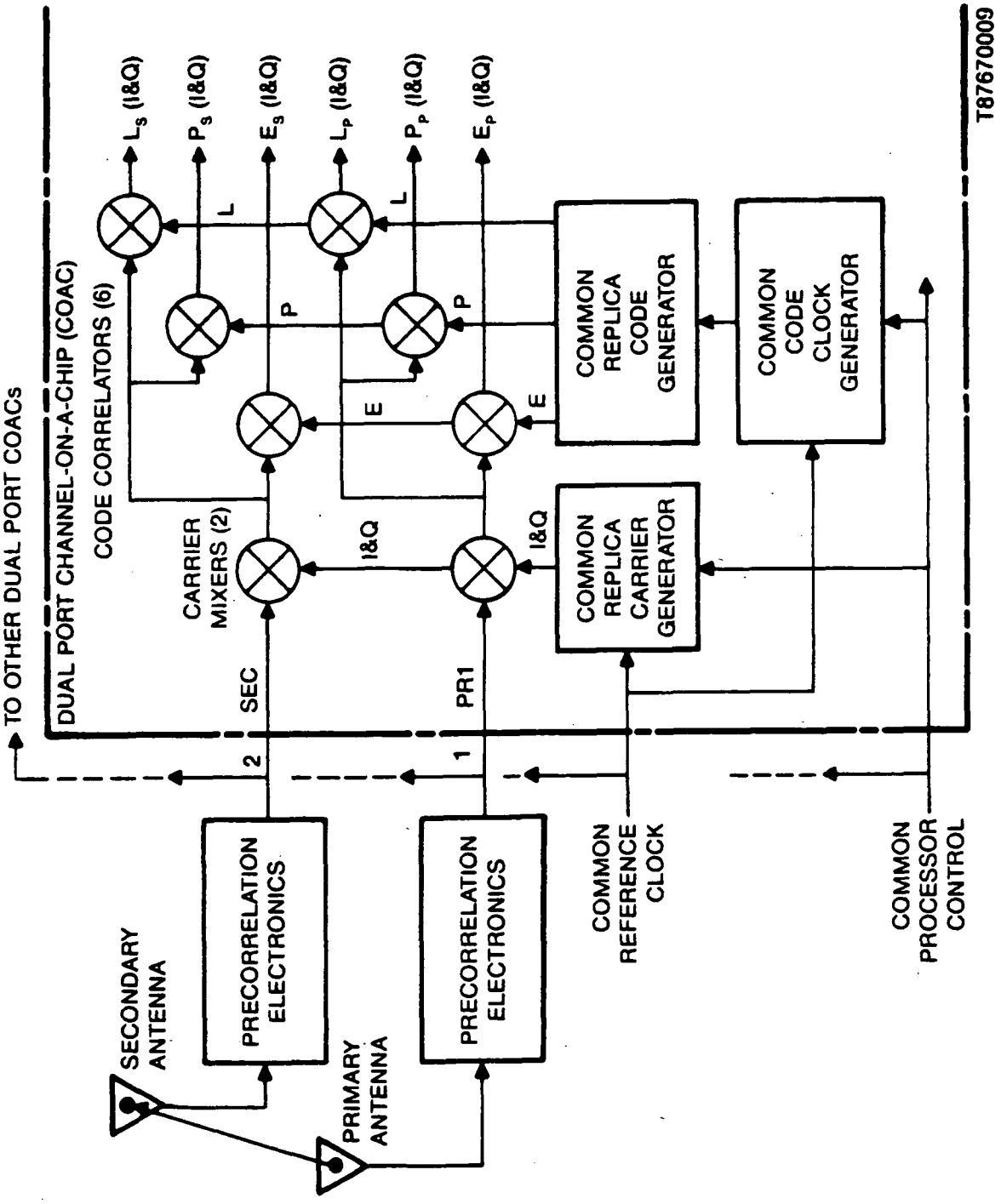

Figure 2-1a. GPS Pointing Invention Block Diagram

produced from the secondary GPS signal which are phase shifted in proportion to the absolute displacement (pointing) of the secondary antenna with respect to the GPS satellite being tracked on the primary antenna. These secondary signals can be combined with the primary signals to obtain the GPS pointing observables for one satellite. No special receiver baseband tracking software is required to track these secondary signals. Only the software to read and process these signals is required. The same process is repeated for each channel in the receiver. In the case of the TI 420, five channels are provided, which provides an oversolution to the GPS pointing computation.

There are other advantages to this invention, besides providing the minimal hardware and baseband software for continuous GPS pointing or attitude measurements. Since the replica carrier and code generators and the oscillator are common to the primary and secondary correlators, all noise contributions from these sources cancels as common mode noise when the observables are differenced to form the pointing or attitude measurements. A high quality oscillator or an atomic standard are not needed since both long term and short term clock noise are common mode and cancel out when the GPS observables are differenced. The assignment of the role of primary antenna is arbitrary, so that the normal GPS tracking function could be switched from one antenna to another if a failure occurred in the antenna or the precorrelation electronics. This provides added redundancy for the normal GPS tracking modes even though the pointing or attitude observables have been reduced.

Although unrelated to the invention, the use of digital mixers and correlators eliminates interchannel bias error.

2.2 TASK 2. STRUCTURAL CONTROL

Structural control of a spacecraft is dependent on the ability to measure structural flexures. The same GPS interferometric techniques used for precise attitude measurement also can be used to measure spacecraft structural flexures, except that more GPS antennas are required. Three GPS antennas arranged in a triangle establish a reference plane. Additional GPS antennas provide a measurement of flexure with respect to the reference plane. When measuring the flexure along a particular beam structure, two GPS antennas placed at the extreme ends of the beam define a line, and an additional GPS antenna in line with and centered between these two antennas could be used to measure flexure of the beam with respect to the line. Since the same techniques are used, the measurement precision is predictable from the attitude measurement simulations.

The same GPS design considerations apply equally to this application and to the GPS attitude measurement application. Given the very mild dynamics of a large spacecraft such as the Space Station and assuming appropriately designed GPS receivers and antennas, the combined noise and error budget in the raw differential carrier doppler phase measurements could be reduced to less than 2 degrees. This corresponds to less than 1 millimeter of measurement uncertainty at L1. Structural deflections can, therefore, be measured with millimeter accuracy using GPS interferometric techniques.

The same limitations also apply equally to this application and to the GPS attitude measurement application. The GPS antenna locations must be selected to minimize obstructions and differential multipath effects. Ideally, the upper hemisphere of the reference plane of GPS antennas should be clear. Practically, some compromise must be made. Typically, obstructions

and multipath are temporary effects because the GPS satellite positions and the platform attitude are changing. One of the benefits of having an oversolution in GPS observables is that an anomalous observable from one satellite, due to masking or multipath, can be detected and rejected before measurement incorporation. There might be some locations on the spacecraft where it is important to monitor deflections continuously, so even temporary signal masking or multipath effects might prevent the use of GPS in this case.

It is important that the carrier doppler phase measurements at the multiple antennas be either simultaneous or multiplexed in a manner which, in effect, provides simultaneous measurements. Otherwise, time skew in the measurements will introduce excessive differential error because the carrier doppler phase is changing so rapidly.

It is advantageous to use a receiver which tracks L1 and L2 simultaneously. This not only provides a continuous absolute measure of the ionospheric delay from the differential range measurements obtained from the dual-code tracking loops, but, also, the dual-carrier doppler phase measurements provide an ultra-precise, continuous time rate of change in the ionospheric delay. The time rate of change of the ionospheric delay is quite well behaved and slow changing, so it provides the only reliable method of determining and correcting carrier cycle slips in real time. By monitoring this L1/L2 differential measurement for sudden step changes, cycle slips can be detected and corrected because the size of a carrier cycle slip is large in comparison to the change in the ionosphere during the measurement observation interval. The size of the step is a measure of which frequency slipped, how many cycles slipped, and which way it slipped. Another advantage of tracking L1 and L2 is that it is easier to resolve the carrier phase wavelength amiguity using both frequencies. The correct solution must coincide with an integer wavelength bias for both L1 and L2, and since these have different wavelengths, they will not coincide every cycle. This greatly reduces the number of acceptable candidates.

2.3 TASK 3. TIME BASE

GPS time is maintained by the GPS Control Segment (CS) with cesium clocks at the Master Control Station. This is not the same as U.S. Naval Observatory time (Universal Coordinated Time/UTC), which periodically requires the addition of leap seconds. GPS time is continuous, starting from midnight Saturday January 5, 1980. The difference between these times is known, and a GPS receiver can put out data in UTC; however, the natural time reference for a GPS receiver is GPS time. This is the time base normally transferred from the GPS receiver, unless otherwise specified by the user.

Before the GPS receiver can provide accurate GPS time, two biases must be corrected: the bias between the satellite clock and GPS time and the bias between the receiver clock and GPS time.

In each satellite, timing is provided by atomic clocks. The offset between GPS time and the satellite time is monitored by the Control Segment. Corrections for this offset are uploaded to the satellites and then broadcast in the navigation message. The GPS receiver decodes the navigation message and reads the clock correction parameters: a_0, a_1, and a_2. The a_0 term defines the offset of the satellite P-code end-of-week epoch from the GPS time Saturday midnight at the Greenwich Meridian. This epoch occurs when the pseudorandom noise (PRN) sequence, which identifies each satellite, starts over each seven days. The identical PRN

sequence then repeats for another seven days. Ideally, each satellite would have its end-of-week rollover coincide with the beginning of the GPS week. In practice, there is an offset between these two and the a_0 term defines this offset. The a_1 term defines the time rate of change of the bias offset (the time bias rate) and the a_2 term defines the next higher rate term. Another way to view the a_1 term from each satellite is as a measure of the offset of the satellite's reference oscillator frequency (which is driving the satellite's PRN code generator) from the GPS time oscillator frequency standard. Each raw pseudorange transmit time must be corrected to GPS time using these correction terms. Likewise, each raw carrier doppler phase measurement must be corrected (using the a_1 term) for the artificial doppler frequency created on the carrier because the local oscillator frequency on the satellite is not exactly at the specified carrier frequency.

After these corrections have been applied to the GPS observables and the measurements incorporated into the navigation state, the natural by-product of the navigation solution is precise time. The GPS navigation process must solve for the time bias and the time bias rate (oscillator frequency offset) between receiver time and GPS time in order to solve for the navigation position and velocity states. Note that bias errors common to all measurements, such as uncalibrated receiver delay paths, will be considered as part of the time bias, so these should be removed by a built-in calibration procedure. Solving for time requires tracking at least four satellites. Once the navigation solution has converged, the receiver maintains precise GPS time and is equivalent to a precise frequency standard.

The time bias and time bias rate are tracked with essentially the same precision as the position and velocity solution. For example, if the absolute position solution is maintained to within 10 meters, the GPS time bias is known within about 30 nanoseconds. This is based on a simple rule of thumb that 1-meter position uncertainty corresponds approximately to a time uncertainty of 3 nanoseconds. The GPS propagation velocity constant is defined to be exactly 0.299792458 meter per nanosecond. Similarly, if the absolute velocity is known to within 0.1 meter per second, the local oscillator frequency uncertainty is known within about 3 Hz in 10^{10} Hz or 3 parts in 10^{10}. This is based on a rule of thumb that 1 meter per second velocity uncertainty corresponds approximately to a receiver frequency uncertainty of 3 Hz in 10^9 Hz. The same rules of thumb also hold for GPS relative navigation. When the relative navigation accuracy performance is improved by the advanced relative navigation techniques developed during this simulations study, so does the relative time accuracy improve. It must also be remembered that there are some relative navigation techniques which result in a reduction of accuracy with the obvious consequence that the relative time accuracy deteriorates proportionally.

GPS receivers do not change the phase of their reference clocks to align with GPS time; they only report the offset and the rate of change of the offset with respect to GPS time. To transfer time, a communication link must be established. A clock pulse in the form of a periodic fast rise time signal derived from the receiver's clock is sent out, along with a message describing the GPS time associated with each pulse and the time bias of the receiver clock. The GPS time which is associated with each pulse is an estimated time which is usually maintained as an integer value whose least significant bit corresponds to the period of the clock pulse. For example, if the period is 1 second, then the estimated GPS time is maintained as integer multiples of 1 second. TI has used both 1 second and 20 milliseconds as the period for the time transfer

clock epochs. Figure 2–2 shows GPS time and the receiver time. By adding the estimated time of the receiver pulse and the receiver's time bias, the GPS time of the pulse is calculated. This time will be accurate to a few nanoseconds.

Now that the concept and expected precision of the GPS time base are understood, spacecraft applications will be discussed. Obviously, GPS time and frequency can be transferred from the receiver to other systems onboard the same spacecraft. If the primary navigation system for the spacecraft is GPS, the primary frequency and time standard should also be derived from GPS. Typically, the GPS receiver's time transfer clock epochs will not be the frequency or phase desired by the other systems. but there are numerous hardware design techniques which can be used to phase and frequency shift the GPS receiver's clock epochs to the desired phase and frequency.

If, to use the GPS receiver as the frequency standard, long-term frequency stability is required, then an atomic frequency standard should be used with the receiver. A tracking GPS receiver does not in any way improve the long-term frequency stability of its local oscillator; it only calculates the frequency deviation from its specified frequency. An atomic frequency standard cannot transfer "time" to the GPS receiver, as is often mistakenly assumed. It is like a clock with very precise ticks, but with no numbers on it. It only stabilizes the long-term frequency drift of the GPS receiver's oscillator. The combination of the atomic frequency standard and a GPS receiver results in an atomic clock which provides a world-wide time reference with long-term frequency stability. If the receiver loses lock on some of the satellites, it still can maintain accurate time for quite a while by relying on the atomic frequency standard.

Another spacecraft application of the GPS time base is the coordination of time-division multiplexed transmissions from numerous spacecraft using the same frequency band and the same transmission technique. The GPS time base prevents multiple transmissions at the same time. The only requirement is that all these spacecraft have a GPS receiver with the appropriate time transfer interface and transmitters with the appropriate time synchronization interface to the GPS receiver. Each spacecraft is assigned an absolute GPS time slot with a guard band that protects against transmission overlap. This guard band must allow for the least precise segment of the time transfer process. A few tenths of a microsecond is a reasonable length of time, which

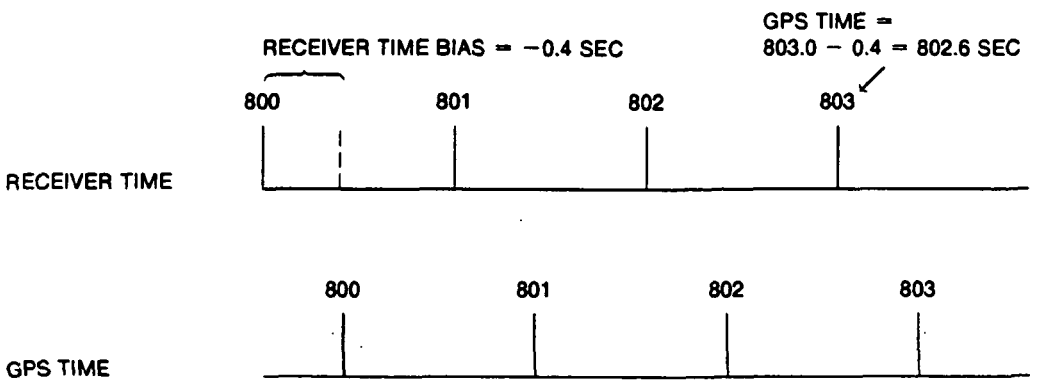

Figure 2-2. Example of GPS and Receiver Time

would not impose severe GPS navigation accuracy or time transfer requirements on any spacecraft. For applications such as this, phase as well as frequency management needs to be applied to the GPS time transfer.

Each time a GPS receiver oscillator is powered down and then powered back up again, the phase of its clock epochs changes with respect to GPS time. A multiplicity of unsynchronized GPS receivers will have different time biases (different clock phases). To coordinate external systems with GPS time, these biases must be removed by phase shifting the reference clock sent by the GPS receiver. The most simple way to implement this would be to shift the phase to coincide with the corresponding GPS time epoch; i.e., if the reference clock is 1 Hz, shift this phase to coincide with the GPS 1-second time epochs. This phase alignment requirement could be accomplished in the GPS receiver. One way to implement this is for the receiver to maintain a time skew counter. To maintain time with an accuracy of 1 second, the least significant bit of the counter would represent seconds. For higher accuracy, the number must be scaled accordingly. When the counter is activated by the receiver's time transfer clock pulse, it begins decrementing until the counter goes to zero and then it sends out the time information over the communication link. The resulting time transfer epoch would be phase coincident with the corresponding time bias estimate and one-half of the reference oscillator period (less than 50 nanoseconds at 10.23 MHz). Rise time, propagation delay time between interfaces, etc., must also be accounted for, but the phase management can be quite accurate with relatively simple circuitry.

Another approach to the GPS receiver clock phase management would be for the navigation processor to provide closed-loop phase and frequency control to its own reference oscillator, driving it by voltage control to maintain phase and frequency alignment with GPS time. This involves significant design analysis complexity since a closed-loop approach to the problem effects the stability of everything in the GPS receiver frequency plan, including the navigation solution itself. This technique could potentially produce the highest precision GPS time phase alignment and time transfer, but unless the application demands this type of specialized design, this approach should be avoided. The skew counter technique is considerably less complex and does not introduce any receiver stability problems.

An important spacecraft application of the GPS time base is the coordination of GPS measurements for precision differential techniques. Differential techniques, such as relative navigation, attitude measurement, and precision navigation relative to an earth-based reference station, all require differencing GPS measurements taken from two locations. Before these measurements can be differenced, they must be aligned in time. The usual technique employed is to propagate the earlier measurement forward to match the time tag of the other measurements. This requires that the measurements include a rate term or that a crude rate term be developed based on differentiating the time sequence of measurements. Both these techniques introduce noise into the measurements and impose additional computational loads and delays on the relative navigation process. When simulations are performed, time skew in the measurements usually is not modeled, so the effects of time skew management are not observed and the performance impact not well understood.

It would seem natural that GPS receiver measurements would be synchronized to occur at the same GPS time, since each receiver has a precise knowledge of absolute GPS time. However, most GPS receiver designs implement the receiver measurement process under the phase

control of the receiver's local oscillator and seldom do any two different GPS receivers provide raw measurements at the same rate. TI has pioneered the advanced concept of synchronized GPS observables in the TI 4100, which was designed for precision differential operation. When it is operating in the low dynamic geodetic modes, the measurements are sychronized to GPS time. Initially, the raw GPS observables are scheduled with zero bias with respect to the TI 4100 clock. After the navigation solution converges, and the time bias is learned, the navigation process begins requesting that the measurements be taken on a schedule that is biased with respect to the TI 4100 clock such that they occur on exact GPS time epochs. In this manner, all TI 4100s in the world which are operating in the geodetic modes (after the navigation solution has converged) are producing GPS observables at the same GPS time without the need for an external synchronizing signal (other than GPS time which the sets derive from the space segment of GPS).

For almost any GPS application, continuously counted integrated doppler measurements every 0.1 second and pseudorange measurements every 1 second, both synchronized to coincide with GPS time epochs, would be an acceptable GPS observable rate. These rates are probably an overkill for most spacecraft differential applications. Since the resulting data rate is not excessively high and could be used for other GPS applications, these rates could be considered as a candidate for standardization of the GPS raw data rate for spacecraft.

In the real world implementation of time-tagged data transfer systems, time skew misunderstandings are probably the number one source of field data processing problems and, in some cases, never are resolved correctly because all the sources of time skew never are determined fully. The predicted precision can be lost by lack of receiver common bias stability or lack of common bias calibration or by the time transfer mechanization.

2.4 TASK 4. TRAFFIC CONTROL

GPS can be used in many ways to provide traffic control. Two interesting alternatives are differential GPS and bent pipe GPS.

2.4.1 Subtask A. GPS Relative Navigation

The classic definition of differential GPS assumes that one stationary reference GPS receiver is used, operating at a known location. Differential corrections are calculated, either from the difference between the individual pseudoranges and the true ranges, or from the difference between the measured position and the true position. These differential corrections can be transmitted to other users in the area and applied in their navigation state solution, making it much more accurate. The increased accuracy comes from the cancellation of bias errors common to both receivers, which are a major component of the total error. Therefore, differential GPS is a cost-effective, straightforward method to significantly improve GPS accuracy.

When operating in space, there is no known location which can serve as a reference. However, there are several techniques which will cancel most bias errors, giving a relative position that has the same level of accuracy as the absolute accuracy of the differential GPS method. For traffic control in space, relative accuracy is the main concern. We will use the term relative navigation to refer to techniques that solve for relative position but do not have a known location reference. Two methods of GPS relative navigation have been investigated in this study: position difference and range difference.

2.4.1.1 Position Difference (Navigation State Vector Difference). In the position difference technique, both receivers solve for their absolute position as in independent navigation. The absolute position solutions (navigation state vectors) then are differenced to get relative position. To ensure that maximum error cancellation occurs, it is important that both receivers track the same satellites.

Many error sources are SV-dependent, such as ephemeris error, SV clock error, and ionospheric error (path-dependent). If different SVs are being used, these errors can add instead of cancel. It is possible to get a relative error which is worse than the absolute error. A mathematical analysis was done to show why this is the case. This analysis is discussed in Section 3. When the same SVs are tracked, the relative navigation error can be four times smaller than the absolute navigation error. If both receivers use identical navigation filters, the accuracy is further improved.

2.4.1.2 Range Difference (Pseudorange Difference). In the range difference technique, the pseudoranges of the reference and remote receivers are differenced, and the solution is the relative position, instead of the absolute position. The measurement can be a single difference or a double difference. A single difference is formed by subtracting the pseudorange of one receiver from the pseudorange for the same SV measured by the other receiver. This eliminates common errors, which include SV clock errors and correlated ionospheric and ephemeris errors. The closer the receivers are to each other, the more these errors will correlate. Beser and Parkinson* quantify this correlation as a function of the receiver separation. For two receivers 35 km apart, after differencing the pseudorange, the residual effect of an ephemeris error of 30 M will be only 5 cm.

The double difference measurement is made by subtracting the first difference for one SV from the first difference of another SV:

$$PR_{DD} = (PR_{Ai} - PR_{Bi}) - (PR_{Aj} - PR_{Bj})$$

In addition to the satellite-dependent errors which cancel in the single difference, this measurement will cancel the receiver clock errors and common receiver channel delays. Receiver interchannel biases will not be removed, but must be minimized by receiver design. As in position difference relative navigation, this error cancellation significantly improves the relative navigation accuracy.

If the single difference is used, the receiver clock errors will fall into the time error term of the solution. Using double differences is a very clean way to simply cancel all common receiver errors before transferring data to the processing station. Note an equivalent form of the double difference measurement is to first subtract the pseudoranges to two SVs as measured by each receiver:

$$PR_{DD} = (PR_{Ai} - PR_{Aj}) - (PR_{Bi} - PR_{Bj})$$

*Beser, J. and B.W. Parkinson, "The Application of NAVSTAR Differential GPS in the Civilian Community," *Global Positioning System: Volume 2.* Institute of Navigation, 1984, 167–196.

Three double differences are formed by using the satellite pairs SV1 and SV2, SV2 and SV3, and SV3 and SV4. The clock term drops out when the differences are formed and the three position components are the solution.

2.4.1.3 Aspects of C/A-Code Operation. The simulations for this study were for P-code operation; however, with a variety of space applications, C/A-code receivers may be used. C/A receivers have many advantages, including smaller size, lighter weight, lower power requirements, slower clock, and smaller bandwidths. The C/A-code performance in tests of the TI420 receiver meets and, in some cases, exceeds the P-code performance. There are several issues to consider in the use of C/A receivers; none are major problems, but the user should be aware of them.

1. Increased signal strength
2. Ionospheric correction without L2
3. Need to track the same SV set
4. Combinations of C/A- and P-code receivers.

- **Increased Signal Strength**

The C/A-code signal is twice as strong as the L1 P-code signal (3 dB) and four times stronger than L2 P-code (6 dB). This means that the 1-sigma noise level is the square root of two less than for L1 P-code. However, because the C/A chip is 10 times longer than the P-code chip, the thermal noise is 10 times higher; therefore, the tracking resolution is not as good. The combination of these effects makes the C/A tracking error $10/\sqrt{2}$ or 7.07 times the L1 P-code tracking error.

- **Ionospheric Correction Without the L2 Signal**

C/A code normally is modulated only on the L1 signal; therefore, the two-frequency ionospheric correction cannot be made. There are parameters for an ionospheric model which are broadcast in the ephemeris. This model has an RSS global error of 50 percent and tends to do better when there is more ionospheric disturbance. That is, the model is biased toward worst case conditions.

For high-altitude applications such as the Space Station, some satellite signal paths would have much less ionosphere to traverse; however, it is also possible to have paths that traverse the ionosphere twice. Satellite selection procedures may need to make adjustments for this.

- **Need to Track the Same SV Set for Relative Navigation**

As the mathematical analysis showed, the most efficient relative navigation requires that both receivers track the same SV set. When they do, the SV clock error and ephemeris error will cancel. This is true for both P-code and C/A-code operation.

- **Combinations of C/A-Code and P-Code Receivers**

There are a couple of error sources found when combining C/A-code data and P-code data which cancel if all data is C/A-code or all is P-code. The first is the "group delay" which results from the satellite's slight delay in broadcasting the L2 signal. This means that the L1 and L2

signals are not sent at precisely the same time, and this will appear to the receiver as an ionospheric error. This delay depends on the hardware path for the signal generation and is measured by the satellite manufacturer before the SV is put into orbit. This measurement is made for only one of the redundant circuits and, if another circuit is switched on, the measurement will be inaccurate. The manufacturer's value is broadcast in the SV navigation message as the TGD term. The error between the actual delay and the TGD term becomes incorporated in the SV clock error by the control segment tracking process. In absolute position navigation, this term is applied and the error drops out and causes no error in the navigation solution. Likewise, in relative navigation with two P-code receivers or two C/A-code receivers, the error drops out. However, when mixing C/A- and P-code, this error will show up. The actual delay can be measured by the reference receiver, if it tracks both C/A- and P-code. This error is about 1 meter.

Another error source is from signal coherence. This means that the C/A-code is not broadcast at precisely the same time as the P-code, resulting in a 1-sigma error of about 5 feet, random across different SVs.

2.4.2 Subtask B. Bent Pipe

The bent pipe technique (often called translator technique) involves the use of a frequency translator in the slave vehicle and a special GPS receiver at the master station which tracks the GPS signals at the translated frequency. In bent pipe applications, the slave vehicle has no need for onboard GPS navigation. Translating the GPS C/A-code to a ground-based tracking system has been used successfully in testing Trident missiles as a range instrumentation system. The GPS signals are received at the slave vehicle antenna, frequency-shifted to a new frequency, then retransmitted from another antenna on the slave vehicle to the master station. The master station receives and tracks the retransmitted signal. The signal also is recorded on a wideband recorder so that it can be post-mission processed, if necessary. The received signal at the master station contains added range and doppler shifts owing to the relative motion of the slave vehicle, but these are common shifts to all the GPS signals and can be removed as common bias terms by the navigation process. Typically, a clock signal is added to the signal by the slave vehicle to provide a reference measure for the common doppler shift, but this is a convenience, not a necessity. The GPS signals are not detected or used onboard the slave vehicle. (The Trident uses an inertial navigation system that does not need GPS for its operation.) Using the C/A-code requires a 2-MHz bandwidth frequency translator and transmitter. The P(Y)-code signals would require 20-MHz bandwidth. To date, there has not been a P(Y)-code version of the bent pipe technique demonstrated, nor is this likely, owing to the added complexity and power of the translator/transmitter design.

A unique C/A-code receiver designed to track the translated GPS signals is required at the master station. A conventional C/A-code receiver also is used to track the same GPS signals at the master station to perform differential navigation to improve tracking accuracy.

The bent pipe technique saves cost in the expendable slave vehicle instrumentation by substituting the translator for the GPS receiver and navigation/interface processor. A telemetry link would be required in either case, but it could be argued that the dedicated specialized and wideband telemetry link used by the bent pipe translator is more expensive than sharing an

existing conventional data link by the low-rate GPS data if this were detected onboard in the form of raw observables and navigation data. For range instrumentation applications where expendable slave vehicles need to be tracked with GPS but do not need onboard GPS navigation (such as the Trident missile testing), the bent pipe technique should be considered. There is presently no known spacecraft application where the bent pipe technique would be applicable.

SECTION 3
ANALYTICAL BASIS FOR STUDY AND SIMULATIONS

3.1 GPS ATTITUDE MEASUREMENT ANALYSIS

3.1.1 Introduction

Using signals from quasars in very-long baseline interferometry experiments to study minute changes in the length and orientation of a baseline on the surface of the earth has been practiced by geodetic astronomers for some time. In recent years, interferometric methods based on signals originating from global-positioning system (GPS) satellites have been used to determine the length of a baseline very accurately. Observations central to these experiments are measurements of the carrier phase of the GPS signals. With advanced digital receivers and associated software, the accuracy of phase measurements to within a few degrees has been achievable. With this attainable accuracy, one can determine the orientation of a baseline. The purpose of this study has been to formulate the problem of attitude determination in terms of single phase differences, identify key parameters which affect the determination of attitude, and simulate the attitude determination process for a system which is moving in space as well as changing its orientation.

3.1.2 Carrier Phase Inteferometry

GPS interferometry techniques have been used extensively in precision geodetic applications. The principle of GPS interferometry is the measurement of carrier doppler phase differences between various antenna phase centers for a signal originating from a given GPS satellite whose position is known. For the GPS receiver to be useful in an interferometric experiment, the carrier phase must be measured with respect to a local oscillator time reference using the digital frequency synthesis method. Using digital GPS receiver tracking loops to measure the carrier doppler phase, a phase difference measurement can be made using two independent phase measurements from two carrier tracking loops. If the measurements are simultaneous and refer to the same local oscillator, the phase noise of the local oscillator is correlated and cancels out in the difference measurements. The cancellation of common mode noise is the primary reason for using differencing techniques. All errors common to each space vehicle (SV) signal are removed by the action of differencing the phase measurements from that SV between two different antenna phase centers. These errors include all SV clock prediction errors and short-term oscillator noise, all SV ephemeris radial prediction errors, and, for closely spaced antenna phase centers, most of the highly correlated ionospheric errors. Errors common to all SVs tracked by a single receiver are removed by the action of differencing that receiver's phase measurements from two different satellites. These errors include all receiver clock short- and long-term errors, all receiver common electrical path bias errors, and any other receiver errors common across all SVs tracked. Thus, single phase differencing measurements involve one SV and two antenna phase centers, whereas double phase difference measurements involve two SVs and two antenna phase centers separated by a baseline whose length and orientation is to be determined. If the multiplexing antenna approach is used, as described in Subsection 2.2.1, then multiple antennas will be connected to the same receiver. In this case, single differences are sufficient.

3.1.3 Geometrical Description, Single and Double Path Differences

The geometrical model used to determine the attitude of a rigid body using GPS observables is described as follows. In Figure 3–1, A and B denote the antenna phase centers, and C denotes the midpoint of the baseline vector $\vec{R}_{AB}$ assumed to be known. It is the orientation of the vector $\vec{R}_{AB}$ that is desired. Let 1 and 2 denote the locations of two GPS satellites, SV1 and SV2, respectively. The formulas for the single path difference, $D_1(AB)$, and the double path difference, $D_{12}(AB)$ are:

$$\begin{aligned} D_1(AB) &= \text{Path difference between points A and B for a signal originating from SV 1.} \\ &= \vec{R}_{AB} \cdot \hat{R}_{C1} \end{aligned} \tag{1}$$

$$\begin{aligned} D_2(AB) &= \text{Path difference between points A and B for a signal originating from SV 2.} \\ &= \vec{R}_{AB} \cdot \hat{R}_{C2} \end{aligned} \tag{2}$$

$$D_{12}(AB) = D_1(AB) - D_2(AB) = \vec{R}_{AB} \cdot (\hat{R}_{C1} - \hat{R}_{C2})$$

where $\vec{R}_{AB}$ is the vector joining points A and B in a certain coordinate system, say earth-centered earth-fixed (ECEF), $\hat{R}_{C1}$ and $\hat{R}_{C2}$ are unit vectors along the lines joining point C to SV 1 and SV 2.

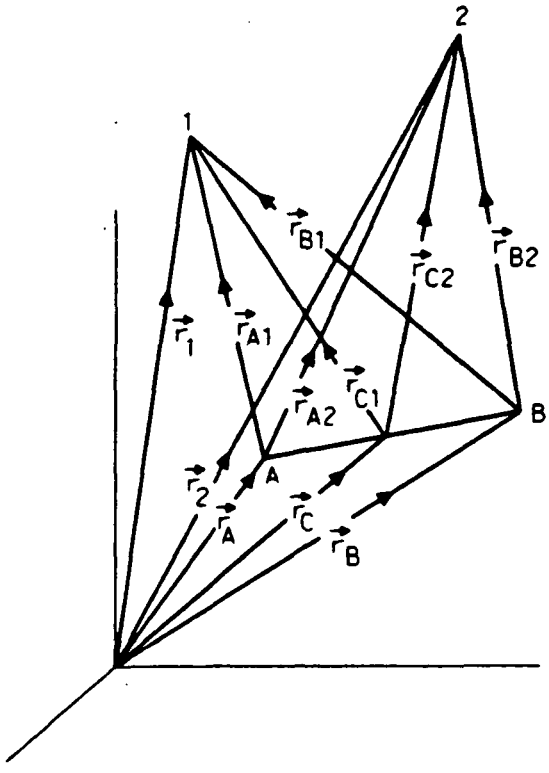

Figure 3-1. Baseline-Satellite Geometry in Three-Dimension

3.1.3.1 Three Antenna Phase Centers and Three SVs, Single Path Difference. In this study, it is assumed that a single GPS receiver with multiplexed GPS antennas is used. Carrier phase difference measurements between phase centers refer to the same receiver clock so it is not necessary to form double difference phase measurements. Phase double differences are useful to eliminate receiver clock errors when carrier phase difference measurements refer to different receiver clocks. If the geometrical model of Subsection 3.1.3 is extended to include three satellites, SV1, SV2 and SV3, then three single path differences can be measured and three equations written as follows:

$$\begin{aligned} \vec{R}_{AB} \cdot \hat{R}_{C1} &= D_1(AB) \\ \vec{R}_{AB} \cdot \hat{R}_{C3} &= D_2(AB) \\ \vec{R}_{AB} \cdot \hat{R}_{C3} &= D_3(AB) \end{aligned} \tag{3}$$

From these three equations in three unknowns, the vector $\vec{R}_{AB}$ can be determined in three dimensions. Vectors $\hat{R}_{C1}$, $\hat{R}_{C2}$, and $\hat{R}_{C3}$ are unit vectors from the midpoint of the baseline to the position of SVs 1, 2, and 3, and are assumed to be known. In the present study, the direction of these unit vectors was taken to be the same as the unit vector from the navigation center to the SVs. This introduces negligible error because the distance to the SVs from the baseline is very long compared to the baselines. It should be noticed that, if there are four or more satellites visible at a given time, many combinations of SV triplets can be made (four combinations for four visible SVs). The baseline can be computed for each choice and averaged, which might improve the definition of the baseline. It is not difficult to see that if there is another antenna phase center at another point, D, then using a similar formula, we can determine the baseline $\vec{R}_{AD}$. The points A, B, and D define a plane if they are not colinear. The two vectors, $\vec{R}_{AB}$ and $\vec{R}_{AD}$, determined from the single path difference measurements will define the attitude of the plane ABD. Methods of expressing attitude of the body which contain the baselines will be discussed in Subsections 3.1.4.1 and 3.1.4.2.

3.1.4 Body-Fixed Coordinate System, ECEF Coordinate System, and the Attitude Matrix

If one has two independent unit vectors ($\vec{u}$ and $\vec{v}$) in three dimensions, then it is possible to construct an orthogonal triad from them as follows.

$$\begin{aligned} \vec{q} &= \vec{u} \\ \vec{r} &= \frac{\vec{u} \times \vec{v}}{|\vec{u} \times \vec{v}|} \\ \vec{s} &= \vec{q} \times \vec{r} \end{aligned} \tag{4}$$

where $\vec{q}$, $\vec{r}$, and $\vec{s}$ constitute an orthogonal triad.

Vectors $\vec{q}$, $\vec{r}$, and $\vec{s}$ are an orthogonal triad in the body-fixed reference frame and $\vec{q}'$, $\vec{r}'$, and $\vec{s}'$ are the same orthogonal triad in the ECEF reference frame. Let matrix M be constructed out of vectors $\vec{q}$, $\vec{r}$, and $\vec{s}$. That is:

$$\begin{aligned} [M] &= [\vec{q}\,|\vec{r}|\,\vec{s}] \text{ and,} \\ [M'] &= [\vec{q}'\,|\vec{r}'|\,\vec{s}'] \end{aligned} \tag{5}$$

The equation relating the ECEF coordinate system to the body-fixed coordinate system can be derived considering two coordinate systems transformations.

3.1.4.1 ECEF to Local Level (North, East, Down) Coordinate Transformation. Let $\vec{X}_L$ denote the position vector of an arbitrary point in the local level coordinate system (north, east, down). Also, let $\vec{X}_{ECEF}$ denote the position vector of the same point in the ECEF coordinate system and $(\vec{X}_o)_{ECEF}$ be the origin of the local level coordinate system also expressed in ECEF reference frame.

Then

$$\vec{X}_L = [U]\,[\vec{X}_{ECEF} - (\vec{X}_o)_{ECEF}]$$

or written in matrix notation

$$\begin{bmatrix} N \\ E \\ D \end{bmatrix} = [U] \left\{ \begin{bmatrix} X \\ Y \\ Z \end{bmatrix}_{ECEF} - \begin{bmatrix} X_o \\ Y_o \\ Z_o \end{bmatrix}_{ECEF} \right\} \tag{6}$$

where

$$[U] = \begin{bmatrix} -\sin\lambda\cos\ell & -\sin\lambda\sin\ell & \cos\lambda \\ -\sin\ell & \cos\ell & 0 \\ -\cos\lambda\cos\ell & -\cos\lambda\sin\ell & -\sin\lambda \end{bmatrix} \tag{7}$$

where λ, ℓ are geodetic latitude and longitude of the origin of the local level coordinate system, respectively.

3.1.4.2 Local Level to Body-Fixed Coordinate System Transformation. If $\vec{X}_B$ denotes the position vector of a point in the body-fixed coordinate system and $\vec{X}_L$ is the position vector of the same point in the local level coordinate system, then:

$$\vec{X}_B = [T]\,\vec{X}_L$$

Written in matrix notation:

$$\begin{bmatrix} X \\ Y \\ Z \end{bmatrix}_B = [T] \begin{bmatrix} N \\ E \\ D \end{bmatrix} \tag{8}$$

where

$$[T] = \begin{bmatrix} \cos\psi\cos\theta & \sin\psi\cos\theta & -\sin\theta \\ \cos\psi\sin\theta\sin\phi - \sin\psi\cos\phi & \sin\psi\sin\theta\sin\phi + \cos\psi\cos\phi & \cos\theta\sin\phi \\ \cos\psi\sin\theta\cos\phi + \sin\psi\sin\phi & \sin\psi\sin\theta\cos\phi - \cos\psi\sin\phi & \cos\theta\cos\phi \end{bmatrix} \tag{9}$$

The attitude angles have been defined as:

Heading angle with respect to north, ψ

Pitch angle with respect to vertical, θ

Roll angle with respect to pitch plane, ϕ.

Using equations 5, 6, and 8, one can express the attitude matrix, T, as:

$$[T] = [M]\,[\,[U]\,[M']]^T \tag{10}$$

Matrix [M] is known because it has been constructed from two known, noncolinear vectors (antenna baselines) in body reference frame [see Equation (5)]. The matrix [U], which is constructed from the geodetic latitude and longitude of the navigation center, is assumed known.

The matrix [M'] is constructed out of antenna baseline vectors in ECEF coordinate system obtained by solving Equation (3). Thus, the elements of matrix [T] can be computed using Equation (10). The attitude angles (heading, pitch, and roll) can be expressed in terms of the matrix elements of matrix [T].

$$\text{Heading angle: } \psi = \tan^{-1}[T_{12}/T_{11}]$$

$$\text{Pitch angle: } \theta = \sin^{-1}[T_{13}] \tag{11}$$

$$\text{Roll angle: } \phi = \tan^{-1}[T_{23}/T_{33}]$$

This completes the discussion on derivation of attitude angles.

3.2 GPS RELATIVE NAVIGATION ANALYSIS

3.2.1 Study Approach

The GPS relative navigation study involved both theoretical analysis and simulation of specific cases. The theoretical segment included a mathematical analysis of the position-difference relative navigation technique to show how the error cancellation takes place, why the same SV set is advantageous, and to provide equations to calculate GPS relative navigation accuracy, given accuracy statistics for a GPS receiver's absolute position and pseudorange measurements. This analysis did not assume a certain receiver type or position solution technique. Also included in the theoretical segment was a formulation of achievable accuracies, based on the system specifications error budget for GPS, SS–GPS–300C. Again, no assumptions are made about receiver types, nor is any reference made to real or simulated data statistics. This gives a theoretical upper bound on GPS relative navigation accuracy.

The GPS relative navigation study involved simulations of both the position-difference and range-difference techniques. Position-difference cases were run, assuming that both receivers were tracking the same four SVs, assuming they were tracking all different SVs, and assuming that some SVs were different. Range difference simulations were run with double-difference

pseudoranges. All simulations assumed that the users were in a Space Station orbit (500 km, 270 nmi) and were 30 meters to 35 kilometers apart (100 feet to 20 nmi). The simulator environment, runs, and results are discussed in detail in Subsection 4.2.

3.2.2 Mathematical Analysis of Relative Navigation Error Position Difference Technique

The goal of this analysis was to derive an expression for the error variance of the relative position and to evaluate this using various satellite set assumptions. The analysis shows which errors cancel when the receivers are both tracking the same four SVs and what happens when different SVs are introduced.

The approach was to first determine a linear relationship between range error and position error. Based on this relationship, the variance of the relative position error was computed. The variance for the absolute error also was computed for comparison purposes. The best relative position solution is the one which minimizes the relative position error variance. Finally, equations were derived for the root-sum-square (RSS) of the standard deviations of the X,Y,Z components of the relative position error $\sigma(\epsilon P_A - \epsilon P_B)$. These may be evaluated for any measurement statistics to see what the relative navigation error will be.

When the receivers are tracking completely different SVs, the equation is $\sqrt{2}$ times the absolute position error.

$$\sigma(\epsilon P_A - \epsilon P_B) = \sqrt{2}\,\sigma(\epsilon R)\,\mathrm{PDOP}$$

where $\sigma(\epsilon R)$ is the standard deviation of the range error. The $\sqrt{2}$ comes from the assumption that both receivers have the same error statistics. If this is not the case, take the RSS of the individual absolute position errors. The range error includes the error in the pseudorange measurement from multipath, thermal noise, and the ionosphere; the satellite clock error; and the satellite ephemeris error. In equation form, this is:

$$\epsilon R = \epsilon PR + \epsilon t + \epsilon E$$

where

- ϵPR is the error in pseudorange from multipath, thermal noise, and ionosphere
- ϵt is the SV clock error
- ϵE is the mapping of the cross-track and along-track SV ephemeris error into relative position error.

When both receivers are tracking the same four SVs, the satellite clock error and ephemeris error components cancel, and the resultant equation depends only on the error of the pseudorange measurement from multipath, thermal noise, and the ionosphere. The best relative position will result from using all the same SVs:

$$\sigma(\epsilon P_A - \epsilon P_B) = \sqrt{2}\,\sigma(\epsilon PR)\,\mathrm{PDOP}$$

In a typical example with $\sigma(\epsilon R) = 6$ meters, $\sigma(\epsilon PR) = 1$ meter, and PDOP = 3:

using the same SVs	$\sigma(\epsilon P_A - \epsilon P_B) = 4.2$ meters
using completely different SVs	$\sigma(\epsilon P_A - \epsilon P_B) = 25.4$ meters

This example uses numbers typical of P-code operation. In actual differential tests of TI equipment at the Yuma Proving Ground, the errors were 4 to 5 meters, which corresponds with the "same SVs" calculation. Note that these same formulas can be applied with C/A-code statistics.

Forming a quality improvement ratio of the relative position (different SVs) divided by the relative position (same SVs):

$$Q_R = \frac{\sqrt{2}\,\sigma(\epsilon R)\,\text{PDOP}}{\sqrt{2}\,\sigma(\epsilon PR)\,\text{PDOP}} = \frac{\sigma(\epsilon R)}{\sigma(\epsilon PR)}$$

This ratio shows that both spacecraft GPS receivers using the same SVs can make the relative position errors approximately an order of magnitude smaller than using different SVs.

Forming a quality improvement ratio of the absolute position error to the relative position error (same SVs):

$$Q_A = \frac{\sigma(\epsilon R)\,\text{PDOP}}{\sqrt{2}\,\sigma(\epsilon PR)\,\text{PDOP}} = \frac{\sigma(\epsilon R)}{\sqrt{2}\,\sigma(\epsilon PR)}$$

This ratio shows that when both spacecraft GPS receivers use the same SVs, the relative navigation error will be approximately four times smaller than the individual absolute position error.

For the cases where some of the SVs are common and some are different, the error will be between these two cases. Simulations were used to show the effects of including different SVs. These plots, shown in Subsection 4.2.2.1, Position-Difference Simulations, demonstrate that a bias in the position solution results from using different SVs. For this particular case, the bias became worse with each additional SV that was not common. In the case with all four SVs different, the bias error was over 15 meters in some of the position components.

The entire mathematical analysis can be found in the appendix to this report.

3.2.3 Upper Bound of GPS Relative Navigation Accuracy Based on SS-GPS-300C (10/27/86)

To identify a GPS relative accuracy definition and be assured that any real data would be within these bounds, the system specification for the GPS user range error budget must be used. This error budget is divided into three segments: space segment errors, control sement errors, and navigation user errors. A user equivalent range error (URE) is given for each segment, and then the total system URE is calculated by taking the root-sum-square of the segments. The URE, when multiplied by the position-dilution-of-precision (PDOP), gives the expected one-sigma position error. The GPS user range error budget from SS–GPS–300C is shown in Table 3–1.

TABLE 3-1. GPS USER RANGE ERROR BUDGET

Source of Error and Responsibility	Error Sources	Error Quantities in Meters (1 σ)
Space	Maximum total segment URE	4.8
Control	Maximum total segment URE	3.6
Navigation user	Maximum total segment URE	3.6
System	Total system URE	7.0

For a PDOP of 3.14, the one-sigma position error would be 21.98 meters. Note that the actual performance of GPS with the current constellation is 10 to 15 meters, much better than this number. The space and control segments have been doing better than the specification, but the specification values must be used to determine expected accuracy limits. This is why these are called "upper bound" accuracies.

Assuming that the space and control segments operate at the specification values, Table 3–2 shows the expected accuracy for the position-difference relative navigation technique (differencing the navigation state vectors). The entries in the table are the RSS of the position accuracies of the individual receivers. PDOP was assumed to be 3.14. Column 1 gives the code type of the two receivers. Various combinations of P(Y)-code and C/A-code are considered, along with the effects of selective availability. Column 2 shows the expected accuracy when both receivers track the same SVs (space and control segment errors cancel). The accuracies are on the 10-meter level, except when selective availability dominates. Column 3 shows the expected accuracy when the receivers track different SVs (cannot assume that space and control segment errors cancel).

TABLE 3-2. EXPECTED ACCURACY OF POSITION DIFFERENCE RELATIVE NAVIGATION (ASSUMES MAXIMUM ERROR SPECIFIED BY SS-GPS-300C DATED 27 OCT 86)

Code Type	RSS Accuracy With Same SVs (Meters)	RSS Accuracy With Different SVs (Meters)
P(Y)-Code and P(Y)-Code	8.9	31.1
P(Y)-Code and C/A both with AS/SA key	9.9	31.2
C/A and C/A both with AS/SA key	10.9	31.4
P(Y)-Code and C/A where C/A without AS/SA key	99.4	101.6
C/A and C/A both without AS/SA key	140.3 10.9*	140.3

*Assumes time synchronization of C/A measurements and identical nav filters to cancel SA time variable bias effect.

The values in column 3, for using different SVs, were calculated using the SS–GPS–300C P-code absolute position URE of 7 meters. TI calculated a comparable C/A absolute position URE of 7.1 meters. This was calculated using the SS–GPS–300C values for the space segment and control segment error components. The navigation user segment error was calculated with:

iono delay = 2.03 M (6.66 feet)
tropo delay = 2.00 M (6.56 feet)
multipath = 1.20 M (3.94 feet)

In addition, the random navigation errors including thermal noise, jitter, quantization noise, and C/N_0 variations, were estimated from a Monte Carlo simulation. This error component was 6.7 meters (21.9 feet), and this was not multiplied by PDOP because geometry does not affect it.

The values in column 2, for position difference relative navigation using the same four SVs, were calculated from the SS–GPS–300C values, taking the space and control segment errors to be zero. These are assumed to cancel completely although differences in navigation filters could leave a small residual error. The navigation user segment residual errors were:

iono and tropo = 0.15 M
multipath = 1.20 M

The total P(Y)-code URE was 2.0 meters and the total C/A-code URE was 2.5 meters.

The P(Y)-code receiver is assumed to have the antisproofing/selective availability (AS/SA) key. If the C/A set has the AS/SA key, then the epsilon and dither error effects are removed and the result is the same as without selective availability. It is a common misconception that C/A-only sets cannot have an AS/SA key, but if the user is authorized, he can use the key with his C/A receivers (provided that they have been designed to accept the key, as TI receivers have). If the C/A receiver does not have the key and accuracy is degraded to 100 meters 2 drms, then this dominates the error. 100 meters 2 drms is a 2-sigma horizontal accuracy number. One-sigma would be 50 meters. Dividing this by a typical horizontal dilution of precision (HDOP), this represents a URE of 31.6 meters. One way to reduce this error is to do relative navigation with two C/A sets, both without the key, whose measurements are synchronized and whose navigation filters are identical. If all of these conditions are met, the SA time variable bias effect will cancel. The absolute position may be considerably off; however, the relative position again will be in the 10-meter range, as shown in column 2, the last entry. The mathematical analysis showed the importance of using the same SVs in position difference relative navigation, and this conclusion can be clearly seen in this table also.

Table 3–3 shows the expected accuracy for the range difference technique. This method guarantees that the same SVs are used, and, therefore, the space and control segment errors cancel.

When the AS/SA key is used in both receivers, the error is in the 10-meter range whether the sets are PY-code or C/A-code. In the last two cases, where at least one of the receivers is not using the AS/SA key, the selective availability effect can be removed by synchronizing measurements and not correcting for SA on either measurement. In this way, when the pseudoranges are subtracted, the SA effect cancels. If the measurements are not synchronized, the time variations will cause the SA effect to be different and cancellation cannot be guaranteed.

TABLE 3-3. EXPECTED ACCURACY OF RANGE DIFFERENCE RELATIVE NAVIGATION (ASSUMES MAXIMUM ERROR SPECIFIED BY SS-GPS-300C DATED 27 OCT 86)

Code Type	RSS Accuracy With Same SVs (Meters)
P(Y)-Code and P(Y)-Code	8.9
P(Y)-Code and C/A both with AS/SA key	9.9
C/A and C/A both with AS/SA key	10.9
P(Y)-Code and C/A where C/A without AS/SA key	99.4 9.9*
C/A and C/A both without AS/SA key	140.3 10.9*

*Assumes time synchronization of all GPS measurements and that effect of SA is not corrected on either measurement.

SECTION 4
SIMULATION RESULTS

4.1 GPS ATTITUDE MEASUREMENT SIMULATION RESULTS

The purpose of the simulation study was to establish the validity of the algorithm for determining the attitude in three dimensions for a moving platform which also is undergoing attitude variation. Since the space shuttle has high attitude dynamics and the Space Station has low dynamics, we chose to simulate our attitude determination algorithms for both cases.

It also was required to examine how accurately the attitude could be measured using GPS in a deterministic fashion, given that there are various sources of error which can corrupt doppler carrier phase measurements. It should be made clear that in the study not *all* error sources were modeled. Those sources of error which can be regarded as gaussian noise were lumped together and made part of a gaussian noise which was added to the carrier phase measurements. The effect of multipath reflection on carrier phase was modeled as described in Subsection 4.1.1.2. From experiments on the ground, it was found that the contribution of multipath errors to carrier phase varied quasi-sinusoidally with a period of 2 to 16 minutes and an amplitude of 2 cm. Clearly, the severity of the problem would depend on the nature of the reflecting surface and physical and electrical characteristics of the antenna. In this study, flat spiral antenna characteristics were modeled. The effect of reflection of signals from large structures in the neighborhood of the antenna is geometry-dependent and has not been considered.

4.1.1 Simulator Environment

4.1.1.1 Truth Data Generation. The simulation study made use of software which was developed within TI for other GPS-related projects. In particular, existing software to generate the user trajectory profile (position, velocity, and acceleration) and the attitude dynamics profile was used. Following is a brief description of this software.

- **SV Constellation**

In this study, the 18-SV constellation (three SVs per plane, six planes) was used to represent GPS SVs. Using the ICD–GPS–200 algorithm with second-order terms neglected, SV position and velocity could be computed at any time in the GPS week. A set of formulas for the position of SVs in the ECEF coordinate system is given below.

$\mu = 3.986008 \times 10^{14} \frac{\text{meters}^3}{\text{sec}^2}$ — WGS 72 value of the earth's universal gravitational parameter

$\dot{\Omega}_0 = 7.292115147 \times 10^{-5} \frac{\text{rad}}{\text{sec}}$ — WGS 72 value of the earth's rotation rate

$A = \sqrt{A^2}$ — Semi-major axis

$n_0 = \sqrt{\frac{\mu}{A^3}}$ — Computed mean motion (radians/second)

$t_k = t - t_{oe}$	Time from ephemeris reference epoch
$n = n_o + \Delta n$	Corrected mean motion
$M_k = M_o + nt_k$	Mean anomaly
$M_k = E_k - e \sin E_k$	Kepler's equation for eccentric anomaly (may be solved by iteration)—radians
$v_k = \tan^{-1}\left[\frac{\sin v_k}{\cos v_k}\right] = \tan^{-1}\left[\frac{\sqrt{1-e^2}\sin E_k / (1 - e\cos E_k)}{(\cos E_k - e)/(1 - e\cos E_k)}\right]$	True anomaly
$E_k = \cos^{-1}\left[\frac{e + \cos v_k}{1 + e\cos v_k}\right]$	Eccentric anomaly
$\Phi_k = v_k + \omega$	Argument of latitude
$\delta u_k = C_{us} \sin 2\Phi_k + C_{uc} \cos 2\Phi_k$	Argument of latitude correction
$\delta r_k = C_{rc} \cos 2\Phi_k + C_{rs} \sin 2\Phi_k$	Radius correction } Second harmonic perturbations
$\delta i_k = C_{ic} \cos 2\Phi_k + C_{is} \sin 2\Phi_k$	Correction to inclination } Second harmonic perturbations
$u_k = \Phi_k + \delta u_k$	Corrected argument of latitude
$r_k = A(1 - e\cos E_k) + \delta r_k$	Corrected radius
$i_k = i_o + \delta i_k + (\text{IDOT})\, t_k$	Corrected inclination
$x'_k = r_k \cos u_k$ $y'_k = r_k \sin u_k$	Positions in orbital plane
$\Omega_k = \Omega_o + (\dot{\Omega} - \dot{\Omega}_e) t_k - \dot{\Omega}_e t_{oe}$	Corrected longitude of ascending node
$x_k = x'_k \cos \Omega_k - y'_k \cos i_k \sin \Omega_k$ $y_k = x'_k \sin \Omega_k - y'_k \cos i_k \cos \Omega_k$ $z_k = y'_k \sin i_k$	Earth-fixed coordinates

- **User Trajectory Generation**

We also have used ICD–GPS–200 algorithms to generate trajectories, both for the space station and the space shuttle. The orbits were taken to be circular with a radius of 6878135 meters. The inclination of the orbits were taken to be 28.5 degrees.

- **Attitude Dynamics of the User**

In this study, the orbital dynamics of the host vehicle were not coupled to its attitude dynamics. Heading, pitch, and roll of the host vehicles could be allowed to vary independent of each other. The attitude variations, in this study, were taken to be a periodic function of the time. Within a full period of attitude variation, by construction, there were two linear and two nonlinear segments. The durations of these segments were determined by the user input parameters to the attitude dynamics model. The input parameters (for each component of the attitude) are:

Maximum value for an attitude component:	θ_{max}
Attitude velocity:	$\dot{\theta}$
Attitude acceleration:	$\ddot{\theta}$

The attitude profile appears in Figure 4–1.

From these, one derives the following quantities:

Time spent in a nonlinear segment:	$T_N = 2\dot{\theta}/\ddot{\theta}$
Change in the amplitude in the nonlinear segment:	$\Delta\theta = 0.5\ \ddot{\theta}\ (T_N/2)^2$
Time spent in a linear segment:	$T_L = 2(\theta_{max} - \Delta\theta)\ /\ \dot{\theta}$

Figure 4–2 describes the duration and amplitude of attitude parameters over a complete cycle (linear and nonlinear segments).

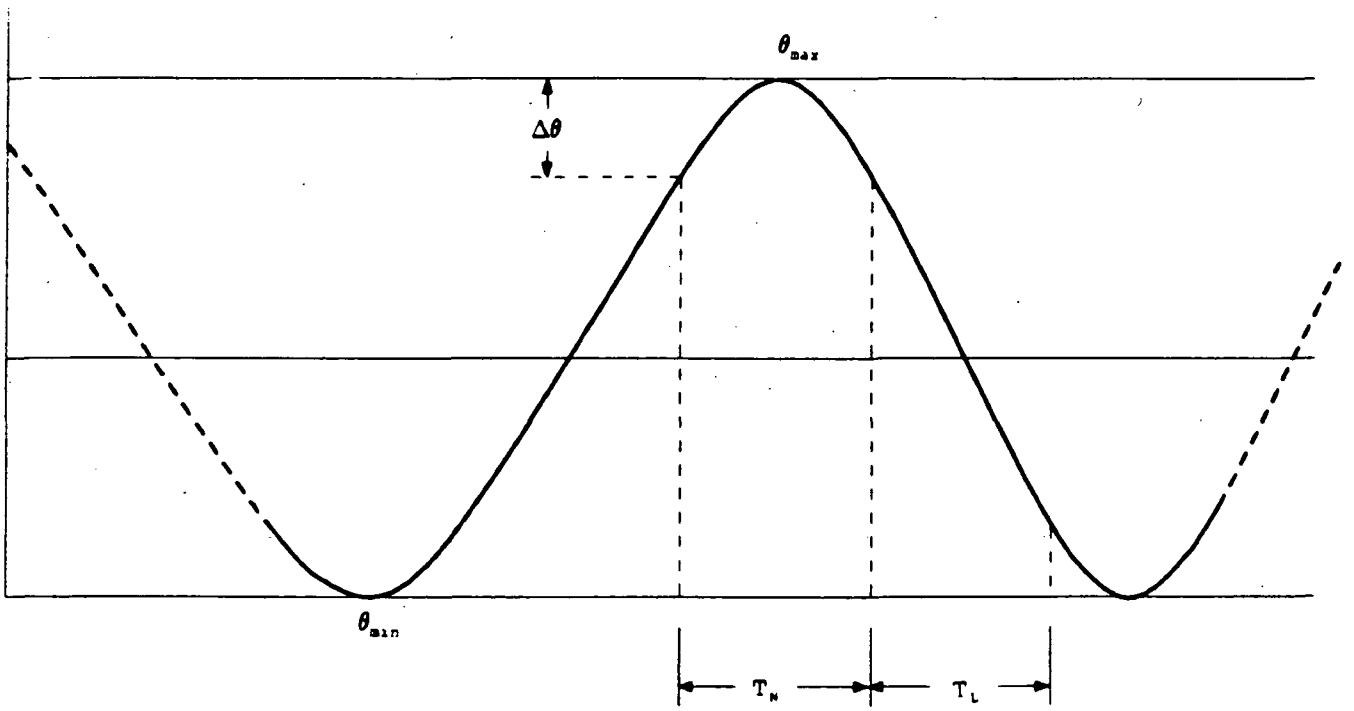

Figure 4-1. Attitude Profile

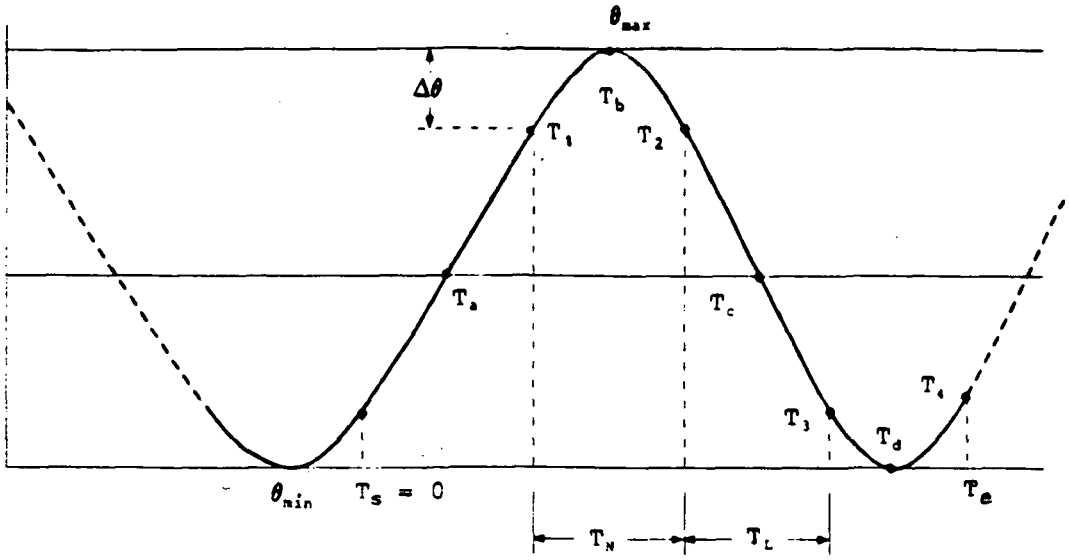

Figure 4-2. Linear and Nonlinear Segments of a Complete Attitude Cycle

Total period ($T_s - T_e$) consists of four segments:

Segment I :	Linear dynamics $T_s - T_1$ T_a is the midpoint of this segment
Segment II:	Nonlinear dynamics $T_1 - T_2$ T_b is the midpoint of the segment
Segment III:	Linear dynamics $T_2 - T_3$ T_c is the midpoint of this segment
Segment IV:	Nonlinear dynamics $T_3 - T_4$ T_d is the midpoint of this segment

Segment I: $\dot{\theta}(t) = \dot{\theta} \times [t - T_a], \quad t \leq T_1$

Segment II: $\theta(t) = \theta_{max} - 0.5\ddot{\theta} \times [t - T_b]^2, \quad t \leq T_2$

Segment III: $\theta(t) = -\dot{\theta} \times [t - T_c], \quad t \leq T_3$

Segment IV: $\dot{\theta}(t) = -\theta_{max} + 0.5[t - T_d]^2\,\ddot{\theta}, \quad t \leq T_4$

with $T_s = 0$

$$T_a = \frac{T_1}{2}, \quad T_b = T_1 + \frac{T_2 - T_1}{2}, \quad T_c = T_2 + T_a, \quad T_d = T_3 + \frac{T_2 - T_1}{2}$$

The function and its first derivatives are continuous at the transition points. The second derivatives, however, are discontinuous.

Table 4–1 shows various attitude parameters used in generating the attitude profiles of the two cases.

TABLE 4-1. PARAMETERS USED IN GENERATING ATTITUDE PROFILE FOR THE SHUTTLE AND SPACE STATION

Parameter	Shuttle	Space Station
Maximum value for yaw	25 degrees	1 degree
Maximum value for pitch	24.30 degrees	5 degrees
Maximum value for roll	27.60 degrees	1 degree
Yaw velocity	0.2 deg/sec	0.02 deg/sec
Pitch velocity	0.2 deg/sec	0.10 deg/sec
Roll velocity	0.2 deg/sec	0.02 deg/sec
Yaw acceleration	0.02 deg/sec^2	0.003 deg/sec^2
Pitch acceleration	0.02 deg/sec^2	0.019 deg/sec^2
Roll acceleration	0.02 deg/sec^2	0.003 deg/sec^2

4.1.1.2 ***Multipath Modeling.*** Self-induced multipath error is caused by reflection of the signal from the host vehicle entering the receiver as opposed to reflections from structures which may be nearby. For example, when the shuttle is orbiting in free space, it sees only the self-induced multipath error; whereas, near the space station, it will see both the reflections from the space station as well as reflections from its own surface. The self-induced multipath is presumably dominant.

Let E be the elevation angle of an SV at a certain time. Ray 1 enters antenna A directly and ray 2 is reflected from the surface and enters the same antenna (Figure 4–3). From the geometry, it can be seen that the path difference between the reflected and direct ray, denoted by Δ_A, is given as

$$\Delta_A = 2\,d \sin E$$

where d is the height of the antenna phase center above the reflecting surface. This path difference corresponds to a phase difference, $\delta\Phi_A$.

$$\delta\Phi_A = 2\pi \frac{2d \sin E}{\lambda}$$

where λ is the wavelength of the signal.

Let a_1 denote the amplitude of the direct ray and a_2 denote the amplitude of the reflected ray. The difference of amplitudes is due to the surface reflectivity. One can write the total disturbance as:

$$Y_a(t) = a_1 \sin \Phi_A + a_2 \sin (\Phi_A + \delta\Phi_a)$$

$$= a \sin (\Phi_A + \delta p_A)$$

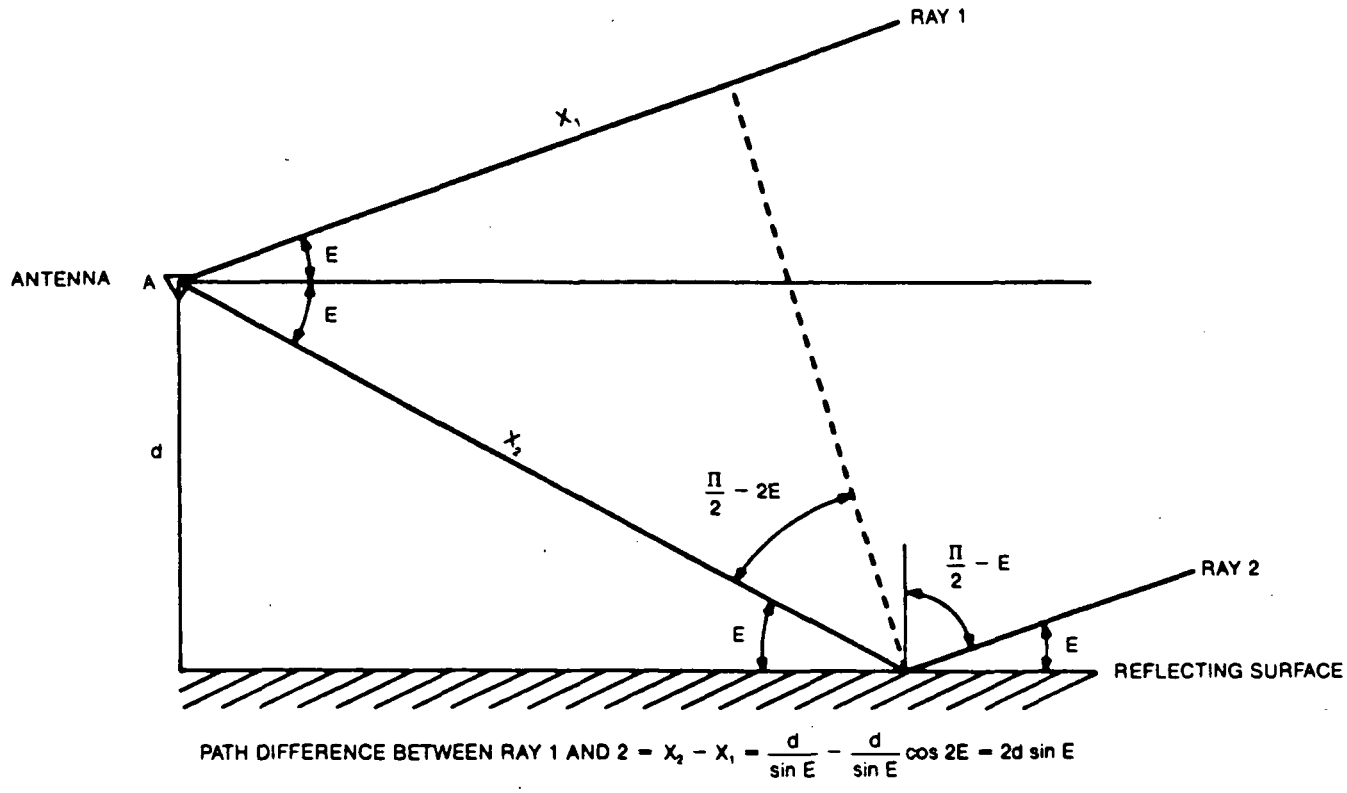

Figure 4-3. Path Difference Between Direct and Reflected Signal

with

$$a = (a_1^2 + a_2^2 + 2\, a_1\, a_2 \cos \delta\Phi_A)^{1/2}$$

$$\tan \delta p_A = \frac{a_2 \sin \delta\Phi_A}{a_1 + a_2 \cos \delta\Phi_A}$$

$$= \frac{(a_2/a_1) \sin \delta\Phi_A}{1 + (a_2/a_1) \cos \delta\Phi_A}$$

δp_A computed from the above equation is the multipath error. The magnitude of the multipath error is studied as a function of various parameters.

It is seen that the multipath error in this model depends on the surface reflectivity, the height of the antenna phase centers above the reflecting surface, and the SV elevation angle with respect to the reflecting surface.

Reflectivity of the mounting surface surrounding the antenna can be dramatically reduced by suitably coating it with material which selectively absorbs microwave energy at the L1 frequency range. With such material, the reflectivity constant (a_2/a_1) can be as low as 0.1.

The attitude determination approach used here makes use of the phase difference of the signal arriving at two different antenna phase centers. Thus, the multipath effect on this phase difference needs to be calculated. In Figure 4–4, A and B are antenna phase centers separated by distance L. The line joining them is not necessarily parallel to the reflecting surface. In practice, there most likely will be a difference in antenna heights.

Figure 4–5 is a plot of phase error δp_A at antenna A as a function of the SV elevation angle (measured from the reflecting plane). The antenna phase center was taken to be 1.9 cm above the reflecting surface. The surface reflectivity was characterized by the ratio $(a_2/a_1) = 0.1$.

Figure 4–6 is a similar plot of phase errors at antenna B which is 5 meters away from antenna A. The line joining the phase centers is canted at an angle of 1 degree with respect to the reflecting surface.

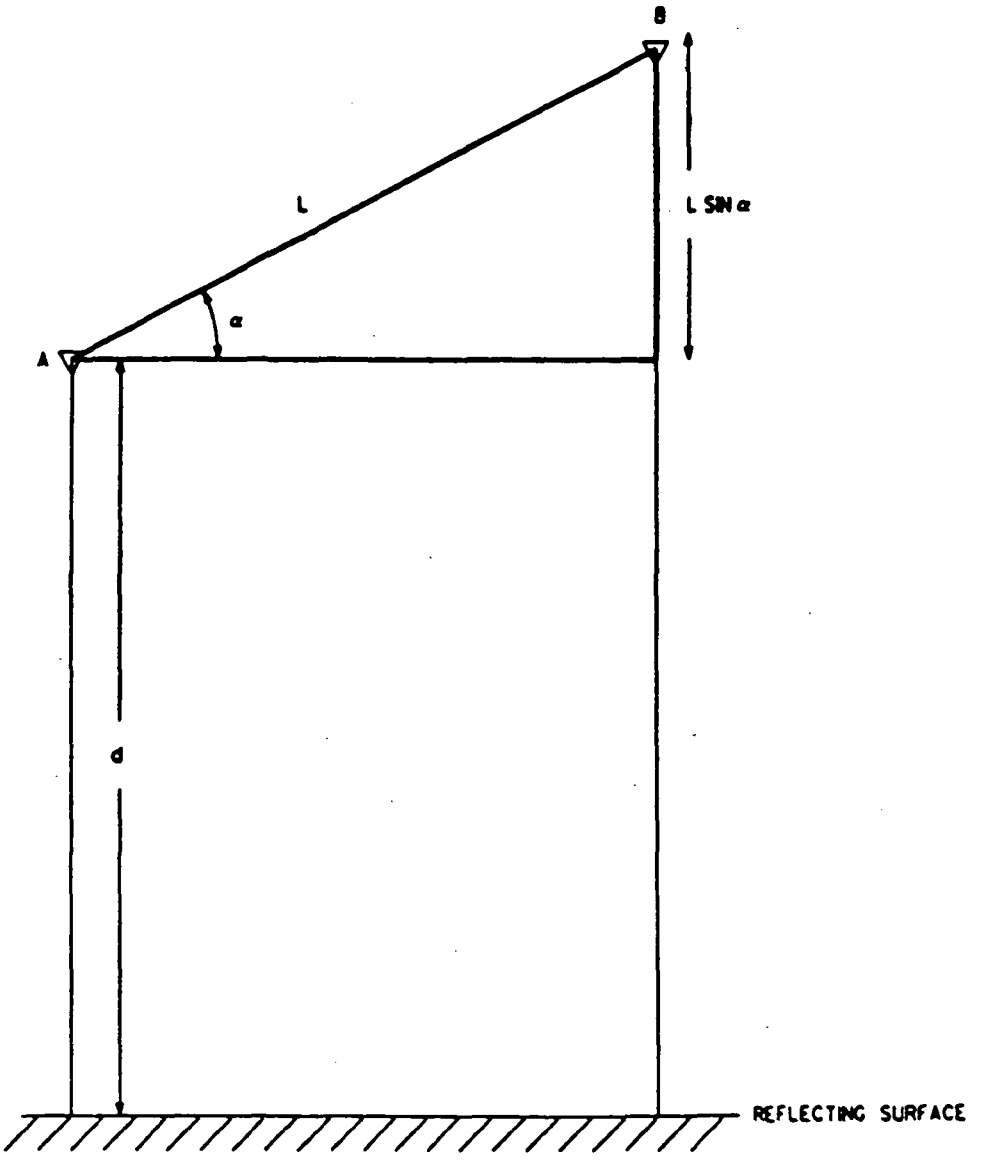

Figure 4-4. Antenna Placement

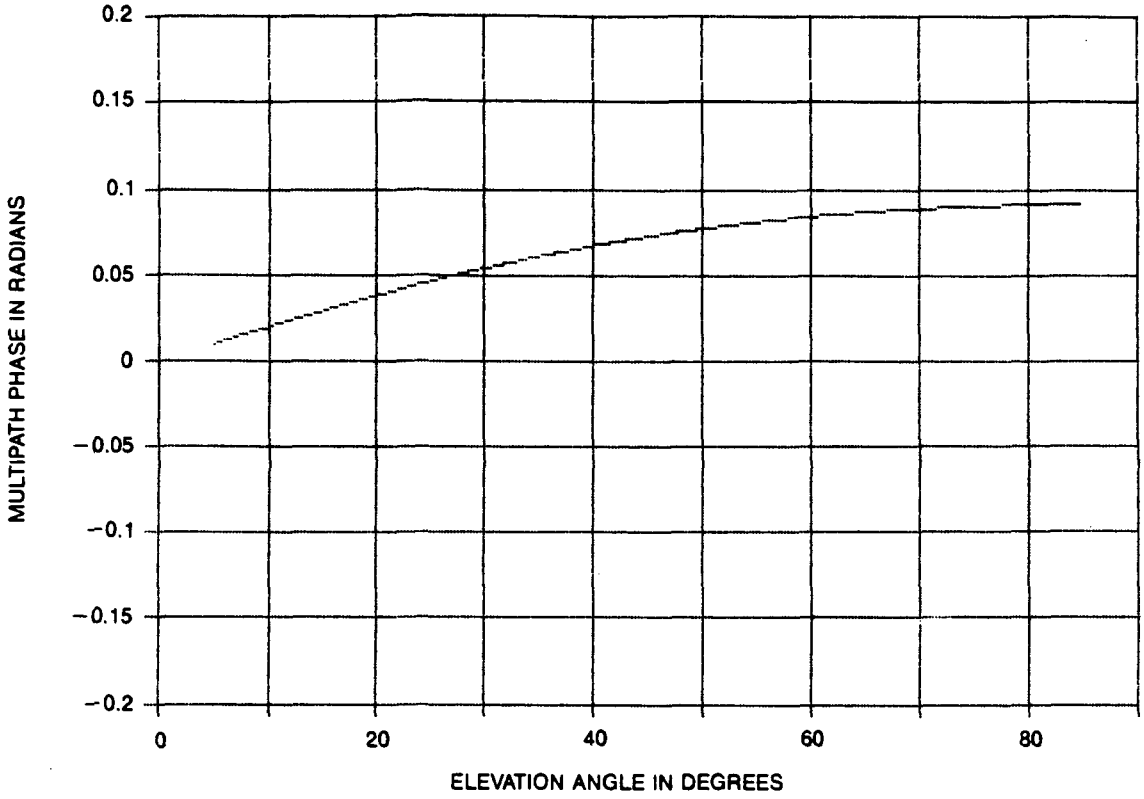

Figure 4-5. Multipath Phase at Antenna A

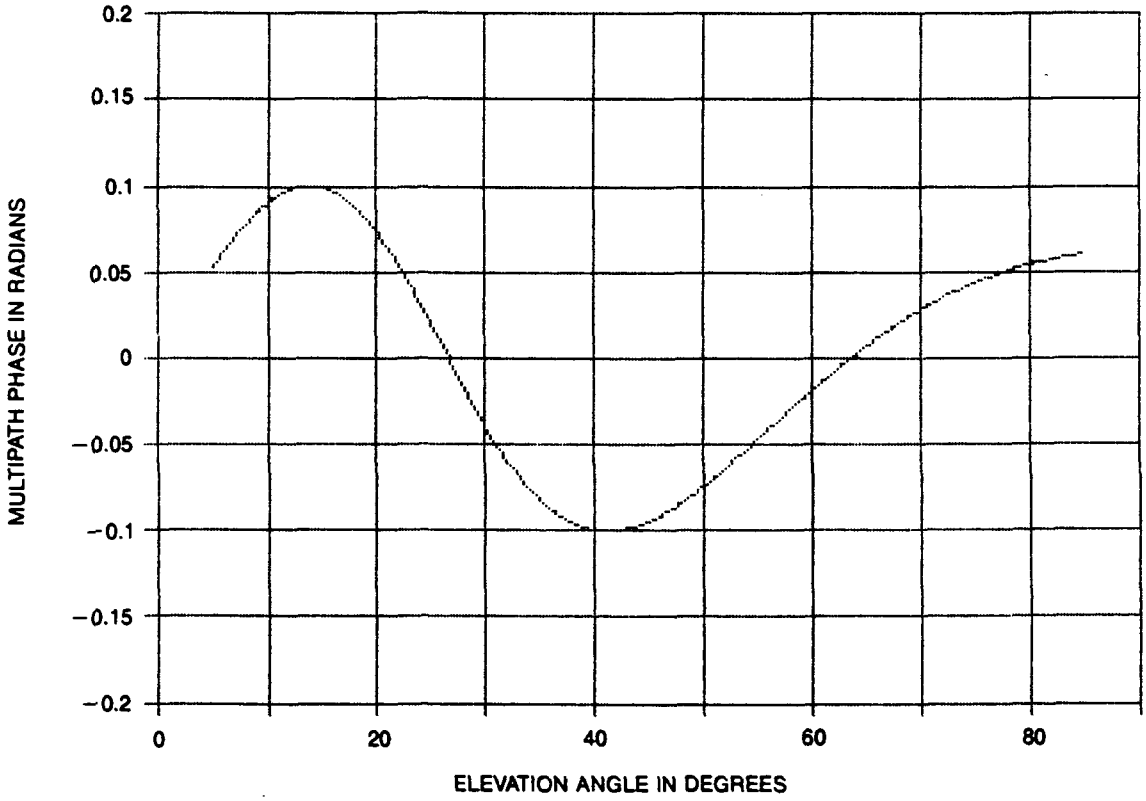

Figure 4-6. Multipath Phase at Antenna B

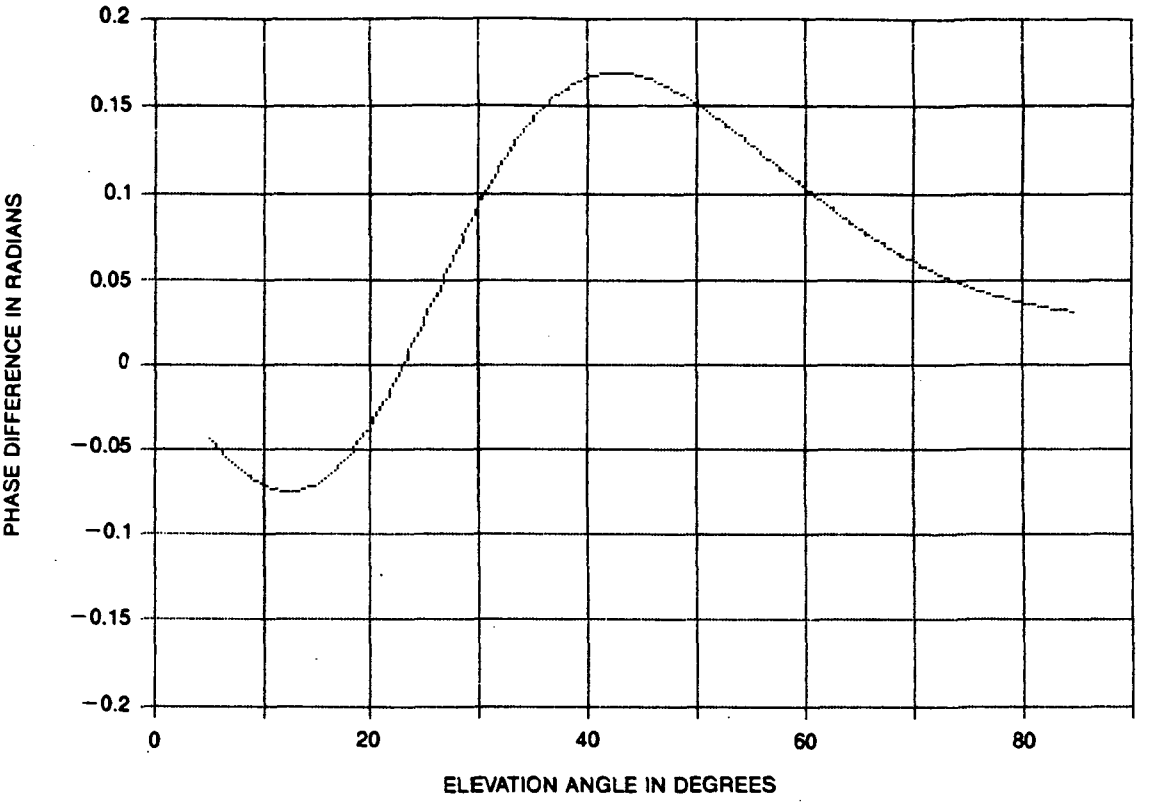

Figure 4-7. Multipath Phase Difference Between Antennas A and B

Figure 4–7 is a plot of differences in phase errors between antenna A and B as a function of SV elevation angle.

In all cases, the assumption is that the antenna gain is uniform for all elevation angles.

4.1.1.3 Antenna Characteristics. The antenna considered for this study was a flat spiral antenna whose phase center was 0.75 inch above the mounting surface. This proximity to the reflecting surface reduced the carrier phase multipath error. The rejection characteristics of this antenna can further reduce the ratio (a_2/a_1). Figure 4–8 represents the gain characteristics of the flat spiral antenna plotted as a function of angle from the boresight. (The elevation angle is 90 degrees minus the boresight angle.) This curve was fitted to a natural cubic spline. Thus, antenna gain (loss) at arbitrary elevation angle can be obtained conveniently.

Let the rejection value for the incident (direct) and reflected rays be X_d and X_r, respectively expressed in dB. It can be seen that the amplitude ratio (a_2/a_1), is multiplied by a factor F to account for the antenna rejection. The factor F is defined by

$$F = 10^{(X_r - X_d)/20}$$

Figures 4–9 and 4–10 result when antenna rejection characteristics are included. Figure 4–11 is a plot of the difference in phase errors between antennas A and B as a function of SV elevation angle with antenna rejection characteristics taken into account. Comparing Figures 4–11 and 4–7, it can be seen that the rejection characteristics of the flat spiral antenna, at low elevation angles, substantially reduced the phase difference errors.

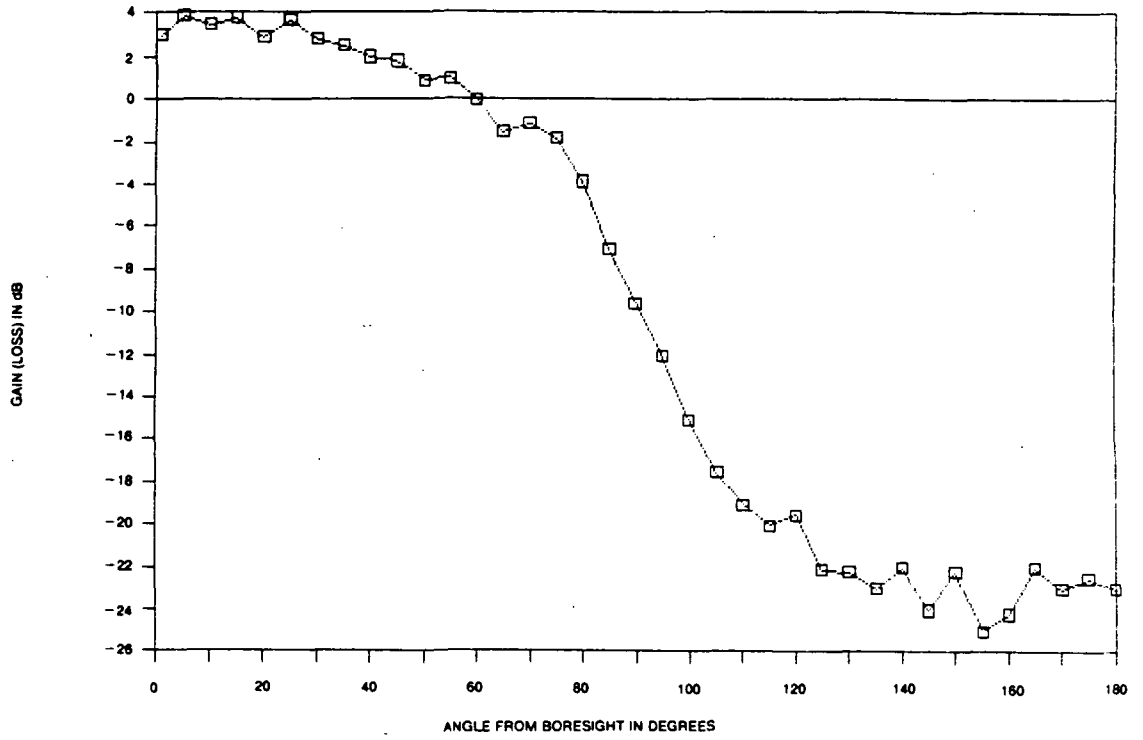

Figure 4-8. Antenna Rejection Characteristics of Flat Spiral Antenna

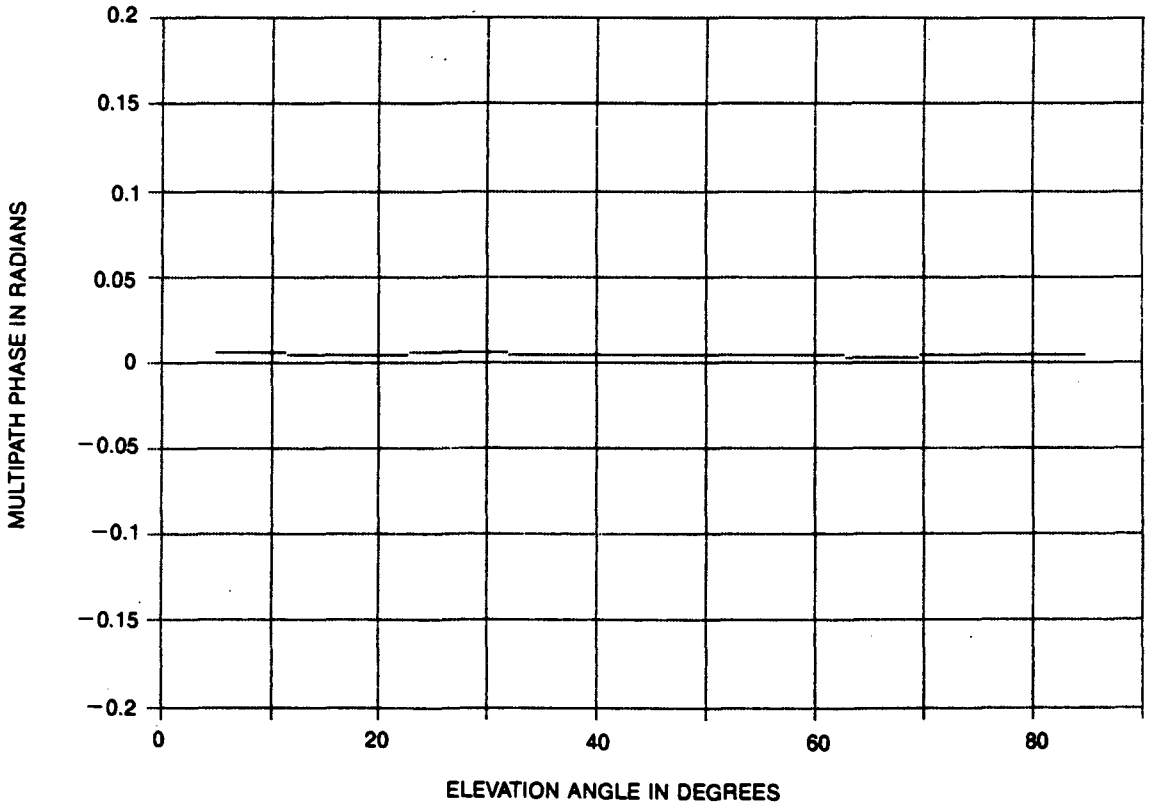

Figure 4-9. Multipath Phase at Antenna A

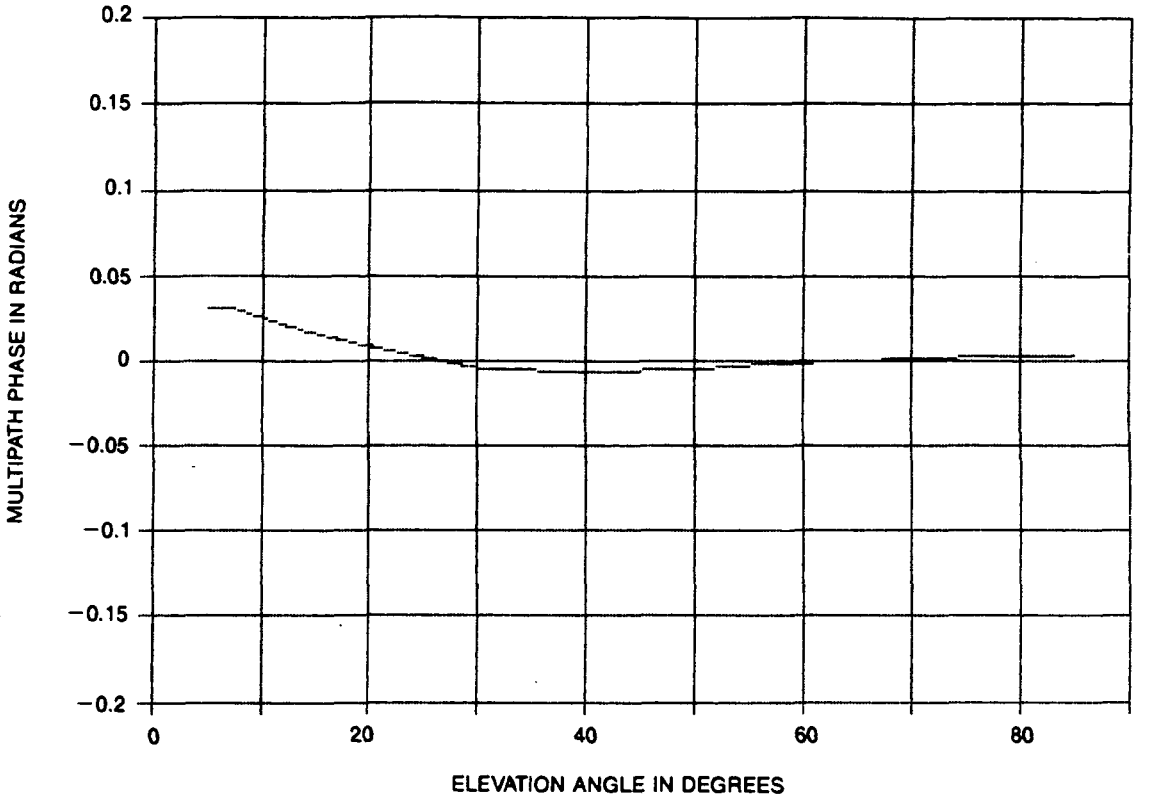

Figure 4-10. Multipath Phase at Antenna B

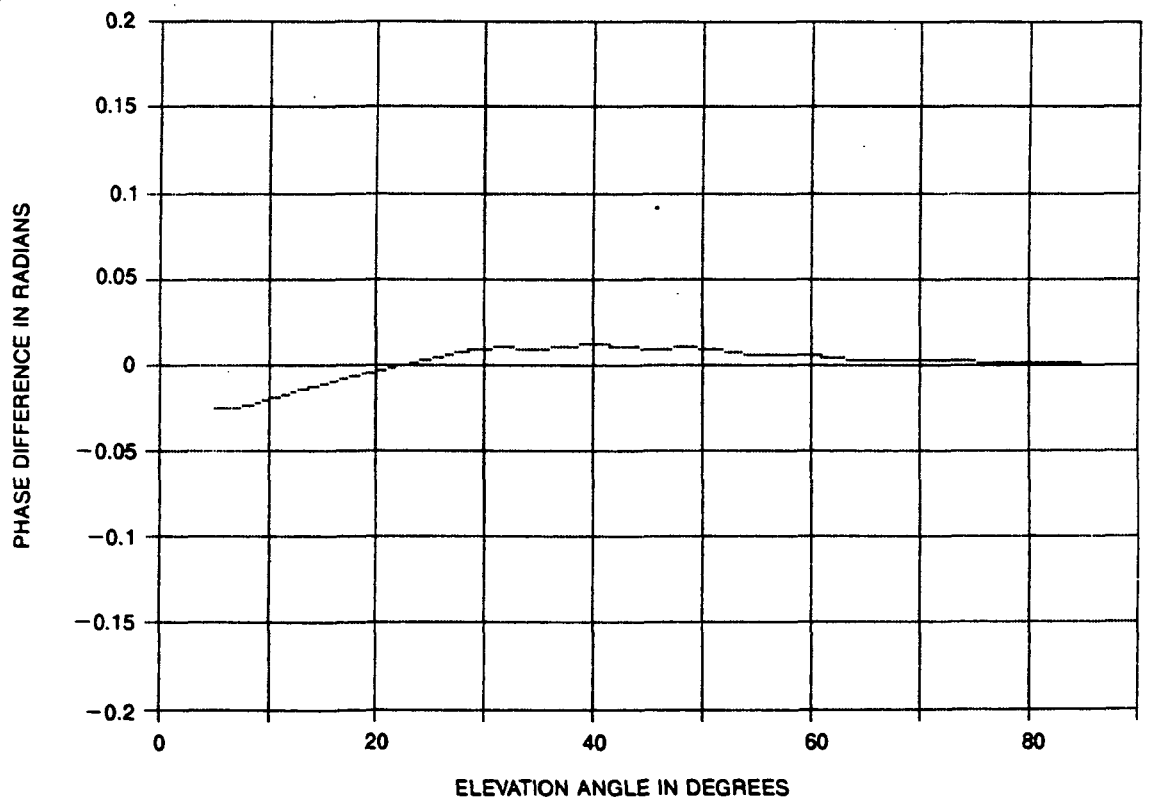

Figure 4-11. Multipath Phase Difference Between Antennas A and B

4.1.1.4 Generation of Observables. The generation of GPS observables in this simulation begins with the assumption that the ECEF position of the navigation center of the platform is computed every second. It is assumed that all measurements are made simultaneously at those time points. Knowing the signal receipt time, the signal transmission time is computed. Using the ICD–GPS–200 algorithm, the SV position in the ECEF coordinate system and the slant range are computed. Note that the antenna positions do not coincide with the navigation centers; hence, a lever arm correction to the slant range from the navigation center to the SV must be made for each antenna phase center. Since the lever arm correction depends on the attitude of the host, heading, pitch, and roll information from the attitude dynamics generator are used to calculate the correction. Also, the elevation angle of the signal which is reflected from the platform surface is dependent on the orientation of the platform. Thus, the elevation angles of SVs with respect to the platform surface at the time of signal receipt are noted and the phase error contribution due to multipath is computed and stored. Thus position, velocity, acceleration, attitude states, and slant range from each SV to each antenna phase center are recorded at 1-second intervals for at least one orbital period. The lever arm corrected slant ranges serve as the observables to the attitude determination program. At this point, it may appear *range measurements* not *carrier doppler phase measurements* are simulated for attitude determination. In this simulation, the issue of carrier doppler phase ambiguity, which is a central issue in the interferometric technique, has not been addressed. An unambiguous carrier doppler phase measurement has been assumed. If we assume that by some means the integer cycle ambiguity has been resolved, then computing the single path difference by (1) differencing the lever arm corrected slant ranges or by (2) computing the phase difference after resolving the phases into fractional part and whole cycles are equivalent. Also, the noise figure used in the generation of observables is appropriate for carrier doppler phase measurements, not pseudorange measurements.

Antenna phase centers were taken to be at A (0, 0, −6.02), B (5, 0, −6.05), and D (0, 5, −6.07) expressed in meters in a rectangular body coordinate system. The reflecting surface was taken arbitrarily to be the $z = -6$ plane and the ratio of reflected amplitude to incident amplitude was taken to be 0.1. The choice of the location of z coordinates of antennas with respect to the reflecting plane could be significant. The z coordinate of antenna A is 2 cm above the reflecting surface on which it is mounted. This is consistent with the physical dimensions of a flat spiral antenna whose phase center is about 0.75 inch above the mounting surface. To account for the fact that the surface may not be perfectly flat, the antenna phase centers B and D were displaced by an additional amount of 3 and 5 cm, respectively.

4.1.2 Attitude Computation and Results.

4.1.2.1 Attitude Compution for the Shuttle. As mentioned in the previous section, platform navigation center position (we are assuming navigation activity is taking place simultaneously) and slant ranges to all SVs from all antenna phase centers are input to an attitude determination program. Gaussian noise of zero mean and 1-sigma value 0.002 M were added to the phase path differences. Also added were the phase errors due to multipath reflections. At each measurement time, the three SVs of highest elevation were chosen to form the single path differences and attitude was computed using the algorithm described earlier (Subsection 3.1.4).

Figures 4–12, 4–13, 4–14 are plots of attitude errors as a function of time. The gaps appearing in the attitude error plots reflect masking of one or more SVs during the simulation. A simple data smoothing procedure of averaging computed attitude over seven data points was used. This procedure clearly smooths the computed attitude. The resulting 1-sigma values for the errors in heading, pitch and roll are 0.017, 0.015 and 0.015 degrees, respectively (Figures 4–15, 4–16 and 4–17).

4.1.2.2 Attitude Computation for the Space Station. Kihara and Okada* have developed an algorithm to choose four satellites for the purpose of navigation. For attitude determination of the Space Station, we made use of the first three of the four satellites selected using their algorithm. Figures 4–18 through 4–23 present the error plots for the raw and smoothed heading, pitch and roll for the Space Station attitude dynamics. The 1-sigma errors based on smoothed attitude were 0.011, 0.015 and 0.012 degrees for heading, pitch and roll, respectively.

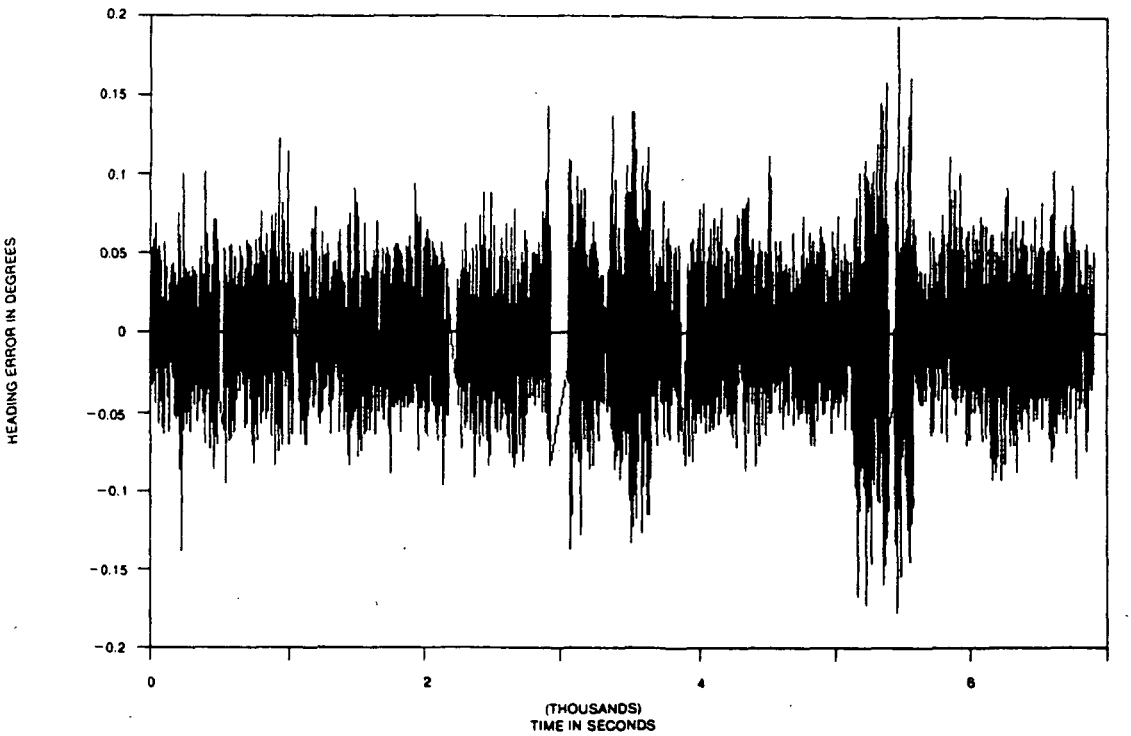

Figure 4-12. Raw Heading Error (High-Attitude Dynamics)

*Kihara, M., and Okada, T., "A Satellite Selection Method and Accuracy for the Global Positioning System," *Navigation*, Vol. 31, No. 1, 1984, pp. 8–20.

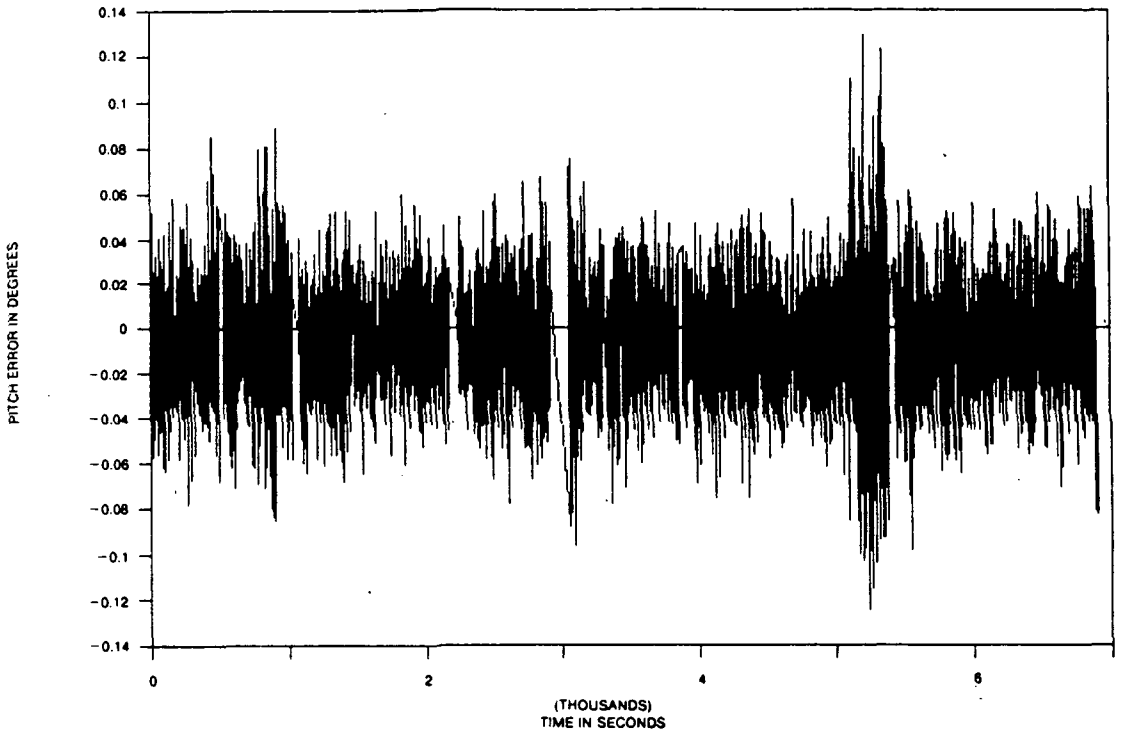

Figure 4-13. Raw Pitch Error (High-Attitude Dynamics)

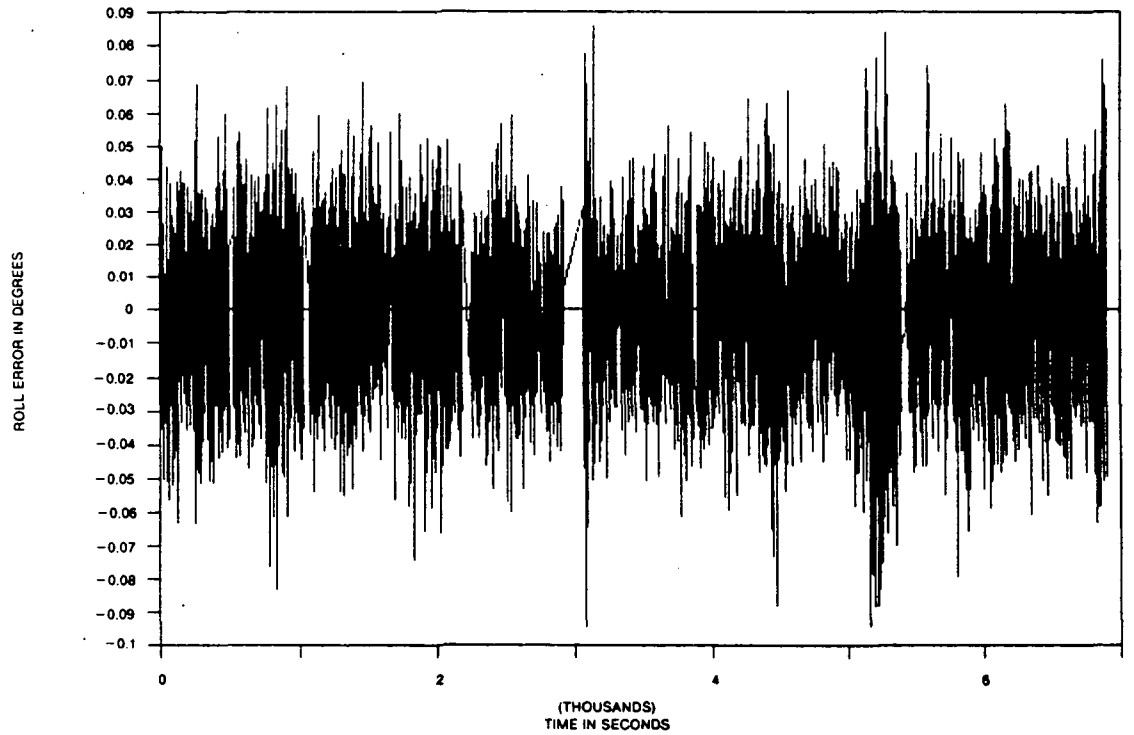

Figure 4-14. Raw Roll Error (High-Attitude Dynamics)

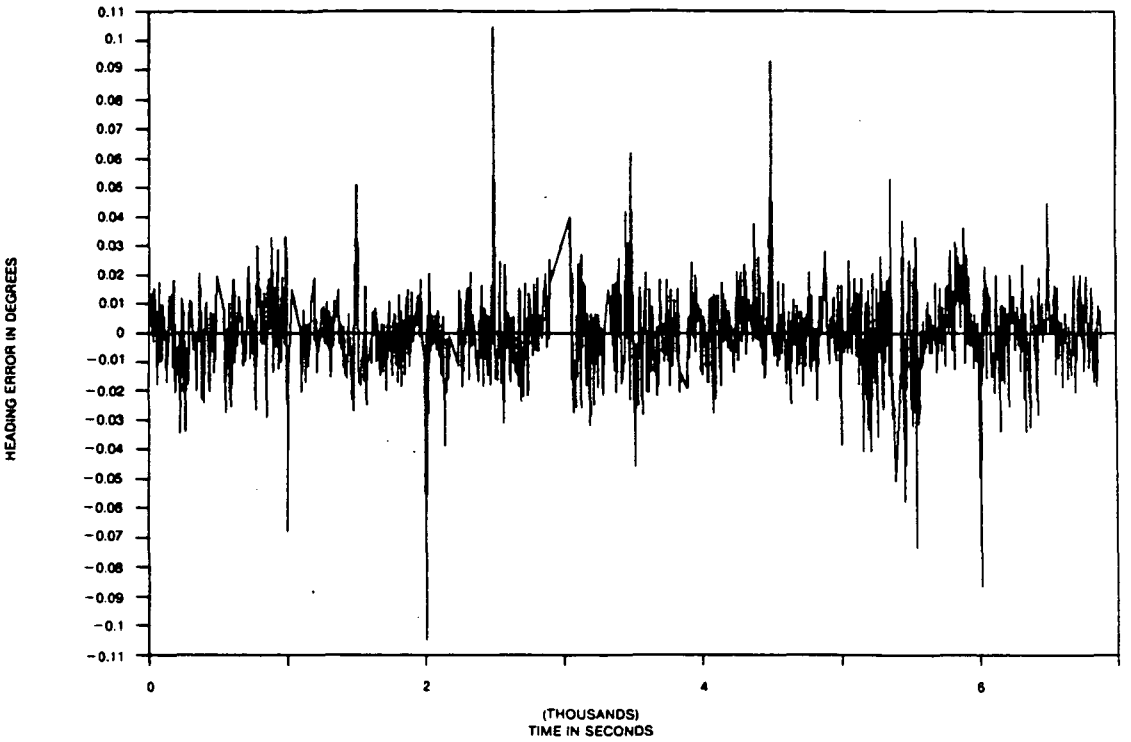

Figure 4-15. Smoothed Heading Error (High-Attitude Dynamics)

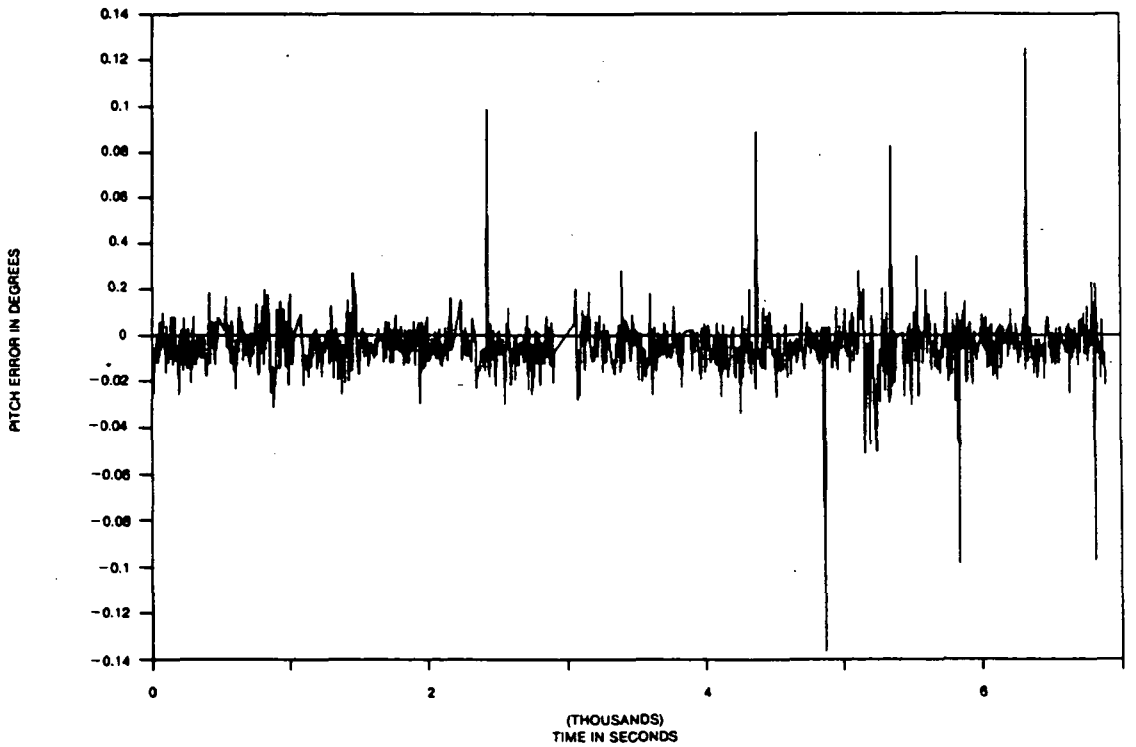

Figure 4-16. Smoothed Pitch Error (High-Attitude Dynamics)

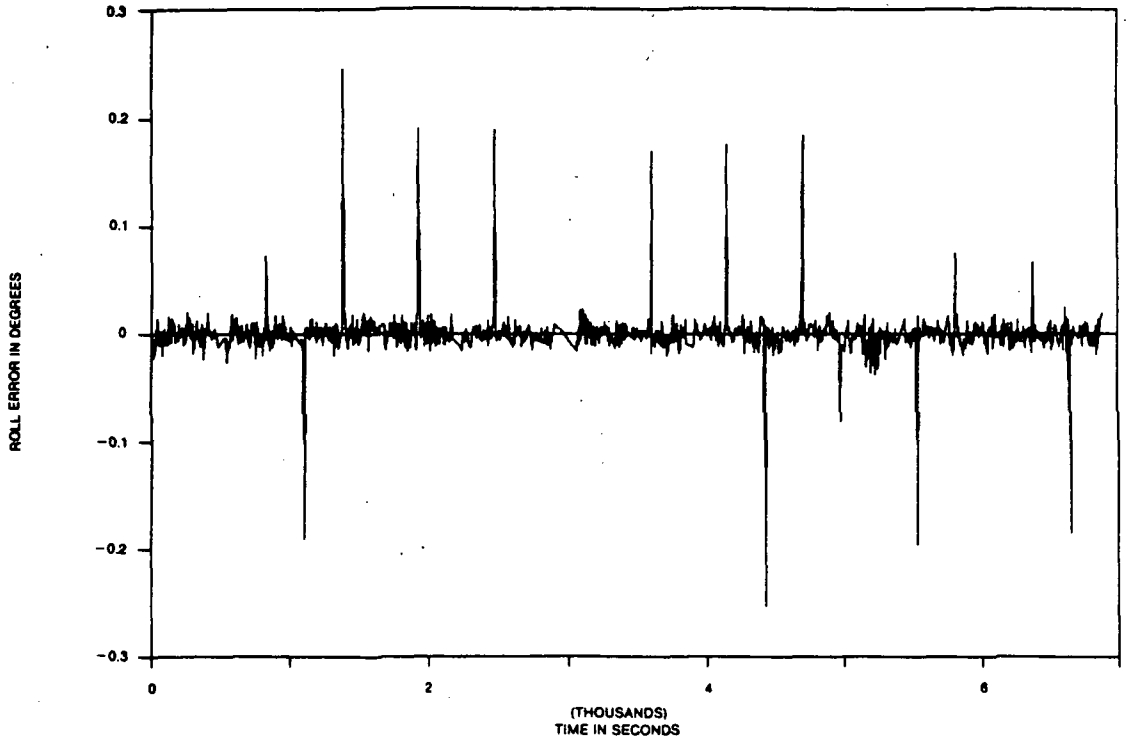

Figure 4-17. Smoothed Roll Error (High-Attitude Dynamics)

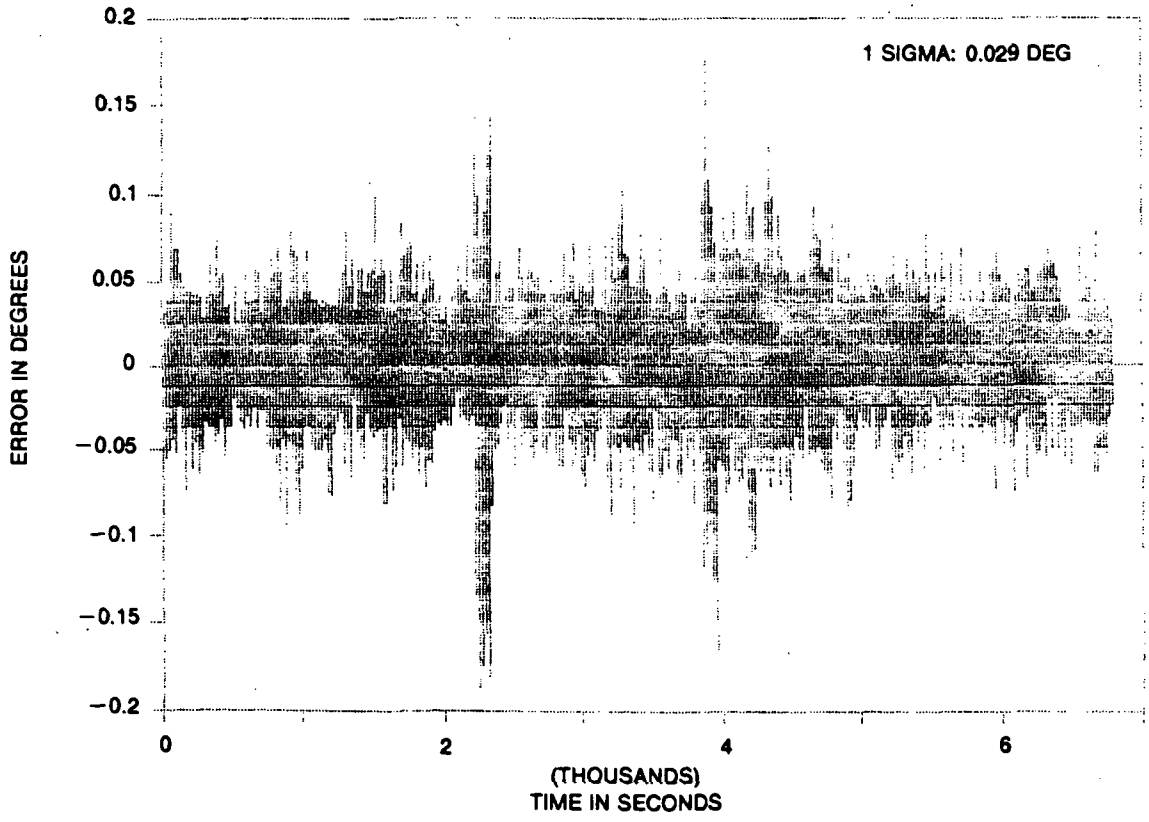

Figure 4-18. Raw Heading Error (Low-Attitude Dynamics)

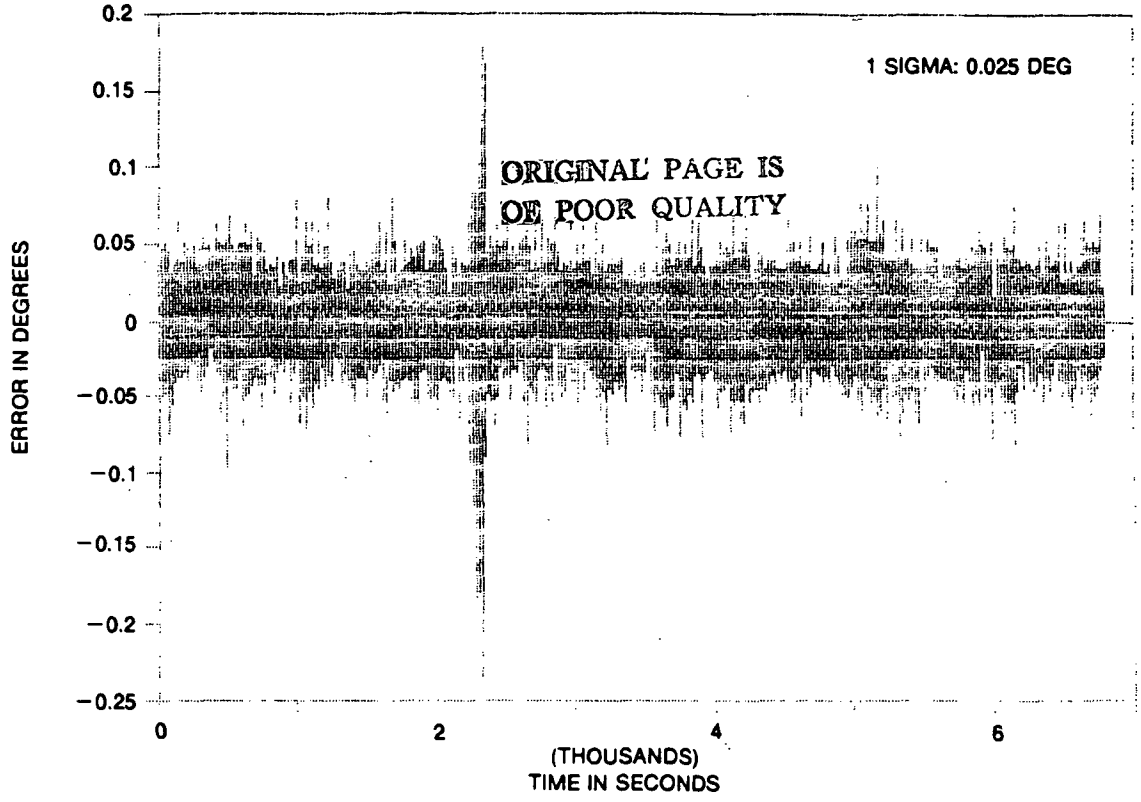

Figure 4-19. Raw Pitch Error (Low-Attitude Dynamics)

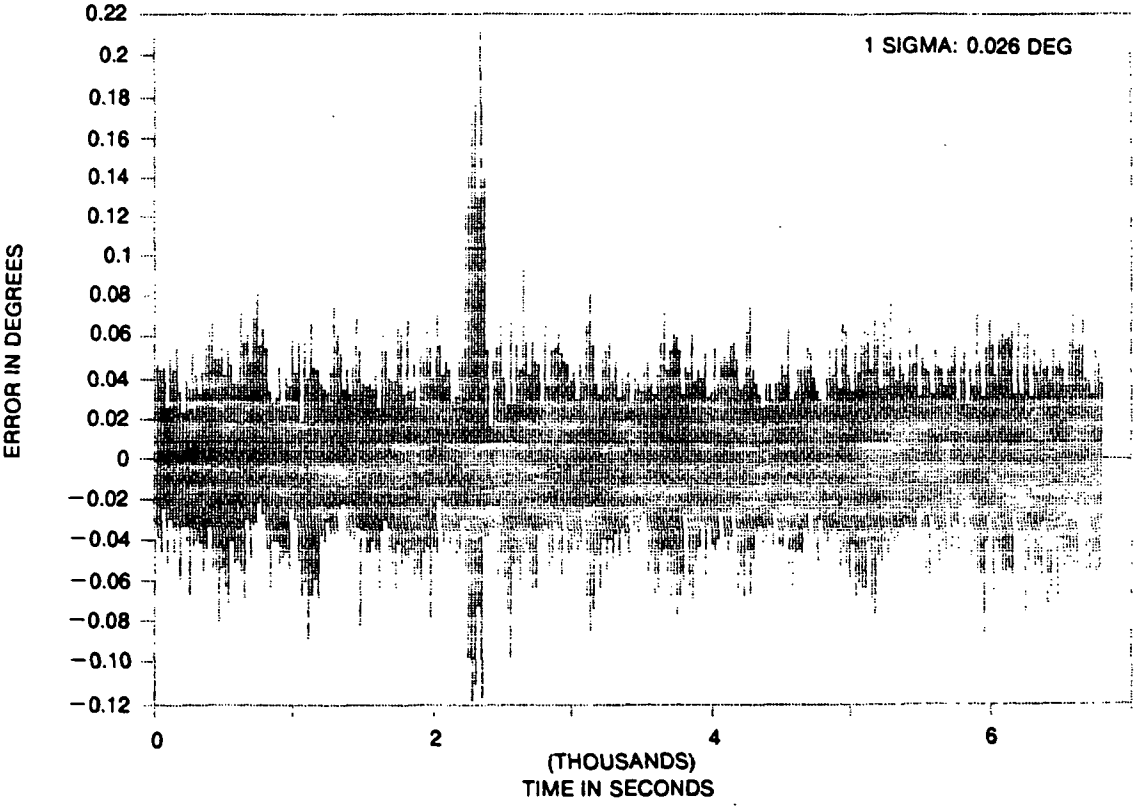

Figure 4-20. Raw Roll Error (Low-Attitude Dynamics)

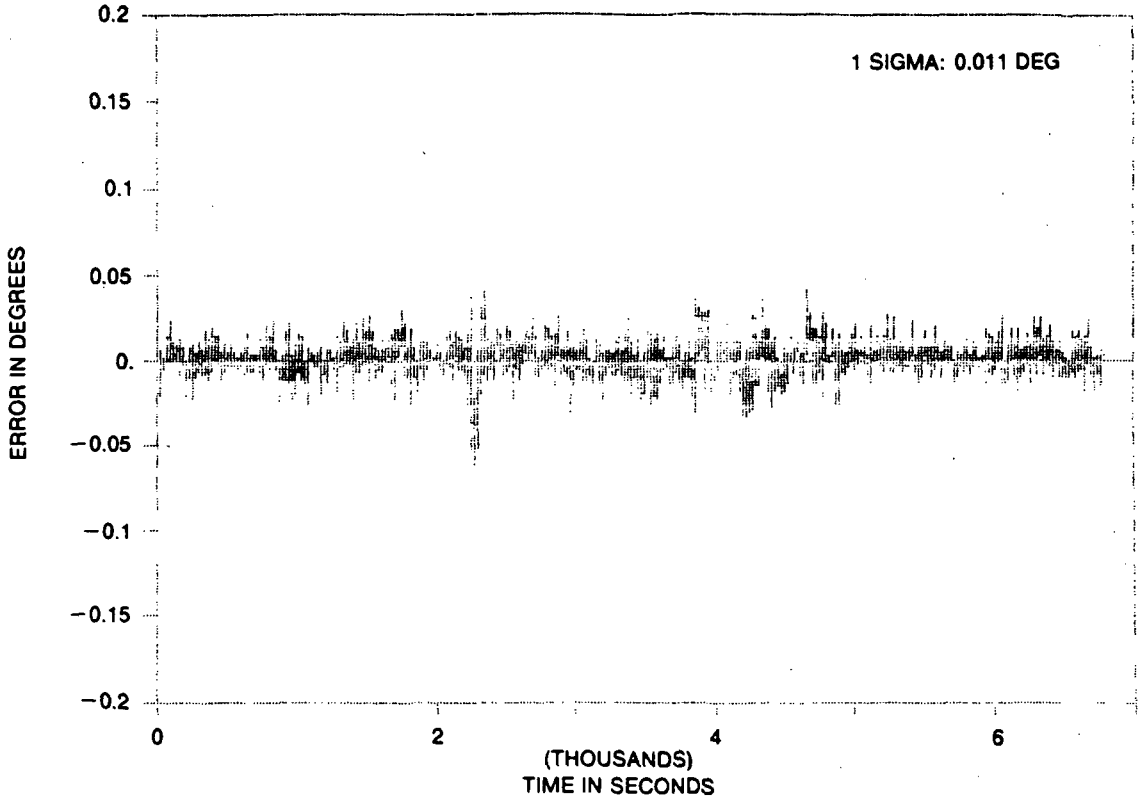

Figure 4-21. Smoothed Heading Error (Low-Attitude Dynamics)

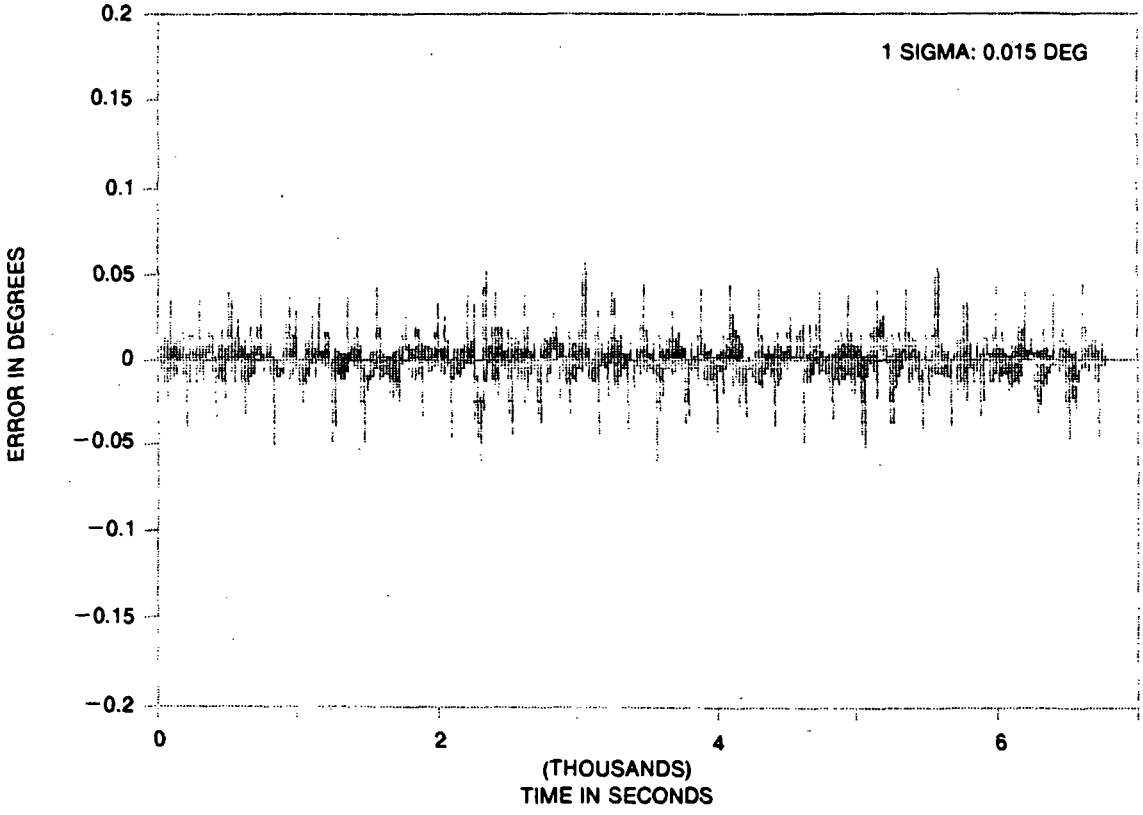

Figure 4-22. Smoothed Pitch Error (Low-Attitude Dynamics)

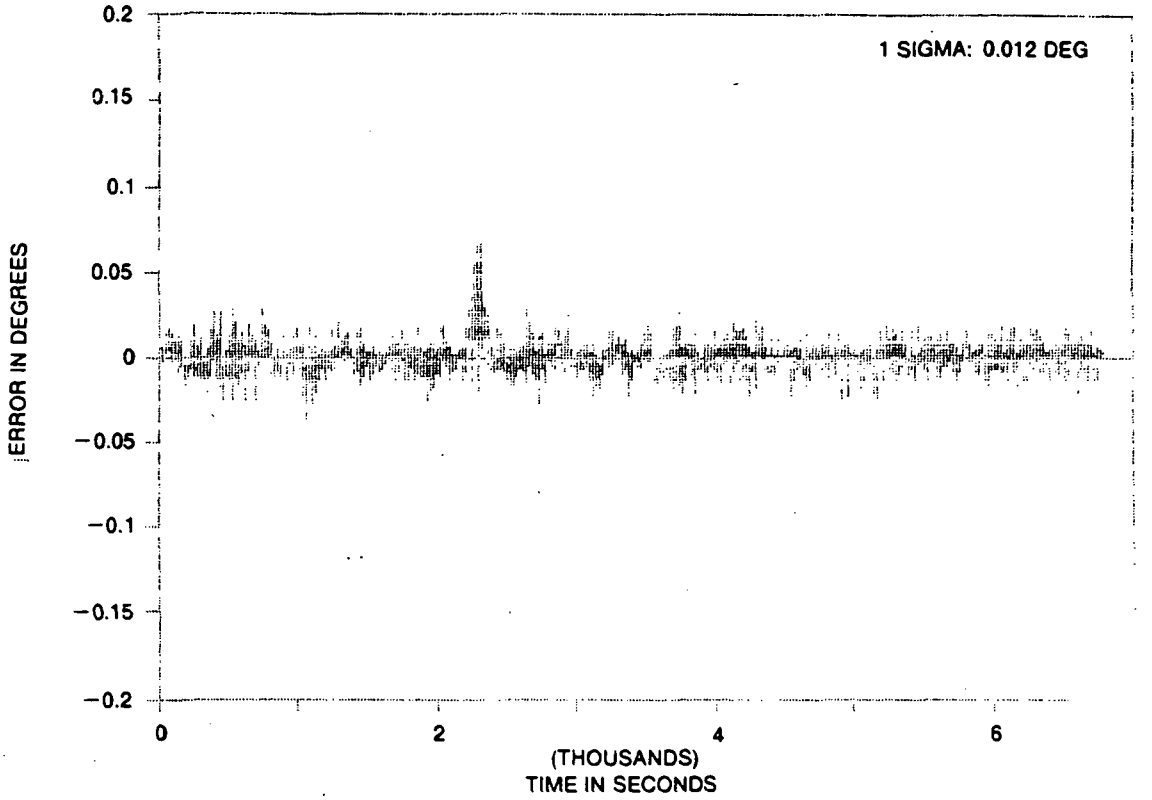

Figure 4-23. Smoothed Roll Error (Low-Attitude Dynamics)

4.2 GPS RELATIVE NAVIGATION SIMULATION RESULTS

4.2.1 Simulator Environment

4.2.1.1 Scenario Generation. The agreed upon scenario was two space vehicles in a 270-nmi (500-km) altitude orbit going from 35-km (20 nmi) separation to 30 M (100 feet) with no docking. We used ICD–GPS–200 algorithms to generate the trajectories. The orbits are circular with an inclination of 28.5 degrees.

The satellite constellation used was the full 18-SV constellation.

4.2.1.2 Generation of Observables. GPS simulated measurements, in the format of the TI 4100 Receiver Measurements outfile file, were generated by the TI legacy measurement generator. The space and control segment errors added to the measurements are consistent with the GPS error budget system specification, SS–GPS–300C. The user errors are consistent with TI 4100 P-code performance.

The following error sources were included:

- Pseudorange thermal noise
- Multipath (P-code effect)
- SV clock error

- User clock error
- Atmospheric errors
- Ephemeris errors.

Each of these is described below.

- **Pseudorange Thermal Noise**

Thermal noise was generated as Gaussian noise. The equation for the pseudorange thermal noise variance is a function of the signal power-to-noise density and the bandwidths:

$$N = BWL \times CN_0 \times (C1 + C2 \times PDBW \times CN_0) \times C3 + C4$$

where

N is PR thermal noise variance

BWL is effective noise bandwidth

CN_0 is signal power-to-noise density in V^2 - Hz. Multiplying BWL by CN_0 gives the signal power-to-noise density without taking into account the type of tracking loop.

C1 and C2 are constants describing a noncoherent tau-dither code tracking loop (C1 = 1; C2 = 2).

PDBW is the predetection bandwidth (1/sample rate).

C3 is a factor for converting chips squared to meters squared (C/A = 85878.3; P-code = 858.783).

C4 is a constant for a minimal noise level regardless of CN_0 (currently set to 0).

For these simulations, nominal signal power-to-noise densities were used:

L_1 C/N_0 = 36 dB	σ = 0.6M (1.9 feet)
L_2 C/N_0 = 33 dB	σ = 1.0M (3.3 feet)

A separate noise sequence was generated for each PR, L_1 and L_2. A representative plot is shown in Figure 4–24.

- **Multipath (P-Code Effect)**

Multipath cannot be modeled adequately as a white noise sequence. The same realistic geometry approach as was used for the attitude work was used here also, except the model was for P-code pseudorange rather than carrier phase. After calculating the angle of the direct and reflected rays, and accounting for surface reflectivity and antenna rejection characteristics, the multipath effect on the P-code was calculated using tracking loop correlation techniques which model the receiver behavior. Multipath was modeled separately for each SV signal path.

The TI 4100 is designed so that if the reflected signal is delayed more than one-and-a-half P-code chips, then the receiver will not be affected by it. This means that there are no multipath effects between vehicles greater than 45 M (147 feet) apart. Multipath between vehicles was not considered in these simulations, just reflections from the vehicle itself. The reflecting surface

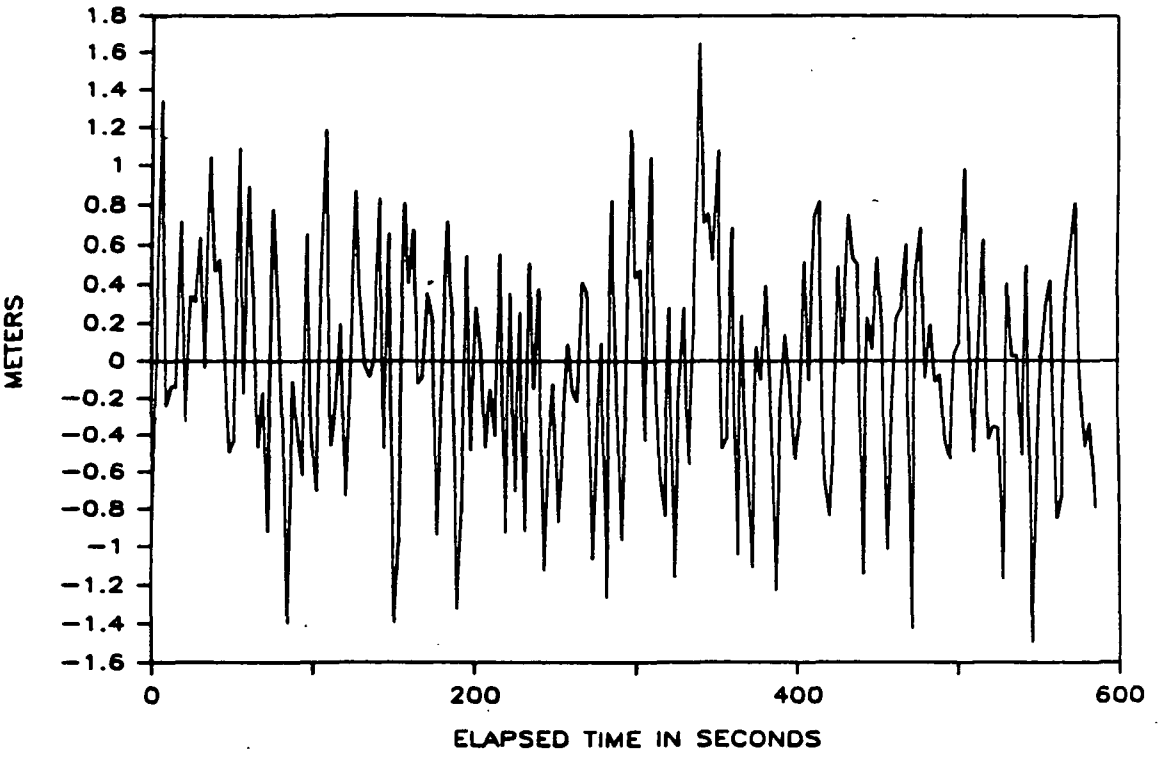

Figure 4-24. PR Thermal Noise, SV 1, L1

suitably designed low-profile, flat-spiral antenna and by putting absorbing material around the antenna. For these simulations, the phase center height was 0.75 inch and the total multipath was on the millimeter level.

- **Satellite Clock Error**

The satellite clock error is estimated by the control segment, and then parameters for a clock-correction polynomial are broadcast in the SV navigation message. The simulated SV clock error is the residual error after applying the broadcast clock error model. Each SV has a different error value. If both receivers are tracking the same SV, the error is the same for both.

The total error consists of a constant part and a random part. The constant part is based on the SS–GPS–300C standard deviation of 2.97 M (9.74 feet). Each SV tracked is assigned a different constant bias, less than or equal to 2.97 meters, and then Gaussian noise is accumulated over the interval to simulate the clock drift of 7×10^{-12} per second (typical of a cesium clock). Figure 4–25 shows the SV clock error for one SV.

- **User Clock Error**

The user clock error was also simulated with a constant part and a random part. Based on SS–GPS–300C, the standard deviation of the constant bias was 2.97 M (9.74 feet), and the, random part was based on an ovenized quartz oscillator clock drift of one part in 10^{11} per second. This error is common to SVs tracked by the same receiver. Figure 4–26 shows the user clock error.

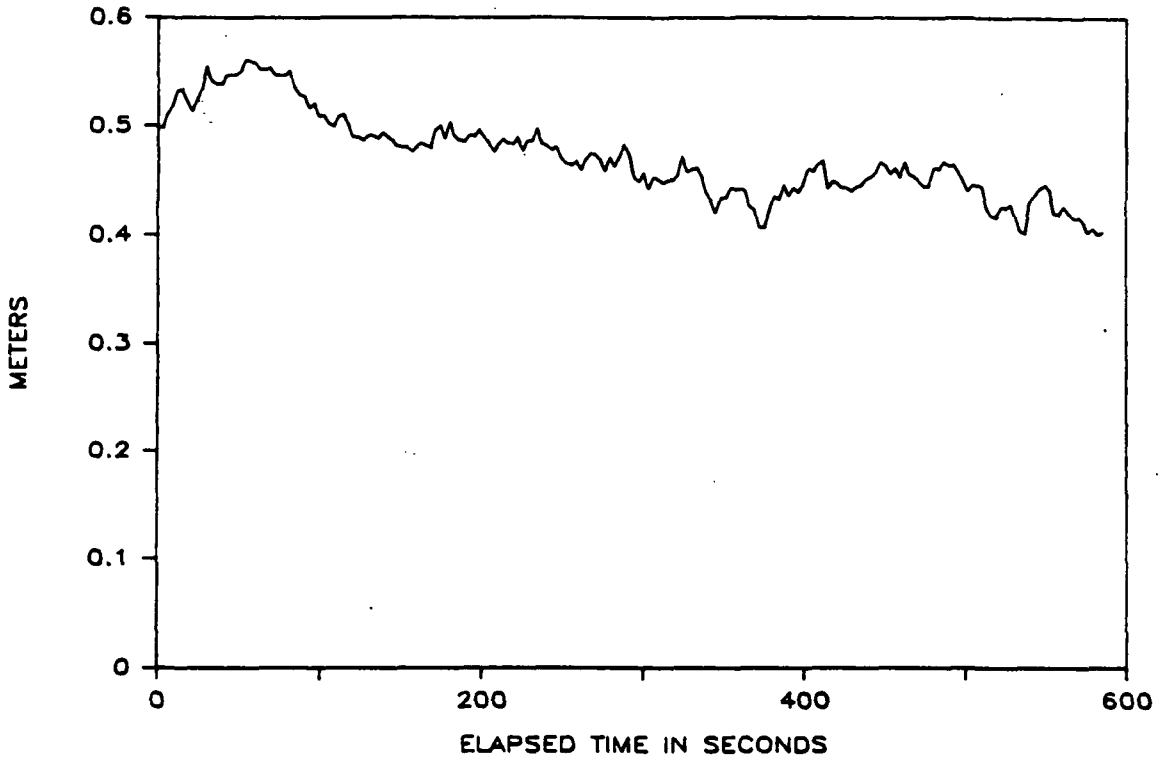

Figure 4-25. Residual SV Clock Error, SV 1, L1

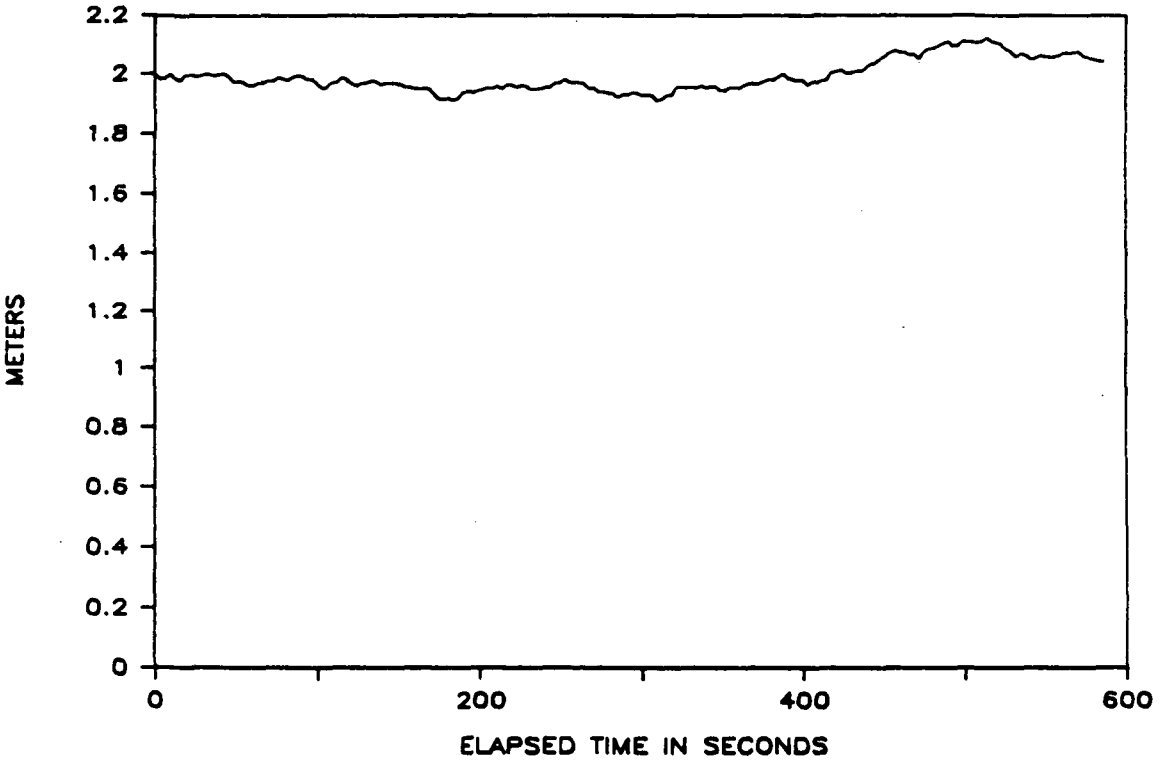

Figure 4-26. User Clock Error, SV 1, L1

- **Composite Error**

Figure 4–27 is the composite error plot of all the above error sources for one receiver.

- **Atmospheric Errors**

Because of the high altitude of the vehicles, tropospheric errors were not considered.

In a P-code, dual-band receiver, the ionospherically corrected PR, $\hat{P}R_{L1}$, is calculated using the L1 and L2 pseudoranges as follows:

$$\hat{P}R_{L1} = PR_{L1} + 1.54572778\,(PR_{L1} - PR_{L2})$$

The second term of this equation is the measure of the ionospheric delay. The error in this measurement is from the error in the L1 and L2 pseudoranges and was not modeled separately.

- **Ephemeris Errors**

Satellite ephemeris errors were modeled by changing the Keplerian orbital parameters which describe the SV orbit. Cross-track error and radial error will cancel in relative navigation. Along-track was simulated by increasing the mean anomaly.

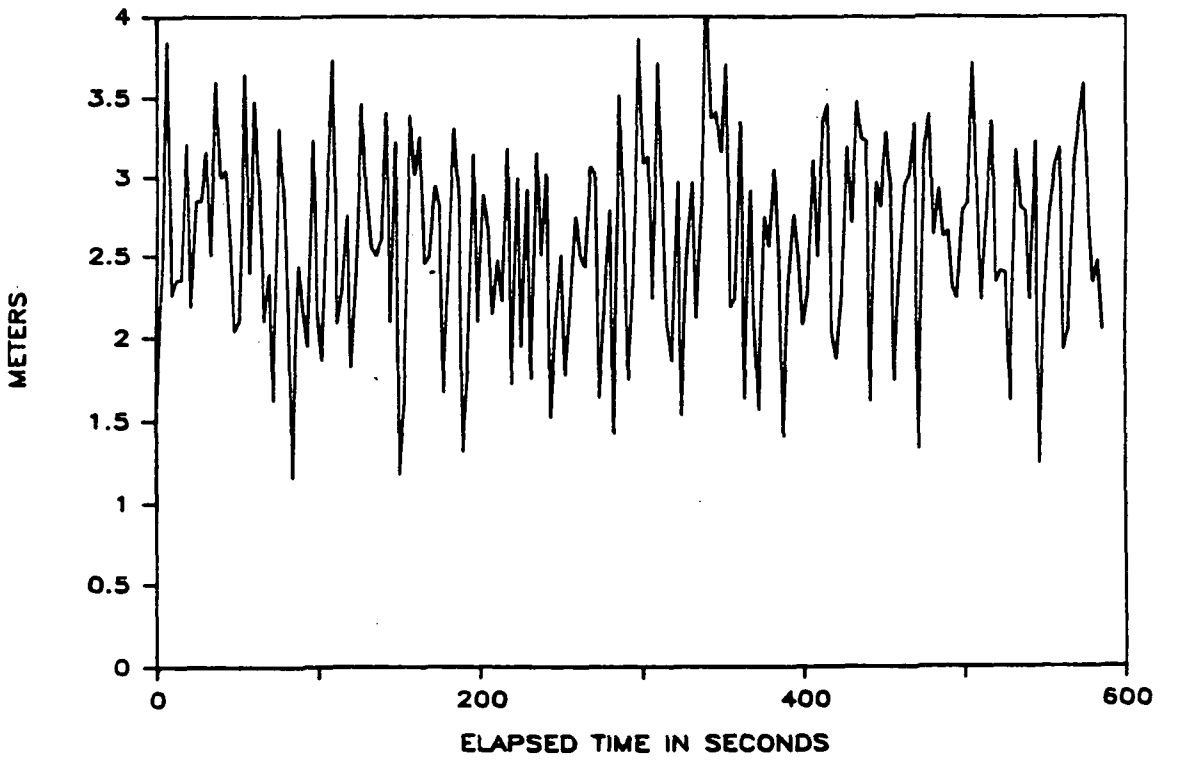

Figure 4-27. Composite Error

4.2.2 GPS Relative Navigation Simulation Runs

4.2.2.1 Position Difference Simulations. In the position difference simulations, the absolute position of receivers A and B were calculated separately (unfiltered). Position B was then subtracted from position A. The baseline vector (in earth-centered/earth-fixed X, Y, Z) was compared to the truth baseline vector.

Position difference simulations were run on five data sets. From the set of all visible satellites, five sets were chosen:

1. All four SVs the same for both spacecraft
2. One SV different
3. Two SVs different
4. Three SVs different
5. All four SVs different.

The PDOP in all cases was close to 2.6, so the results can be directly compared without compensating for PDOP differences. The simulation interval was chosen when eight SVs were visible so that all cases could be run. This resulted in a rather short simulation interval and also in PDOPs that were slightly better than the nominal value of 3.14 quoted for the final constellation.

Figures 4–28 through 4–32 correspond to the five cases listed above. Case 1, all SVs the same, resulted in a one-sigma RSS relative position error of 3.5 M (11.5 feet). This corresponds to the value expected by looking at the math analysis and using this slightly smaller PDOP. With a knowledge of the orbital dynamics, these results could be filtered to remove the noise. Cases 2 through 5, which introduce different SVs, have approximately the same standard deviation of the relative position error; however, there are now biases which no amount of filtering could remove. The "all four SVs different" case had the worst bias errors of 19 M (62 feet). This clearly shows the advantages of using the same four SVs for position difference relative navigation.

The means and standard deviations of all cases are as follows:

1. All four SVs the same (Figure 4–28)

mean X error	=	−0.3 meter	(−1.0 foot)
mean Y error	=	0.2 meter	(0.7 foot)
mean Z error	=	−0.1 meter	(−0.3 foot)
root-sum-square error	=	0.4 meters	(1.3 feet)
one-sigma X error	=	2.7 meters	(8.9 feet)
one-sigma Y error	=	1.9 meters	(6.2 feet)
one-sigma Z error	=	1.1 meters	(3.6 feet)
root-sum-square error	=	3.5 meters	(11.5 feet)

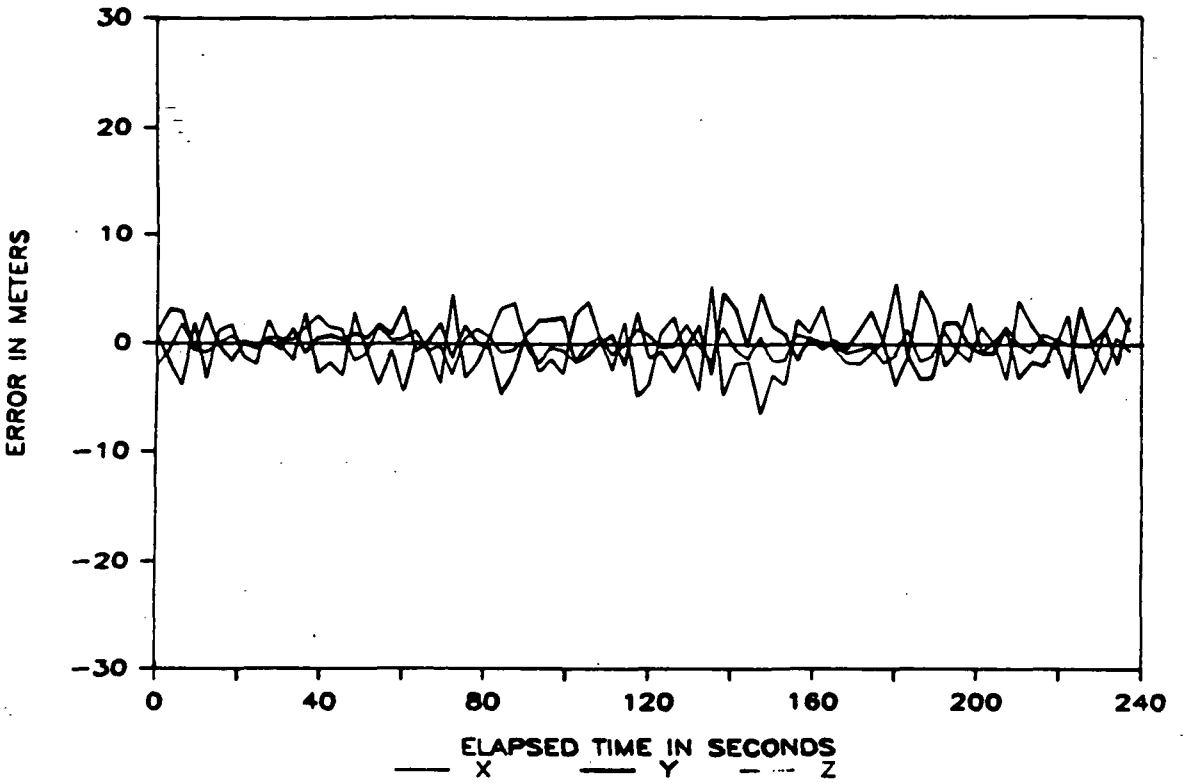

Figure 4-28. Position Difference Simulations (All Four SVs Same) (PDOP = 2.6)

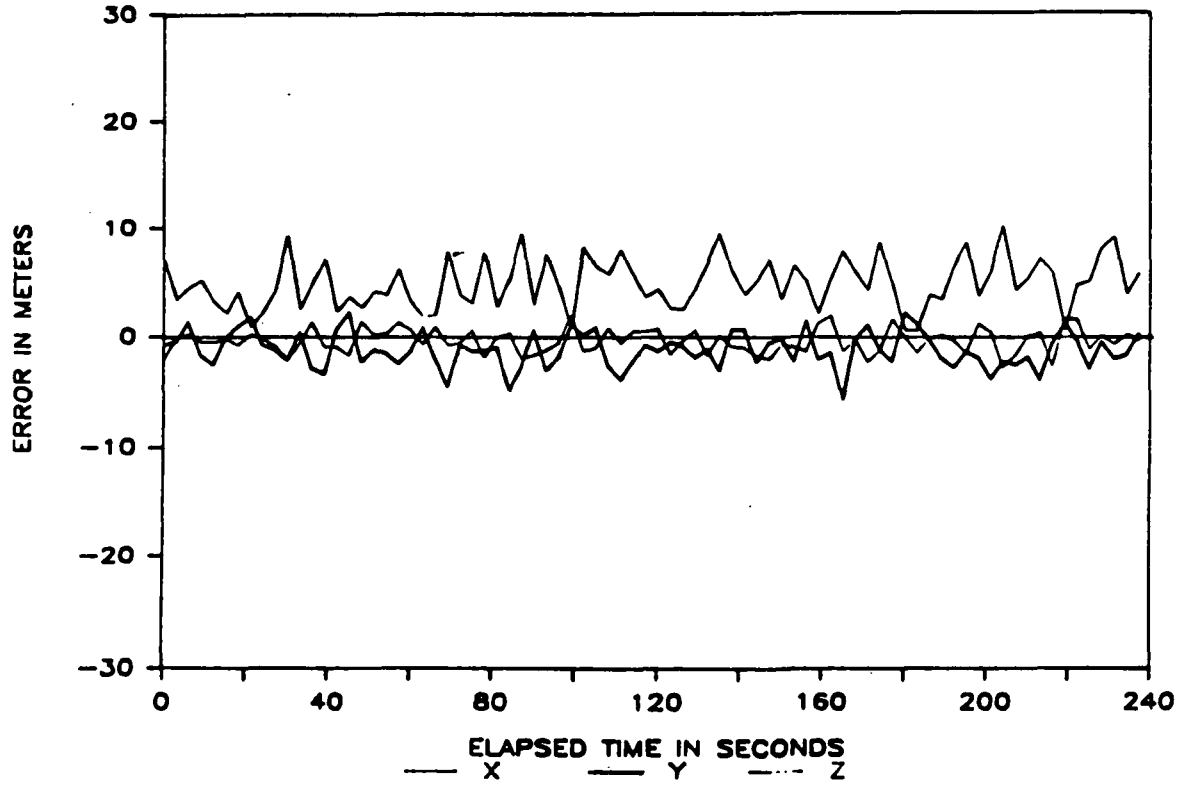

Figure 4-29. Position Difference Simulations (One SV Different) (PDOP = 2.6)

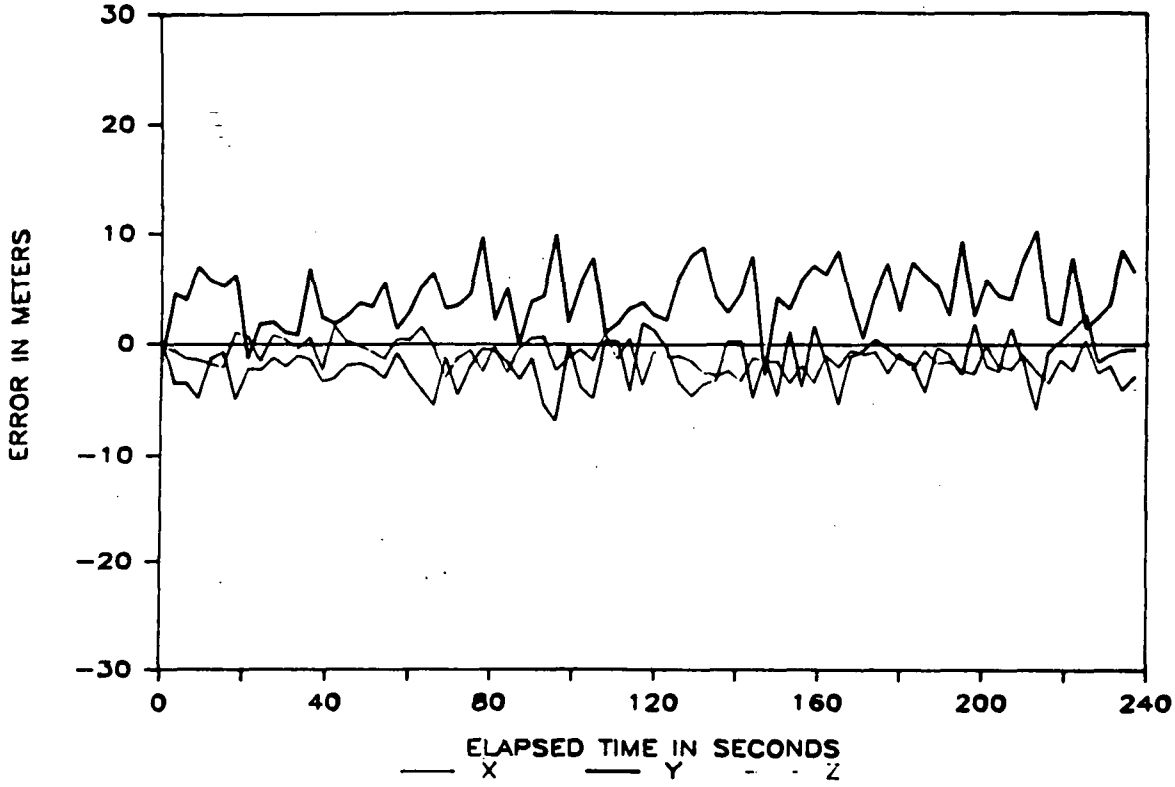

Figure 4-30. Position Difference Simulations (Two SVs Different) (PDOP = 2.6)

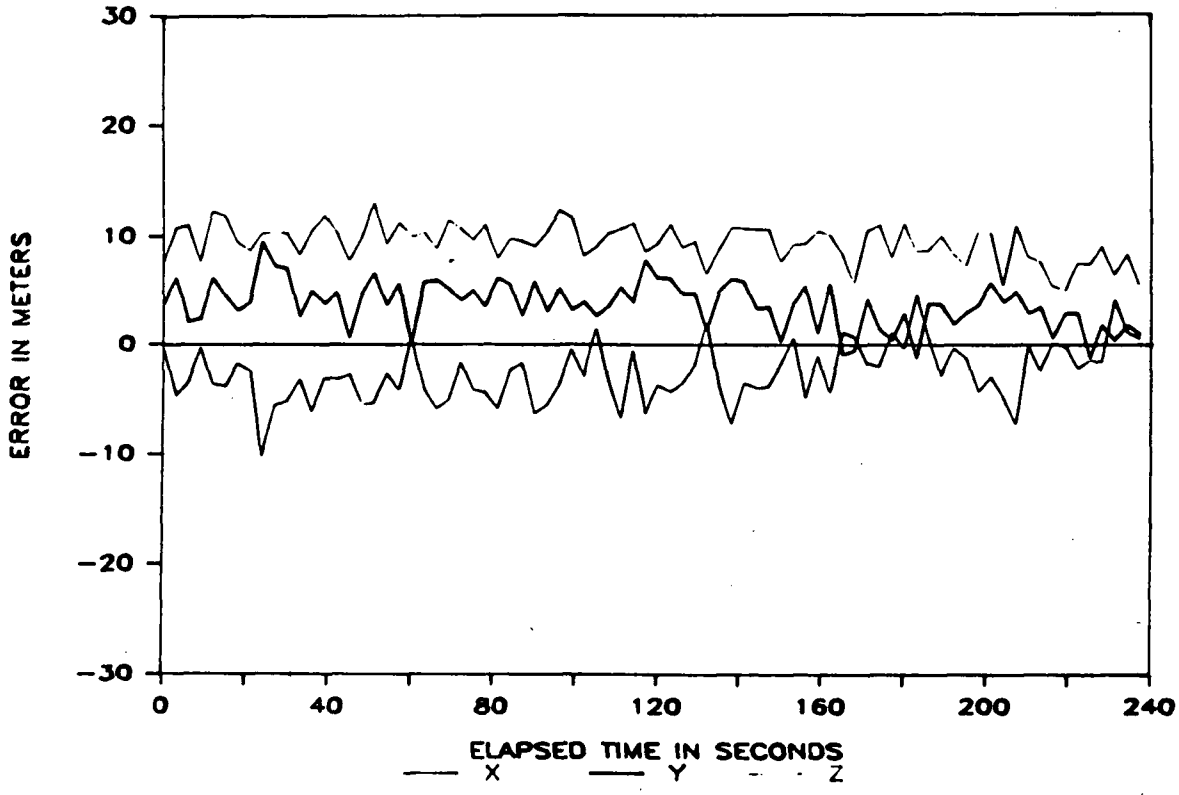

Figure 4-31. Position Difference Simulations (Three SVs Different) (PDOP = 2.6)

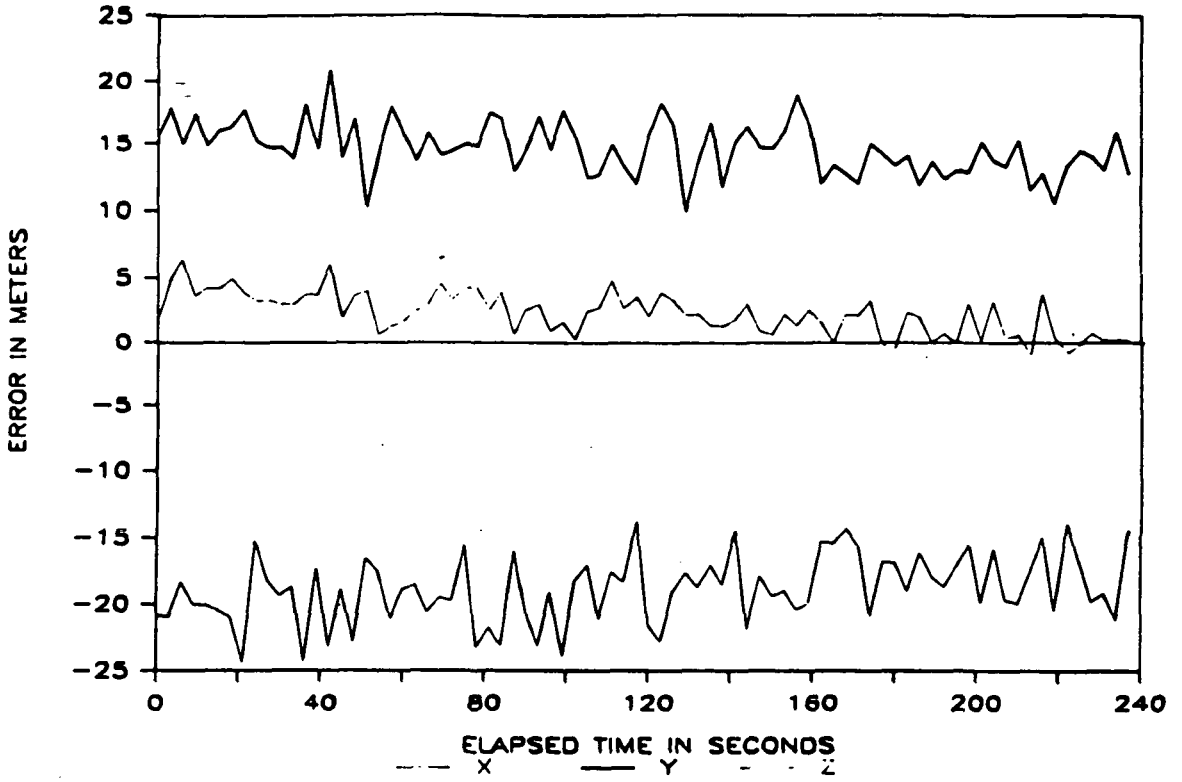

Figure 4-32. Position Difference Simulations (All Four SVs Different) (PDOP = 2.6)

2. One SV different (Figure 4–29)

mean X error	=	4.9 meters (16.1 feet)
mean Y error	=	−1.2 meters (−3.9 feet)
mean Z error	=	−0.4 meter (−1.3 feet)
root-sum-square error	=	5.1 meters (16.7 feet)
one-sigma X error	=	2.8 meters (9.2 feet)
one-sigma Y error	=	1.7 meters (5.6 feet)
one-sigma Z error	=	1.1 meters (3.6 feet)
root-sum-square error	=	3.5 meters (11.5 feet)

3. Two SVs different (Figure 4–30)

mean X error	=	−1.9 meters (−6.2 feet)
mean Y error	=	4.3 meters (14.1 feet)
mean Z error	=	−1.3 meters (−4.3 feet)
root-sum-square error	=	4.9 meters (16.1 feet)
one-sigma X error	=	2.1 meters (6.9 feet)
one-sigma Y error	=	2.7 meters (8.9 feet)
one-sigma Z error	=	1.3 meters (4.3 feet)
root-sum-square error	=	3.7 meters (12.1 feet)

4. Three SVs different (Figure 4–31)

mean X error	=	− 2.7 meters	(−8.9 feet)
mean Y error	=	3.7 meters	(12.1 feet)
mean Z error	=	9.4 meters	(30.8 feet)
root-sum-square error	=	10.5 meters	(34.4 feet)
one-sigma X error	=	2.7 meters	(8.9 feet)
one-sigma Y error	=	2.2 meters	(7.2 feet)
one-sigma Z error	=	1.7 meters	(5.6 feet)
root-sum-square error	=	3.9 meters	(12.8 feet)

5. All four SVs different (Figure 4–32)

mean X error	=	−18.9 meters	(−62.0 feet)
mean Y error	=	14.7 meters	(48.2 feet)
mean Z error	=	2.3 meters	(7.5 feet)
root-sum-square error	=	24.1 meters	(79.0 feet)
one-sigma X error	=	2.6 meters	(8.5 feet)
one-sigma Y error	=	2.0 meters	(6.6 feet)
one-sigma Z error	=	1.7 meters	(5.6 feet)
root-sum-square error	=	3.7 meters	(12.1 feet)

4.2.2.2 Range Difference Simulation

- **Range Differential Theory**

The term range difference refers to the GPS relative navigation technique where the measurement is the difference of pseudoranges. Specifically, a double-difference pseudorange (PR) measurement was used for these simulations. The solution of the navigation process is the relative position vector: X, Y, Z (earth-centered/earth-fixed). Below is a definition, first of single differences and then of double differences.

- **Single Difference**

To form the single-difference PR measurement, the PR of the remote receiver is subtracted from the PR of the reference.

$$PR_{SDi} = PR_{Ai} - PR_{Bi} \qquad i = 1, 2, 3, 4$$

Before discussing the measurement observation matrix for PR single difference measurements, it would be helpful to go through the mathematics for the absolute position case.

When calculating absolute position using a Kalman filter, the measurement observation matrix relates change in the pseudorange to change in absolute position. This matrix has elements which are the partial derivatives of the PR with respect to the components of the receiver's position.

For example, the partial derivative of the PR from receiver B to SV_i with respect to the X component of the receiver position is:

$$\frac{\partial\, PR_{Bi}}{\partial\, X_B}\,[(\hat{X}_i - X_B)^2 + (\hat{Y}_i - Y_B)^2 + (\hat{Z}_i - Z_B)^2]^{1/2} + \Delta t_B$$

$$= \frac{\frac{1}{2}\left[\frac{\partial}{\partial X_B}(\hat{X}_i^2 - 2\hat{X}_i X_B + X_B^2)\right]}{[(\hat{X}_i - X_B)^2 + (\hat{Y}_i - Y_B)^2 + (\hat{Z}_i - Z_B)^2]^{1/2}}$$

$$= \frac{\frac{1}{2}(-2\hat{X}_i + 2X_B)}{[(\hat{X}_i - X_B)^2 + (\hat{Y}_i - Y_B)^2 + (\hat{Z}_i - Z_B)^2]^{1/2}}$$

$$= \frac{-(\hat{X}_i - X_B)}{[(\hat{X}_i - X_B)^2 + (\hat{Y}_i - Y_B)^2 + (\hat{Z}_i - Z_B)^2]^{1/2}}$$

$$= -\ell_{XBi}$$

where

PR_{Bi} = SV_i PR corrected for atmospheric delay and SV clock error

X_B, Y_B, Z_B = the earth-centered/earth-fixed (ECEF) position of receiver B

$\hat{X}_i, \hat{Y}_i, \hat{Z}_i$ = SV position predicted from the SV nav message

Δt_B = user clock error in meters

ℓ_{XBi} = the X component of the line-of-sight vector from receiver B to SV_i.

The partial derivatives with respect to the Y and Z components are similar. The partial derivative with respect to the receiver clock error is:

$$\frac{\partial PR_{Bi}}{\partial \Delta t_B} = 1$$

For single difference measurements, the measurement observation matrix relates change in the PR single difference to change in relative position. In formulating the measurement observation matrix, we assume that the error in relative position is from error in the position of receiver B. So the partial derivative of the PR single difference with respect to the components of position of receiver B is calculated:

$$\frac{\partial PR_{SDi}}{\partial X_B} = \frac{\partial PR_{Ai}}{\partial X_B} - \frac{\partial PR_{Bi}}{\partial X_b} = +\ell_{XBi}$$

The terms for PR_{Ai} drop out. The sign is opposite that for the absolute position. Likewise for the receiver clock error component:

$$\frac{\partial PR_{SDi}}{\partial \Delta t_B} = -1$$

- **Double Difference**

The double-difference measurement is the single-difference PR for SV_i minus the single-difference PR for SV_j. Four SVs are tracked and three double differences are formed with the SV pairs.

$$\begin{aligned} PR_{DDij} &= (PR_{Ai} - PR_{Bi}) - (PR_{Aj} - PR_{Bj}) \qquad i = 1, 2, 3 \\ &= (PR_{Ai} - PR_{Aj}) - (PR_{Bi} - PR_{Bj}) \qquad j = 2, 3, 4 \end{aligned}$$

where PR_{Ai} is the pseudorange from user A to SV_i.

When the double difference is formed, the receiver clock term drops out. The partial derivatives of the PR double difference with respect to the position components are:

$$\frac{\partial PR_{DDij}}{\partial X_B} = \frac{\partial PR_{SDi}}{\partial X_B} - \frac{\partial PR_{SDj}}{\partial X_B}$$

$$= \ell_{XBi} - \ell_{XBj}$$

and similarly for the Y and Z components. The measurement observation matrix is a 3-by-3 matrix with one row for each SV pair.

- **Simulation Results**

Processing was done using a six-state Kalman filter. Three states are the X, Y, Z of the relative position and three states are X, Y, Z of the relative velocity. To make the maximum use of the legacy code from which the simulator was derived and to avoid getting bogged down in side issues, several things were done which might not be included in a navigation system implementation but are sufficient for a study of this scope. First, the relative position states were propagated linearly instead of along the orbit. Using three-second measurements reduces the propagation error, and acceleration data was provided to make this comparable to orbital propagation. Also, the legacy filter uses line-of-sight vectors from the reference and remote locations to form the H matrix. These absolute positions do not have to be known very accurately, so these simulations assume that an absolute position for the target vehicle (accurate to about 10 or 20 M; 30 to 60 feet) is sent over.

The target and chaser are both in a typical 270-nmi space station orbit. The simulated vehicle separation was 35 km to 30 M (20 nmi to 100 feet). Three segments were run: 35 km apart, 17 km apart, and 30 M apart. Figures 4–33 through 4–38 are plots of the simulation results, a relative position and relative velocity plot for each of the three segments. Table 4–2 summarizes the results, showing the root-sum-square of the X, Y, Z error components.

TABLE 4-2. SUMMARY OF RANGE DIFFERENCE RELATIVE NAVIGATION SIMULATIONS

Simulation	Mean of Position Error (M)	(Ft)	Standard Dev. of Position Error (M)	(Ft)	Mean of Velocity Error (M/sec)	(Ft/sec)	Standard Dev. of Velocity Error (M/sec)	(Ft/sec)
35 km	0.27	(0.89)	1.60	(5.25)	0.12	(0.39)	0.15	(0.49)
17 km	0.27	(0.89)	1.60	(5.25)	0.06	(0.20)	0.16	(0.52)
30 M	0.26	(0.85)	1.60	(5.25)	0.01	(0.03)	0.15	(0.49)

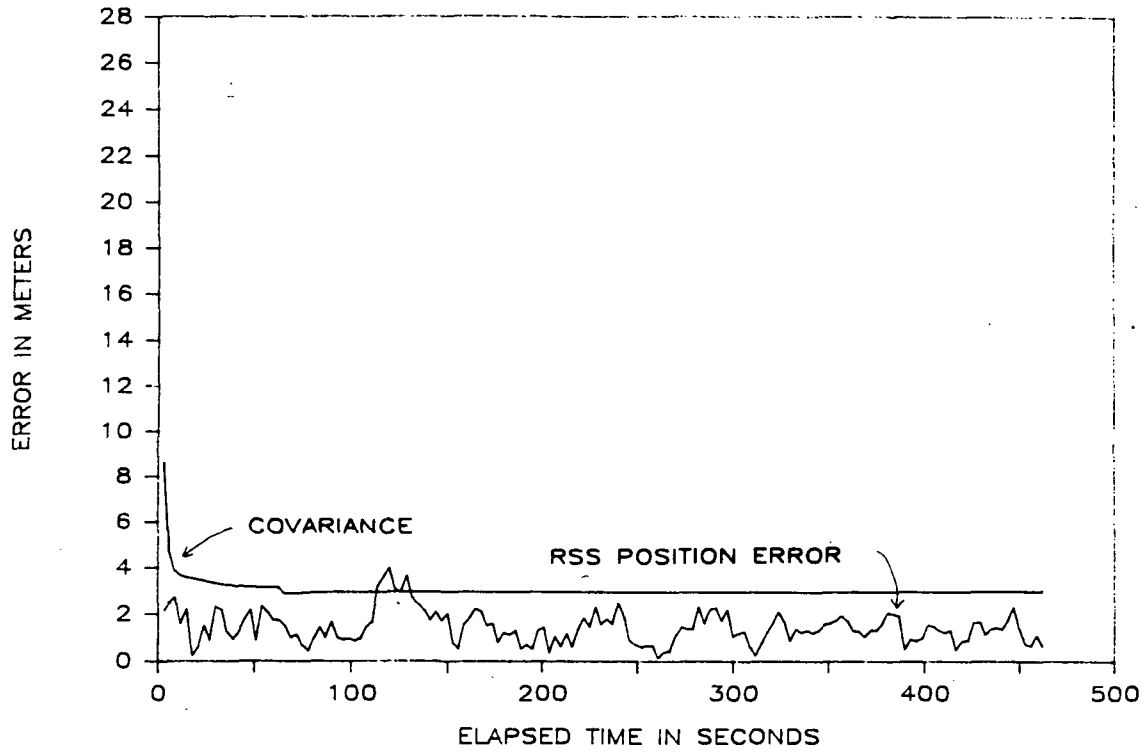

Figure 4-33. Range Difference Simulations—Position Error (35-km Separation) (PDOP = 3.0-2.6)

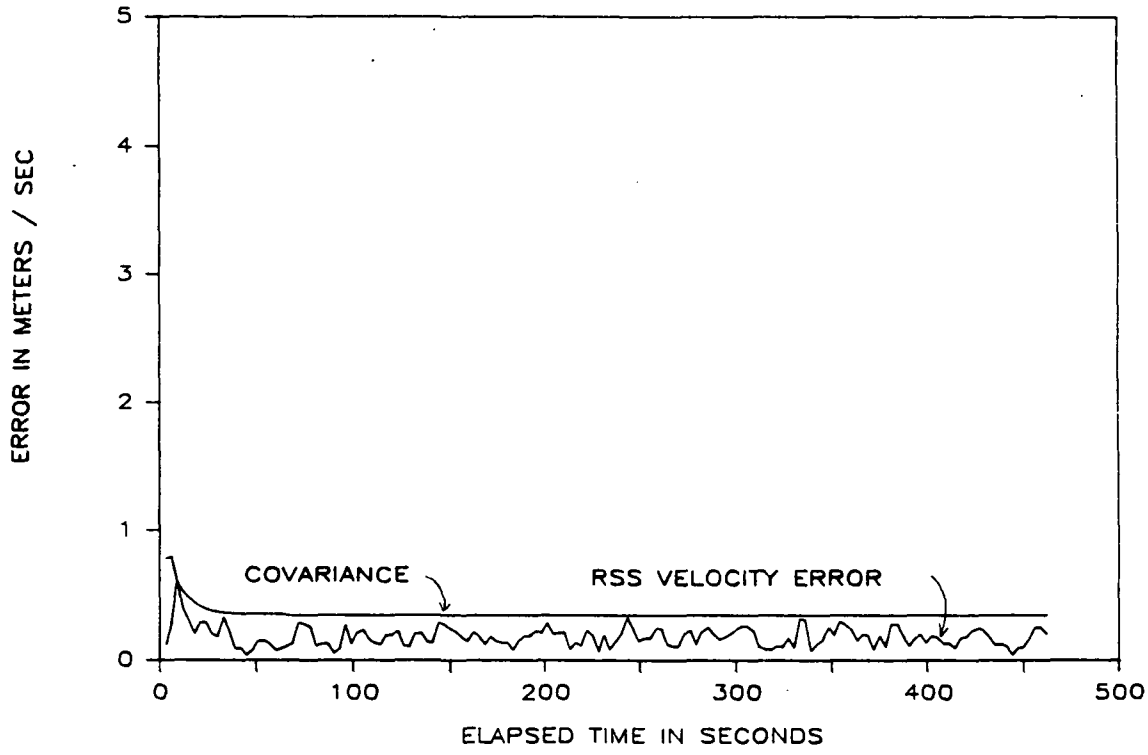

Figure 4-34. Range Difference Simulations—Velocity Error (35-km Separation) (PDOP = 3.0-2.6)

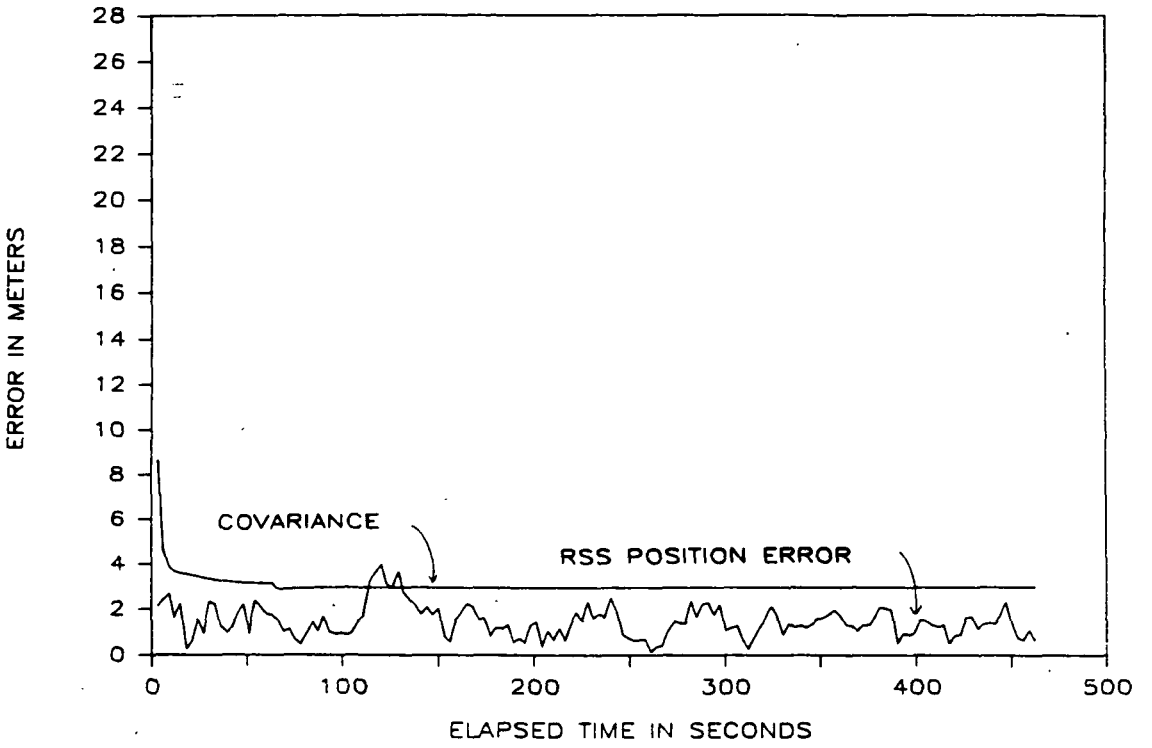

Figure 4-35. Range Difference Simulations—Position Error (17-km Separation) (PDOP = 3.0-2.6)

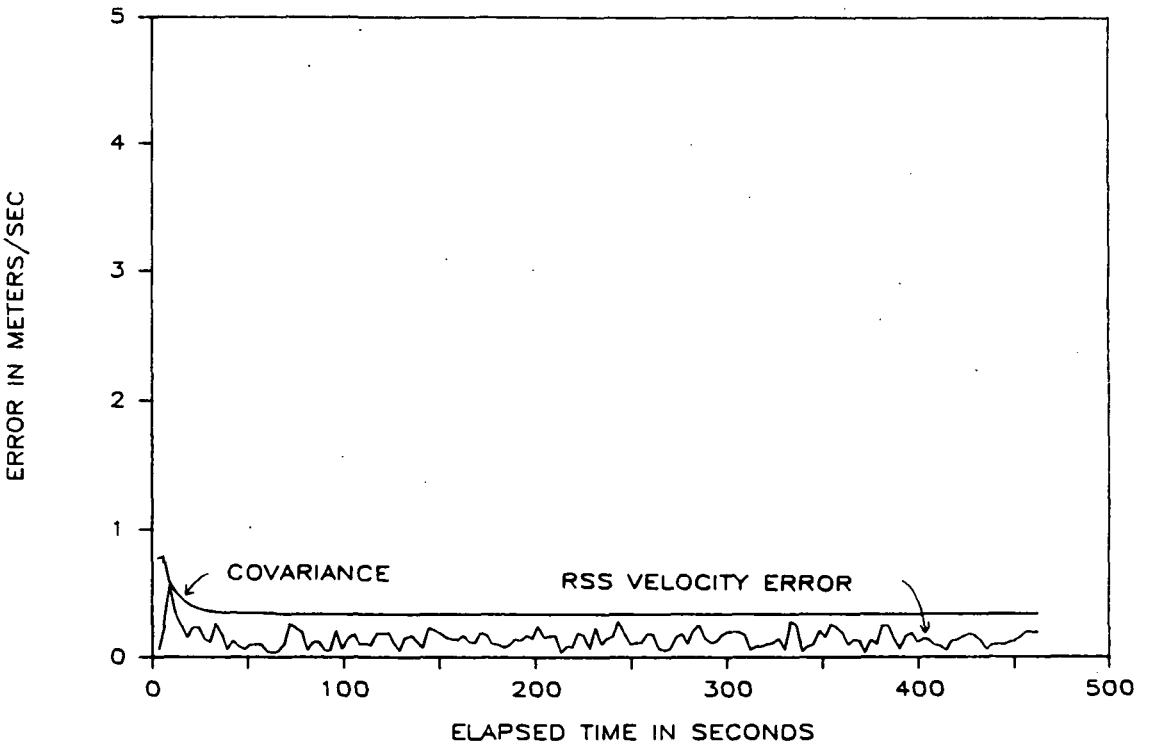

Figure 4-36. Range Difference Simulations—Velocity Error (17-km Separation) (PDOP = 3.0-2.6)

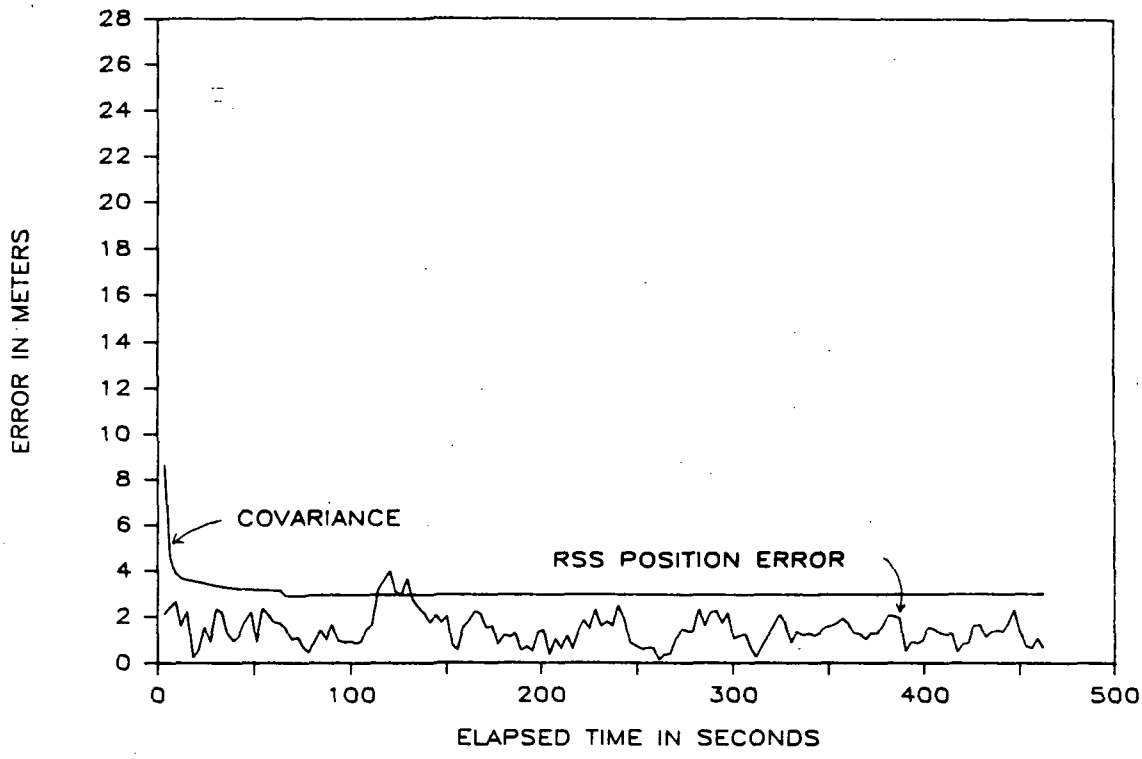

Figure 4-37. Range Difference Simulations—Position Error (30-M Separation) (PDOP = 3.0-2.6)

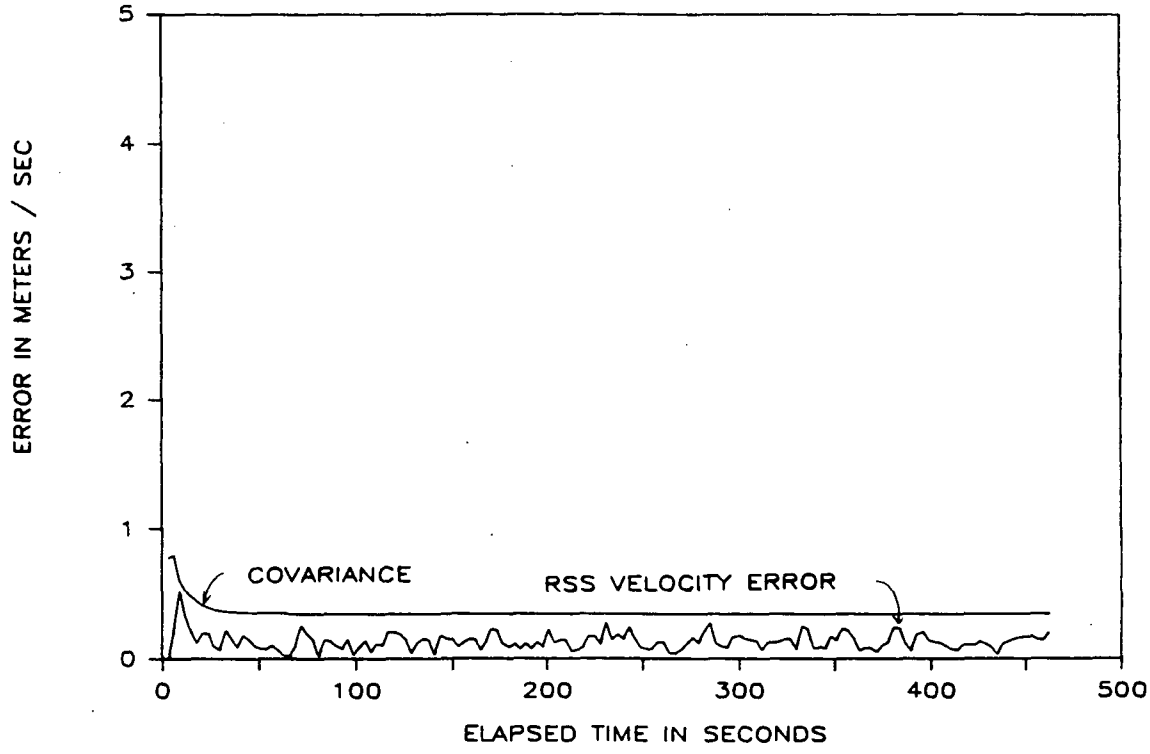

Figure 4-38. Range Difference Simulations—Velocity Error (30-M Separation) (PDOP = 3.0-2.6)

APPENDIX

MATHEMATICAL ANALYSIS OF DIFFERENTIAL NAVIGATION ERROR

MATHEMATICAL ANALYSIS OF DIFFERENTIAL NAVIGATION ERROR

GOAL

- DERIVE AN EXPRESSION OF THE ERROR VARIANCE IN DIFFERENTIAL POSITION
- EVALUATE THE EXPRESSION FOR VARIOUS SV SET ASSUMPTIONS

APPROACH

- DETERMINE A LINEAR RELATIONSHIP BETWEEN RANGE ERROR AND POSITION ERROR (RELATIVE ERROR BETWEEN TWO USERS)
- COMPUTE THE ERROR VARIANCE OF RELATIVE POSITION BASED ON THE LINEAR RELATIONSHIP AND ASSUMED MEASUREMENT ERROR STATISTICS
- ASSUMES MAXIMUM USER SEPARATION OF 35 KM.

DETERMINATION OF A LINEAR RELATIONSHIP BETWEEN RANGE ERROR AND POSITION ERROR

- GPS POSITION IS FOUND BY SOLVING 4 NON-LINEAR PR EQUATIONS IN 4 UNKNOWNS (X_u, Y_u, Z_u AND Δt_u)

$$PR_i' = \left[\left(\hat{X}_i - X_u\right)^2 + \left(\hat{Y}_i - Y_u\right)^2 + \left(\hat{Z}_i - Z_u\right)^2\right]^{1/2}$$

$$+ c\Delta t_u + n_i \qquad i = 1, 2, 3, 4$$

PR_i' = SV_i PR CORRECTED FOR ATMOSPHERIC DELAY AND SV CLOCK ERROR

X_u, Y_u, Z_u = THE USER'S EARTH-CENTERED/EARTH-FIXED (ECEF) POSITION

$\hat{X}_i$, $\hat{Y}_i$, $\hat{Z}_i$ = PREDICTED SV POSITION FROM THE SV NAV MESSAGE

Δt_u = USER CLOCK ERROR

c = SPEED OF LIGHT

n_i = NOISE

- PLEASE NOTE THAT GPS RECEIVERS DO NOT SOLVE FOR POSITION USING 4 NON-LINEAR EQUATIONS, BUT THIS APPROACH IS USED HERE TO FACILITATE THE ANALYSIS.
- IF THE APPROXIMATE USER POSITION IS KNOWN, A SOLUTION MAY BE FOUND USING A NEWTON-RAPHSON ITERATIVE METHOD
- A TAYLOR POLYNOMIAL FOR THE PR EQUATIONS IS EXPANDED ABOUT THE APPROXIMATE POSITION

$$PR_i' = PR_i'\Big|_{\underline{\hat{u}}} + \frac{\partial PR_i'}{\partial \underline{u}}\Big|_{\underline{\hat{u}}} \underline{\Delta u} + \varnothing + n_i$$

AND

$$\Delta PR_i = PR_i' - PR_i'\Big|_{\underline{\hat{u}}} = \frac{\partial PR_i'}{\partial \underline{u}}\Big|_{\underline{\hat{u}}} \underline{\Delta u} + \varnothing + n_i$$

WHERE

ΔPR_i = DIFFERENCE BETWEEN ACTUAL AND USER PREDICTED PR

PR_i' = CORRECTED PSEUDORANGE

$\underline{\hat{u}}$ = ESTIMATE OF USER POSITION

$\underline{\Delta u}$ = THE ERROR BETWEEN THE ESTIMATE AND THE TRUE POSITION

$\varnothing$ = HIGHER ORDER TERMS

n_i = NOISE

- A G MATRIX IS FORMED OF THE PARTIAL DERIVATIVES OF THE PR WITH RESPECT TO THE COMPONENTS OF USER POSITION. THE DERIVATIVES TURN OUT TO BE LINE-OF-SIGHT VECTORS TO THE SVs.

$$G = \begin{bmatrix} \frac{\partial PR_1'}{\partial \underline{u}} \\ \vdots \\ \frac{\partial PR_4'}{\partial \underline{u}} \end{bmatrix}\Bigg|_{\underline{\hat{u}}} = \begin{bmatrix} -\ell_{1x} & -\ell_{1y} & -\ell_{1z} & 1 \\ -\ell_{2x} & -\ell_{2y} & -\ell_{2z} & 1 \\ -\ell_{3x} & -\ell_{3y} & -\ell_{3z} & 1 \\ -\ell_{4x} & -\ell_{4y} & -\ell_{4z} & 1 \end{bmatrix}$$

WHERE PR_i' = SV_i PR CORRECTED FOR ATMOSPHERIC DELAY AND SV CLOCK ERROR

$\underline{u}$ = USER ECEF POSITION

$\hat{\underline{u}}$ = APPROXIMATE USER POSITION

$-\ell_{1x}$ = THE X COMPONENT OF THE LINE-OF-SIGHT VECTOR TO SV_1

$-\ell_{1x}$ =

$$\frac{-(\hat{X}_1 - X_u)}{\left[(\hat{X}_1 - X_u)^2 + (\hat{Y}_1 - Y_u)^2 + (\hat{Z}_1 - Z_u)^2\right]^{1/2}}$$

- THEN THE RELATIONSHIP BETWEEN THE RANGE ERROR AND THE USER POSITION ERROR CAN BE EXPRESSED AS FOLLOWS:

$\underline{\varepsilon R} = G\ \underline{\varepsilon U}$

WHERE $\underline{\varepsilon R}$ = DIFFERENCE BETWEEN ACTUAL AND USER PREDICTED RANGE

$$\underline{\varepsilon U} = \begin{bmatrix} \varepsilon X_u \\ \varepsilon Y_u \\ \varepsilon Z_u \\ \Delta t_u \end{bmatrix}$$

X_u, Y_u, Z_u = THE USER'S EARTH-CENTERED/EARTH-FIXED (ECEF) POSITION

Δt_u = USER CLOCK ERROR

COMPUTATION OF THE ERROR VARIANCE OF ABSOLUTE POSITION

- AN EQUATION FOR THE ABSOLUTE ERROR OF USER A (INCLUDING TIME ERROR) WOULD BE:

$$\underline{\varepsilon U}_A = G_A^{-1}\, \underline{\varepsilon R}_A$$

WHERE $\underline{\varepsilon R}_A = \underline{\varepsilon PR}_A + \underline{\varepsilon t}_A + \underline{\varepsilon E}_A$

$\underline{\varepsilon PR}_A$ IS THE ERROR IN PSEUDORANGE FROM MULTIPATH, THERMAL NOISE AND IONOSPHERE

$\underline{\varepsilon t}_A$ IS THE SV CLOCK ERROR

$\underline{\varepsilon E}_A$ IS THE MAPPING OF THE CROSS TRACK AND ALONG TRACK SV EPHEMERIS ERROR INTO DIFFERENTIAL POSITION ERROR.

SINCE THE MEAN OF THE RANGE ERROR IS ZERO, THE VARIANCE OF THE ABSOLUTE ERROR IS:

$$\begin{aligned}
\mathrm{Var}(\underline{\varepsilon U}_A) &= \mathrm{Var}(G_A^{-1}\, \underline{\varepsilon R}_A) \\
&= E\left[(G_A^{-1}\, \underline{\varepsilon R}_A)(G_A^{-1}\, \underline{\varepsilon R}_A)^T\right] \\
&= E\left[G_A^{-1}\, (\underline{\varepsilon R}_A)(\underline{\varepsilon R}_A)^T\, G_A^{-T}\right] \\
&= G_A^{-1}\; E\left[(\underline{\varepsilon R}_A)(\underline{\varepsilon R}_A)^T\right]\, G_A^{-T}
\end{aligned}$$

NOW WE MAKE SOME ASSUMPTIONS, AND PLEASE NOTE THAT THESE ARE REALISTIC ASSUMPTIONS, NOT MERELY FOR SIMPLIFICATION.

FIRST, ASSUMING THAT THE RANGE ERRORS ARE UNCORRELATED FOR INDEPENDENT PSEUDORANGES TO EACH OF FOUR SVs, THEN THE OFF-DIAGONAL TERMS OF $E\left[(\underline{\varepsilon R}_A)(\underline{\varepsilon R}_A)^T\right]$ WILL BE ZERO. ASSUMING THAT THE PSEUDORANGE ERRORS ARE STATISTICALLY EQUIVALENT, THAT IS: $\sigma(\varepsilon R_1) = \sigma(\varepsilon R_2) = \sigma(\varepsilon R_3) = \sigma(\varepsilon R_4) = \sigma(\varepsilon R)$. THEN:

$$\mathrm{Var}(\underline{\varepsilon U}_A) = \sigma(\varepsilon R)^2\, (G_A^{-1}\, G_A^{-T}).$$

THE DIAGONAL ELEMENTS OF THE MATRIX VAR ($\underline{\varepsilon U}_A$) ARE THE ECEF POSITION AND TIME ERROR VARIANCES. THE SQUARE ROOT OF THE TRACE OF THE MATRIX ($G_A^{-1}\, G_A^{-T}$) IS KNOWN AS GEOMETRIC DILUTION OF PRECISION (GDOP). GDOP TIMES THE RANGE ERRORS YIELDS POSITION AND TIME ERRORS FOR A GIVEN SV GEOMETRY.

$\sigma(\underline{\varepsilon U}_A) = \sigma(\varepsilon R)$ GDOP

FOR POSITION ONLY, THE 3 X 3 MATRIX CALLED PDOP IS USED. DEFINING $\sigma(\varepsilon P_A)$ AS THE ABSOLUTE POSITION ERROR OF USER A, THEN IT FOLLOWS THAT $\sigma(\underline{\varepsilon P}_A) = \sigma(\varepsilon R)$ PDOP

WHERE $\underline{\varepsilon P}_A = \begin{bmatrix} \varepsilon X_u \\ \varepsilon Y_u \\ \varepsilon Z_u \end{bmatrix}$

$\sigma(\underline{\varepsilon P}_A)$ IS THE ROOT-SUM- SQUARE OF THE X,Y,Z ERRORS

COMPUTATION OF THE ERROR VARIANCE OF RELATIVE POSITION

- THE BEST RELATIVE POSITION SOLUTION WILL MINIMIZE THE VARIANCE:

$$\begin{aligned}
&\text{VAR}(\underline{\varepsilon U}_A - \underline{\varepsilon U}_B) \\
&= \text{Var}(G_A^{-1}\,\underline{\varepsilon R}_A - G_B^{-1}\,\underline{\varepsilon R}_B) \\
&= \text{Var}(G_A^{-1}(\underline{\varepsilon PR}_A + \underline{\varepsilon t}_A + \underline{\varepsilon E}_A) - G_B^{-1}(\underline{\varepsilon PR}_B + \underline{\varepsilon t}_B + \underline{\varepsilon E}_B)) \\
&= \text{Var}(G_A^{-1}\,\underline{\varepsilon PR}_A + G_A^{-1}\,\underline{\varepsilon t}_A + G_A^{-1}\,\underline{\varepsilon E}_A - G_B^{-1}\,\underline{\varepsilon PR}_B - G_B^{-1}\,\underline{\varepsilon t}_B \\
&\quad - G_B^{-1}\,\underline{\varepsilon E}_B) \\
&= \text{Var}(G_A^{-1}\,\underline{\varepsilon PR}_A) + \text{Var}(G_B^{-1}\,\underline{\varepsilon PR}_B) \\
&\quad + \text{Var}(G_A^{-1}\,\underline{\varepsilon t}_A) + \text{Var}(G_B^{-1}\,\underline{\varepsilon t}_B) \\
&\quad + \text{Var}(G_A^{-1}\,\underline{\varepsilon E}_A) + \text{Var}(G_B^{-1}\,\underline{\varepsilon E}_B) \qquad \text{(EQ. 1)} \\
&\quad - 2\,\text{Cov}(G_A^{-1}\,\underline{\varepsilon PR}_A, G_B^{-1}\,\underline{\varepsilon PR}_B) \\
&\quad - 2\,\text{Cov}(G_A^{-1}\,\underline{\varepsilon t}_A, G_B^{-1}\,\underline{\varepsilon t}_B) \\
&\quad - 2\,\text{Cov}(G_A^{-1}\,\underline{\varepsilon E}_A, G_B^{-1}\,\underline{\varepsilon E}_B)
\end{aligned}$$

AND THE COVARIANCE TERMS FOR COMBINATIONS OF εPR, εt, AND εE ARE ZERO BECAUSE THESE ERRORS ARE INDEPENDENT, IN ALL CASES.

- CASE 1 ALL SVs DIFFERENT

  IN THIS CASE THE 3 COVARIANCE TERMS OF EQUATION 1 ARE ZERO BECAUSE THE ERRORS ARE INDEPENDENT. EQUATION 1 BECOMES:

  $$\text{VAR}(\underline{\varepsilon U}_A - \underline{\varepsilon U}_B)$$

  $$= \text{Var}(G_A^{-1}\,\underline{\varepsilon PR}_A) + \text{Var}(G_B^{-1}\,\underline{\varepsilon PR}_B)$$

  $$+ \text{Var}(G_A^{-1}\,\underline{\varepsilon t}_A) + \text{Var}(G_B^{-1}\,\underline{\varepsilon t}_B)$$

  $$+ \text{Var}(G_A^{-1}\,\underline{\varepsilon E}_A) + \text{Var}(G_B^{-1}\,\underline{\varepsilon E}_B)$$

  $$= \text{Var}(G_A^{-1}\,\underline{\varepsilon R}_A) + \text{Var}(G_B^{-1}\,\underline{\varepsilon R}_B)$$

  ASSUMING THAT THE RANGE ERRORS ARE STATISTICALLY EQUIVALENT FOR BOTH USERS, A AND B, AND ASSUMING THAT FOR SEPARATIONS LESS THAN 35 KM $G_A = G_B = G$, THEN:

  $$\text{VAR}(\underline{\varepsilon U}_A - \underline{\varepsilon U}_B) = 2\,G^{-1}\,\text{Var}(\underline{\varepsilon R})\,G^{-T}$$

  ASSUMING THAT THE RANGE ERRORS FOR DIFFERENT SVs ARE UNCORRELATED:

  $$\sigma(\underline{\varepsilon U}_A - \underline{\varepsilon U}_B) = \sqrt{2}\;\sigma(\varepsilon R)\;\text{GDOP}$$

  WHICH IS 2 TIMES THE ABSOLUTE ERROR. AGAIN, CONSIDERING ONLY POSITION ERROR: $\sigma(\underline{\varepsilon P}_A - \underline{\varepsilon P}_B) = \sqrt{2}\;\sigma(\varepsilon R)\;\text{PDOP}$.

- CASE 2 ALL SVs SAME

  IN THIS CASE, SV DEPENDENT ERRORS WILL CANCEL AND STATION DEPENDENT ERRORS WILL REMAIN. BASED ON EQUATION 1:

  $$\text{VAR}(\underline{\varepsilon U}_A - \underline{\varepsilon U}_B)$$

  $$= \text{Var}(G_A^{-1}\,\underline{\varepsilon PR}_A) + \text{Var}(G_B^{-1}\,\underline{\varepsilon PR}_B)$$

  $$+ \text{Var}(G_A^{-1}\,\underline{\varepsilon t}_A) + \text{Var}(G_B^{-1}\,\underline{\varepsilon t}_B)$$

  $$+ \text{Var}(G_A^{-1}\,\underline{\varepsilon E}_A) + \text{Var}(G_B^{-1}\,\underline{\varepsilon E}_B)$$

  $$- 2\,\text{Cov}(G_A^{-1}\,\underline{\varepsilon t}_A, G_B^{-1}\,\underline{\varepsilon t}_B)$$

  $$- 2\,\text{Cov}(G_A^{-1}\,\underline{\varepsilon E}_A, G_B^{-1}\,\underline{\varepsilon E}_B)$$

WHERE $-2\,\mathrm{Cov}(G_A^{-1}\,\underline{\varepsilon PR}_A, G_B^{-1}\,\underline{\varepsilon PR}_B) = 0$ BECAUSE THE ERRORS ARE RECEIVER DEPENDENT. SINCE RECEIVER A AND B ARE TRACKING THE SAME SVs, $\underline{\varepsilon t}_A$ AND $\underline{\varepsilon t}_B$ ARE THE CLOCK ERROR FOR THE SAME SV. THE DIFFERENCE BETWEEN RECEIVERS OF THE RANGE ERROR CAUSED BY THE SV CLOCK IS NEGLIGIBLE, SO IT IS ASSUMED THAT $\underline{\varepsilon t}_A = \underline{\varepsilon t}_B$. ASSUMING THAT $G_A = G_B = G$ FOR CLOSE STATIONS, THEN:

$$-2\,\mathrm{Cov}(G_A^{-1}\,\underline{\varepsilon t}_A, G_B^{-1}\,\underline{\varepsilon t}_B) = -2\,\mathrm{Var}(G^{-1}\,\underline{\varepsilon t})$$

AND THIS WILL CANCEL WITH $\mathrm{Var}(G_A^{-1}\,\underline{\varepsilon t}_A) + \mathrm{Var}(G_B^{-1}\,\underline{\varepsilon t}_B)$.

SIMILARLY THE EPHEMERIS ERROR IS REFERENCED TO THE SAME SV. IN THE INSTITUTE OF NAVIGATION PAPER "THE APPLICATION OF NAVSTAR DIFFERENTIAL GPS IN THE CIVILIAN COMMUNITY" BY BESER AND PARKINSON, THEY SHOW THAT THE MAGNITUDE OF

$$\left| \varepsilon E_A - \varepsilon E_B \right| < \frac{\delta d}{r}$$

WHERE δ = THE USER SEPARATION, d IS THE MAGNITUDE OF THE EPHEMERIS ERROR AND r IS THE TRUE RANGE TO THE SV. FOR AN EPHEMERIS ERROR OF 30 M AND USER SEPARATION OF 35 KM, THIS IS 5CM.

THEREFORE, ASSUMING $\underline{\varepsilon E}_A = \underline{\varepsilon E}_B$, THE VARIANCE TERMS

$\mathrm{Var}(G_A^{-1}\,\underline{\varepsilon E}_A)$ and $\mathrm{Var}(G_B^{-1}\,\underline{\varepsilon E}_B)$ WILL CANCEL WITH
$-2\,\mathrm{Cov}(G_A^{-1}\,\underline{\varepsilon E}_A, G_B^{-1}\,\underline{\varepsilon E}_B)$.

THEN

$$\mathrm{VAR}(\underline{\varepsilon U}_A - \underline{\varepsilon U}_B)$$

$$= \mathrm{Var}(G_A^{-1}\,\underline{\varepsilon PR}_A) + \mathrm{Var}(G_B^{-1}\,\underline{\varepsilon PR}_B)$$

ASSUMING THE STATISTICS ARE THE SAME FOR εPR FOR BOTH RECEIVERS, THEN

$$\mathrm{VAR}(\underline{\varepsilon U}_A - \underline{\varepsilon U}_B) = 2\,G^{-1}\,\mathrm{Var}(\varepsilon PR)\,G^{-T}$$

$$\sigma(\underline{\varepsilon U}_A - \underline{\varepsilon U}_B) = \sqrt{2}\;\sigma(\varepsilon PR)\;\mathrm{GDOP}$$

CONSIDERING ONLY POSITION ERROR:

$$\sigma(\underline{\varepsilon P}_A - \underline{\varepsilon P}_B) = \sqrt{2}\;\sigma(\varepsilon PR)\;\mathrm{PDOP}$$

- CASE 3. PARTIALLY COMMON SVs

AGAIN BASED ON EQUATION 1:

$$\text{VAR}(\underline{\varepsilon U}_A - \underline{\varepsilon U}_B)$$

$$= \text{Var}(G_A^{-1}\,\underline{\varepsilon PR}_A) + \text{Var}(G_B^{-1}\,\underline{\varepsilon PR}_B)$$

$$+ \text{Var}(G_A^{-1}\,\underline{\varepsilon t}_A) + \text{Var}(G_B^{-1}\,\underline{\varepsilon t}_B)$$

$$+ \text{Var}(G_A^{-1}\,\underline{\varepsilon E}_A) + \text{Var}(G_B^{-1}\,\underline{\varepsilon E}_B)$$

$$- 2\,\text{Cov}(G_A^{-1}\,\underline{\varepsilon t}_A, G_B^{-1}\,\underline{\varepsilon t}_B)$$

$$- 2\,\text{Cov}(G_A^{-1}\,\underline{\varepsilon E}_A, G_B^{-1}\,\underline{\varepsilon E}_B)$$

WHERE $-2\,\text{Cov}(G_A^{-1}\,\underline{\varepsilon PR}_A, G_B^{-1}\,\underline{\varepsilon PR}_B) = 0$ BECAUSE THE ERRORS ARE RECEIVER DEPENDENT.

LOOKING AT THE SV CLOCK TERM, $2\,\text{Cov}(G_A^{-1}\,\varepsilon t_A, G_B^{-1}\,\varepsilon t_B)$, SOME ELEMENTS OF THE COVARIANCE MATRIX WILL BE ZERO (COVARIANCE FOR DIFFERENT SVs) AND SOME ELEMENTS WILL BE NON-ZERO (COVARIANCE FOR COMMON SVs). THE RESULT IS AN ERROR DUE TO THE SV CLOCKS WHICH IS IN BETWEEN THE VALUE FOR CASE 1 (ALL SVs DIFFERENT) AND THE VALUE FOR CASE 2 (ALL SVs SAME).

IN THE SAME WAY, THE ERROR DUE TO SV EPHEMERIS ERROR WILL BE BETWEEN THE CASE 1 AND CASE 2 VALUES. IT IS DIFFICULT TO SHOW ANALYTICALLY THE EFFECT OF HAVING SOME SVs WHICH ARE DIFFERENT BECAUSE ALL OF THE ELEMENTS OF THE MATRIX INVERSES HAVE DIFFERING SVs. THE SIMULATIONS OF THESE CASES WILL SHOW HOW MUCH THE ACCURACY IS AFFECTED BY INTRODUCING DIFFERENT SVs.

CONCLUSIONS

NOTE: THE NOTATION $\sigma(\varepsilon P_A - \varepsilon P_B)$ MEANS THE ROOT SUM SQUARE OF THE X, Y, Z ERROR.

- THE BEST RELATIVE POSITION SOLUTION WILL RESULT FROM USING ALL OF THE SAME SVs.

  $$\sigma(\underline{\varepsilon P}_A - \underline{\varepsilon P}_B) = \sqrt{2}\ \sigma(\varepsilon PR)\ PDOP \qquad (EQ.\ 2)$$

- USING COMPLETELY DIFFERENT SVs HAS NO ADVANTAGE OVER ABSOLUTE POSITIONING.

  $$\sigma(\underline{\varepsilon P}_A - \underline{\varepsilon P}_B) = \sqrt{2}\ \sigma(\varepsilon R)\ PDOP \qquad (EQ.\ 3)$$

  WHERE $\varepsilon R = \varepsilon PR + \varepsilon t + \varepsilon E$

- IN A TYPICAL EXAMPLE WITH $\sigma(\varepsilon R)$ = 6 METERS, $\sigma(\varepsilon PR)$ = 1 METER AND PDOP = 3,

  USING THE SAME SVs (EQ. 2) $\sigma(\underline{\varepsilon P}_A - \underline{\varepsilon P}_B)$ = 4.2 METERS

  USING COMPLETELY DIFFERENT SVs (EQ 3) $\sigma(\underline{\varepsilon P}_A - \underline{\varepsilon P}_B)$ = 25.4 METERS

  USING PARTIALLY COMMON SVs WILL RESULT IN AN ERROR WHICH WILL TEND TO BE IN BETWEEN THE 25.4 METER ERROR AND THE 4.2 METER ERROR RESULT.

- FORMING A QUALITY IMPROVEMENT RATIO OF THE RELATIVE POSITION (DIFFERENT SVs) DIVIDED BY THE RELATIVE POSITION (SAME SVs):

$$Q_R = \frac{\sqrt{2}\,\sigma(\varepsilon R)\ PDOP}{\sqrt{2}\,\sigma(\varepsilon PR)\ PDOP} = \frac{\sigma(\varepsilon R)}{\sigma(\varepsilon PR)}$$

- THIS RATIO SHOWS THAT BOTH SPACECRAFT GPS RECEIVERS USING THE SAME SVs CAN MAKE THE RELATIVE POSITION ERRORS APPROXIMATELY AN ORDER OF MAGNITUDE SMALLER THAN USING DIFFERENT SVs.

- FORMING A QUALITY IMPROVEMENT RATIO OF THE ABSOLUTE POSITION ERROR TO THE RELATIVE POSITION EFFOR (SAME SVs):

$$Q_A = \frac{\sigma(\varepsilon R)\ PDOP}{\sqrt{2}\,\sigma(\varepsilon PR)\ PDOP} = \frac{\sigma(\varepsilon R)}{\sqrt{2}\,\sigma(\varepsilon PR)}$$

- THIS RATIO SHOWS THAT WHEN BOTH SPACECRAFT GPS RECEIVERS USE THE SAME SVs, THE RELATIVE NAVIGATION ERROR WILL BE APPROXIMATLEY FOUR TIMES SMALLER THAN THEIR INDIVIDUAL ABSOLUTE POSITION ERROR.